الجمهورية الجزائرية الديمقراطية الشعبية
People's Democratic Republic of Algeria
وزارة التعليم العالي والبحث العلمي
Ministry of Higher Education and scientific research
المدرسة الوطنية العليا للتكنولوجيا
National High School of Technology
Department of Industrial Engineering And Maintenance

Final Year Project to Obtain the Diploma of Engineering

- Field –
Electromechanics
-Speciality-
Mechatronics
- Subject -

Contribution to modeling and stabilizing control laws design for hexacopter guidance

Realized by
MEKHERBECHE Abdelkrim

Members of The Jury :

Dr BOUHIRED Saâdi (MCB) - ENST	Président
Dr BOUADI Hakim (MCA) - ENST	Supervisor
Dr HOUARI FOUAD (MCB) - ENST	Examinator

Algiers, the 07/03/2023

Academic year 2022 –2023

Dedication

To my mother Thank you for your boundless love and nurturing nature. Your strength, patience, and sacrifices have always been an inspiration to me. You have been my rock, providing unwavering support in every step of my educational pursuit. Your belief in me has instilled confidence in my abilities, and I am forever grateful for your unwavering presence in my life.

To my father Thank you for being my role model and mentor. Your wisdom, guidance, and constant encouragement have pushed me to strive for excellence. Your dedication to providing me with the best opportunities and resources has been instrumental in my academic achievements. Your belief in my potential has fueled my ambition and determination.

Acknowledgement

I would like to express my heartfelt gratitude to all those who have contributed to the successful completion of this thesis. Without their support, guidance, and encouragement, this research would not have been possible.

I would like to thank my supervisor, Dr. BOUADi Hakim for his invaluable guidance throughout the entire process. His expertise, patience, and unwavering support have been instrumental in shaping this thesis. I am truly grateful for his insightful feedback, which has significantly enriched my work.

My thanks also go to Prof. NEMRA Abdelkrim and the entire team of the Guidance and Navigation laboratory at the Military Polytechnic School.

In conclusion, I would like to express my deepest appreciation to everyone who has played a part, big or small, in the completion of this thesis. Your contributions have been invaluable, and I am truly grateful for your support.

Thank you.

Contents

Contents III

List of Figures VI

List of Tables VIII

1 Overview of multicopters 1
- 1.1 Introduction . . . 2
- 1.2 Unmanned Aircraft System (UAS) . . . 3
  - 1.2.1 Unmanned Aerial Vehicles (UAVs) and model aircraft . . . 3
  - 1.2.2 Classification of Unmanned Aerial Vehicles "UAV" . . . 3
- 1.3 Historical Overview of multicopters . . . 6
  - 1.3.1 The Maturation Period (pre-1990) . . . 6
  - 1.3.2 The Growth Period (1990 - 2005) . . . 7
  - 1.3.3 The Development Period (2005-2010) . . . 8
  - 1.3.4 The Activity Period (2010-2013) . . . 9
  - 1.3.5 The period of prosperity (+2013) . . . 10
  - 1.3.6 Conclusion . . . 11
- 1.4 Evaluation of multicopter Performance . . . 12
  - 1.4.1 Ease of use . . . 12
  - 1.4.2 Reliability . . . 12
  - 1.4.3 Ease of maintenance . . . 12
  - 1.4.4 Autonomy . . . 13
  - 1.4.5 Maximum payload weight . . . 13
- 1.5 Bottleneck . . . 14
- 1.6 Missions of multicopters . . . 15
  - 1.6.1 Civil Domain . . . 15
  - 1.6.2 Military Domain . . . 16
- 1.7 Challenges of Hexacopters . . . 16
  - 1.7.1 Endurance . . . 16
  - 1.7.2 Motion and Obstacle Detection . . . 16
  - 1.7.3 Localization . . . 17
  - 1.7.4 Communication and Information Security . . . 18
  - 1.7.5 Open-source/Closed-source Autopilot . . . 18
  - 1.7.6 Mechanical Structure and Propulsion System . . . 18
- 1.8 Conclusion . . . 19

2 Modeling of the Hexacopter **20**
2.1 Introduction . . . 21
2.2 Principle of operation of the Hexacopter . . . 21
2.2.1 Vertical Movement . . . 21
2.2.2 Roll movement and lateral displacement along the axis . . . 21
2.2.3 Pitch movement and longitudinal displacement . . . 21
2.2.4 Yaw movement . . . 21
2.3 General Description of the Modeling . . . 22
2.3.1 Kinematic model of a rigid body . . . 22
2.3.2 The dynamic model of a rigid body . . . 22
2.3.3 Control efficiency model . . . 23
2.3.4 Propeller model . . . 23
2.4 Modeling assumptions . . . 23
2.5 Definition of reference frames . . . 23
2.6 Modeling of the Hexacopter . . . 24
2.6.1 Kinematic Modeling . . . 24
2.6.2 Dynamic Modeling . . . 26
2.6.3 Control Efficiency Model . . . 28
2.6.4 Rotor Model . . . 30
2.7 Control Synthesis Model . . . 31
2.8 Conclusion . . . 32

3 Control Techniques **33**
3.1 Introduction . . . 34
3.2 State of the art on the control of multicopters . . . 35
3.3 Linear Approaches . . . 36
3.4 Nonlinear Approaches . . . 36
3.5 General Control Structure . . . 37
3.6 Synthesis of PID Control Laws . . . 37
3.6.1 Principle of Control . . . 37
3.6.2 Control objectives . . . 38
3.6.3 Control Laws . . . 39
3.7 Synthesis of Backstepping Control Laws . . . 45
3.7.1 Backstepping theory . . . 45
3.7.2 Control objective . . . 45
3.7.3 Description of the design steps . . . 45
3.8 Synthesis of Sliding Mode Control Laws . . . 53
3.8.1 Control objective . . . 53
3.8.2 Description of the design steps . . . 53
3.9 conclusion . . . 60

Bibliography **62**

Symbols and notations

R_E:	Inertial Earth frame
x, y, z:	The position of the hexacopter in the reference frame R_E
ϕ, θ, ψ:	Orientation of the hexacopter in the reference frame R_E
R_B:	Frame of reference associated with the hexacopter
u, v, w:	The speed of the hexacopter in the frame of reference R_B
p, q, r:	The orientation of the hexacopter in the frame of reference R_E
R_{EB}:	Homogeneous transformation matrix from R_E to R_B
m:	Total mass of the hexacopter
g:	Acceleration of gravity
K_{ft}:	Coefficients of drag force
J:	Inertia matrix of the hexacopter
K_{fa}:	Coefficients of aerodynamic friction
ω:	Rotational speed of a motor
J_r:	Inertia of the motor
C_L:	Lift coefficient of the propeller
C_D:	Drag coefficient of the propeller
d:	Half-span of the hexacopter
k_e:	Electrical torque constant
C_s:	Dry friction
k_r:	Load torque constant
k_m:	Mechanical torque constant
r:	Motor resistance

List of Figures

1.1 The trend of aircraft sales. . . . 2
1.2 Unmanned Aircraft System (UAS) . . . 3
1.3 The three models of unmanned aerial vehicles . . . 4
1.4 The trend of using quadcopters and hexacopters. . . . 5
1.5 Two highly recognized multicopter models. . . . 5
1.6 combination of The three models of unmanned aerial vehicles . . . 5
1.7 Diagram illustrating the technological evolution of multicopters. . . . 6
1.8 Gyroplane Breguet-Richet in flight. . . . 6
1.9 Gyroplane Breguet-Richet No. 1. . . . 6
1.10 Oehmichen Model No. 2. . . . 7
1.11 The Convertawings Model "A". . . . 7
1.12 The Curtiss-Wright VZ-7 prototype. . . . 8
1.13 Drones developed during the growth period. . . . 8
1.14 Number of publications related to multicopters.[1] . . . 9
1.15 Two drones from the company Microdrones. . . . 9
1.16 Estimation of the number of articles related to multicopters. . . . 11
1.17 Prime Air delivery octocopter. . . . 12
1.18 The movements performed by the arms of the Remote Controller. . . . 14
1.19 The VC-200 transport UAV . . . 15
1.20 UAV HYCOPTER with a hydrogen fuel cell. . . . 17
1.21 Radar detection system onboard a hexacopter drone. . . . 17
1.22 The RQ-170 drone. . . . 18

2.1 Configurations used to achieve the six degrees of freedom. . . . 22
2.2 The two main frames. . . . 24
2.3 Block diagram presenting the complete model of the hexacopter. . . . 24
2.4 Transformation from the Earth frame to the body frame. . . . 25
2.5 Geometric configuration of the rotors. . . . 29

3.1 The aerodrome circuit navigation scenario . . . 35
3.2 Diagram of the General Control Structure. . . . 38
3.3 Structure of PID Control. . . . 39
3.4 PID attitude hovering . . . 40
3.5 PID position hovering . . . 40
3.6 PID thrust and moments hovering. . . . 41
3.7 trajectory tracking using PID . . . 42
3.8 PID attitude trajectory . . . 43

3.9 PID position trajectory 43
3.10 PID thrust and moments trajectory. 44
3.11 backstepping attitude hovering 48
3.12 backstepping position hovering 48
3.13 backstepping thrust and moments hovering. 49
3.14 trajectory tracking using backstepping 50
3.15 backstepping attitude trajectory 51
3.16 backstepping position trajectory 51
3.17 backstepping thrust and moments hovering. 52
3.18 sliding mode attitude hovering 55
3.19 sliding mode position hovering 55
3.20 backstepping thrust and moments hovering. 56
3.21 trajectory tracking using sliding mode 57
3.22 sliding mode attitude trajectory 58
3.23 sliding mode position trajectory 58
3.24 sliding mode thrust and moments trajectory. 59

List of Tables

1.1 Main Comparisons between UAVs and MAs 3
1.2 Open-Source Autopilot Systems 10
1.3 Drone Specifications 10
1.4 Drone Specifications 10
1.5 Commercialized drones from 2013 to 2015. 13
1.6 Comparison of Fixed-Wing, Helicopters, and multicopters 14
1.7 Open Source vs Closed Source 18

3.1 Simulation parameters 34

Introduction

An unmanned aerial vehicle (UAV), commonly known as a drone, is a flying vehicle without a human pilot, crew, or passengers on board. Drones are a component of an unmanned aircraft system (UAS), which additionally includes a ground controller and a communication system with the drone [2]. Drones can be flown under the remote control of a human operator, as a remotely piloted aircraft (RPA), Drones can have varying degrees of autonomy, and in ascending order of autonomy, the levels are: No Drone Autonomy, Low Drone Autonomy, Partial Drone Autonomy, Conditional Drone Autonomy, High Autonomy, up to fully autonomous aircraft that do not require any human intervention.

While unmanned aerial vehicles are primarily used in military applications today (surveillance, reconnaissance, damage assessment, etc.)[3], drones can also perform scientific, public safety, and commercial tasks such as data and image acquisition in disaster areas, mapping, communication relays, search and rescue operations, traffic management, and more [4].

In addition to the limitations of fixed-wing drones and the complexity of helicopter drones, multicopter drones have garnered significant attention from the scientific community. One of the reasons for this attention is related to the fact that rotary-wing configurations offer the possibility of hovering flight, which is essential for ensuring clear identification.

Hovering flight is also a means of easily taking off and landing without complex procedures, such as a prepared aerodrome or a specific landing device. Additionally, multicopters are easy to manufacture and relatively simple to fly indoors. While quadcopters were almost the only available multicopters ten years ago, newer multicopters now include Hexacopters, octacopters, and various combinations of coaxial multicopters.

With six propellers, Hexacopter drones provide excellent flight stabilization and are more resistant to windy conditions [5], which can be crucial for a professional drone capable of flying and filming in hovering flight even in difficult weather.

Furthermore, having six rotors allows for motor redundancy. In other words, a Hexacopter is capable of compensating for the failure of one motor during flight, enabling the drone to continue to be piloted and safely brought back without any issues.

Hexacopters have undergone incredible evolution in recent years. Universities, students, and researchers are continuously working to introduce more robust controllers and modeling and control techniques [5]. However, from an automation perspective, the mathematical model of drones, in general, is characterized by coupling between its variables and strong nonlinearity. In particular, the dynamic model of the Hexacopter involves a non-invertible control effectiveness matrix (dimension 4 X 6), which poses a challenge during control. Today, the evolution of drones is accompanied by advancements in control techniques. Traditional control methods can be applied within a limited range and under certain constraints on the behavior of these systems, which may limit their application in certain scenarios. In order to work across the full range of system variables, advanced control techniques provide a promising alternative. Another factor influencing the evolution of drones is the advancement of flight controllers. These controllers are necessary to manage the attitude and navigation of the vehicle when no human intervention is desired.

Various autopilot systems are available, ranging from more expensive options in the market to relatively cheaper and open-source alternatives like the Ardupilot series.
The objective is to provide a mathematical description of a system's behavior (Modeling) , followed by simulation-based control using various techniques.
The complete mathematical model of the hexacopter primarily consists of:

- Kinematic equations that establish a relationship between the vehicle's position and velocity.
- Dynamic model equations that define the relationship governing applied forces and resulting accelerations.

Regarding simulation, the hexacopter was controlled using three different control techniques:

- PID control as a classical technique.
- Backstepping control
- sliding mode

Chapter 1

Overview of multicopters

1.1 Introduction

The commonly used unmanned aerial vehicles, weighing less than 20 kg or 25 kg [6], can be classified into fixed-wing aircraft, helicopters, and multicopters [7], among which multicopters are currently the most popular. In fact, before 2010, fixed-wing aircraft and helicopters largely dominated the aerospace field and aeromodelling, but subsequently, multicopters became the new trend due to their ease of use. Figure 1.1 below shows the evolution of aircraft usage between 2004-2022.[8]

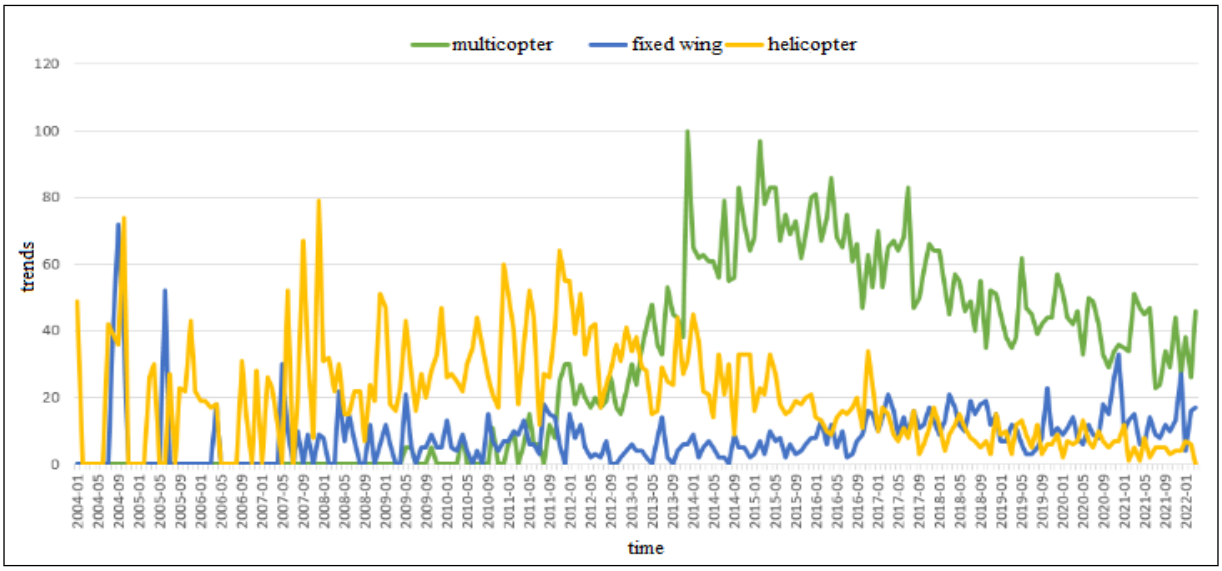

Figure 1.1: The trend of aircraft sales.

This evolution is particularly marked by the launch at the end of 2012 by DJI (Da-Jiang Innovations Science and Technology Co., Ltd.) of an all-in-one solution, namely the ready-to-fly Quadcopter "Phantom," and in 2017, the Hexacopter "MATRICE 600 PRO" [9], with significant advantages. Prior to 2010, multicopters were often assembled only by professional personnel (typically the manufacturer) due to the separate sale of autopilots and other aerospace components, and the cumbersome adjustment of flight parameters was done based on payload and flight time.

The main advantages of the Hexacopter "MATRICE 600 PRO" are: quick user piloting, low acquisition cost of approximately one thousand dollars, which represents significant savings compared to some commercial multicopters such as the MD4-200 and MD4-1000 from Microdrones GmbH in Germany, and positive contribution to reducing the difficulties and cost of aerial photography. These advantages have granted it a prominent position in the market.

In the wake of the development of UAVs, and thanks to several factors, including extensive publications by numerous media outlets after 2012, providing abundant information about multicopters in terms of technologies, products, applications, and innovations, as well as successful flight attempts, the development of open-source autopilot boards, and unprecedented investment in this field, multicopters have solidified their market share in the small aircraft industry. As a result, their development is becoming increasingly popular.

This chapter aims to answer the following question: Why are multicopters ultimately chosen? The answer to this question is based on the aforementioned introduction, which includes an overview of unmanned aerial systems, a brief historical background on multicopters, an evaluation of aircraft performance, and the challenges associated with multicopters.

1.2 Unmanned Aircraft System (UAS)

A Unmanned Aircraft System (UAS) is depicted in Figure 1.2 below. It consists of several subsystems, including the aircraft (often referred to as UAV or unmanned aerial vehicle), the payload, one or more control stations, the launch and recovery system for the flying vehicle, the communication system, and the transportation system. Their global usage is subject to rules, regulations, and disciplines of aviation [9].

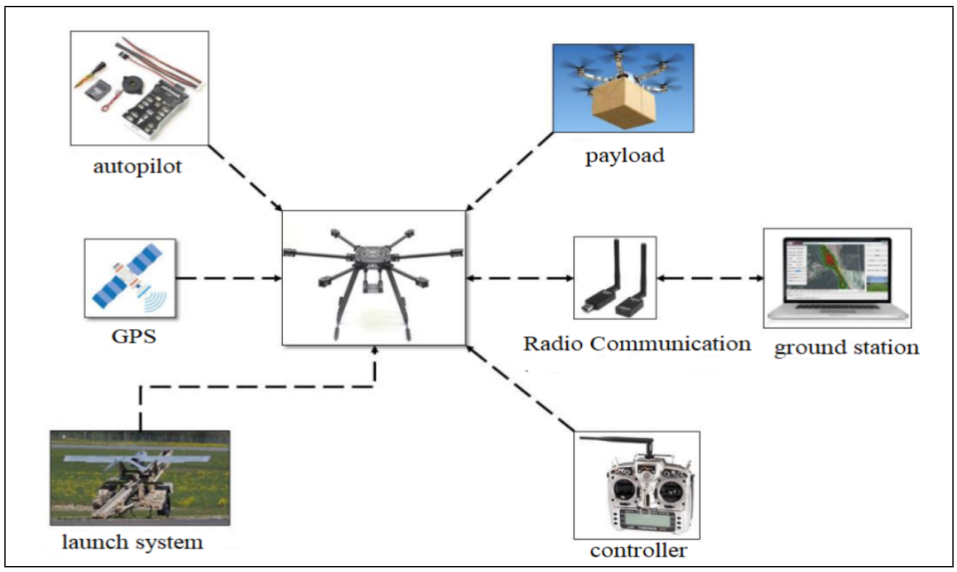

Figure 1.2: Unmanned Aircraft System (UAS)

1.2.1 Unmanned Aerial Vehicles (UAVs) and model aircraft

Unmanned Aerial Vehicles (UAVs) : The flight of UAVs can be controlled either autonomously by on-board computers or by remote control from a ground-based pilot or from another vehicle.
The model aircraft (MA): The flight of model aircraft can only be conducted if the aircraft remains within the visual line of sight (VLOS) of the ground-based pilot. These aircraft, which can fly with or without propulsion systems, are used for aerial competitions, sports, or recreational purposes. The regulatory parameters for operating a model aircraft are described in [9]. The Table 1.1 below shows the main comparisons between UAVs and MAs.

Aspect	**UAV**	**MA**
Composition	Complex	Simple
Operation	Autonomous and Remote Controlled	Remote Controlled
Role	Military or Civil Applications	Hobbies

Table 1.1: Main Comparisons between UAVs and MAs

1.2.2 Classification of Unmanned Aerial Vehicles ”UAV”

Today, several models of UAVs are available based on their application areas. Among these models, there are fixed-wing UAVs, helicopters, and multicopters which are the focus of our work. As shown in Figure

1.3, unmanned aircraft are classified into three types:

Fixed-wing

Fixed-wing aircraft have wings that are permanently attached to the fuselage of the aircraft. Most civil and military fighter aircraft are of the fixed-wing type. The necessary lift to balance the weight of the vehicle is generated by the wings. According to this principle, fixed-wing aircraft, as shown in Figure 1.3(a), need to maintain a certain speed and therefore cannot take off and land vertically. The major disadvantage of this type of aircraft is the requirement for a runway/launcher for takeoff and landing.

Helicopter

A helicopter is an aircraft in which lift and propulsion are provided by a rotating wing (see Figure 1.3(b). The majority of helicopters use a single main rotor for lift and a tail rotor or other anti-torque device. Based on the above introduction, it is understood that a helicopter has the ability to take off and land vertically (VTOL). Therefore, no runway or launcher is required for takeoff and landing.

multicopter

Considered a type of remote-controlled or autonomous helicopter with three or more propellers, this type has the ability to fly in VTOL (Vertical Takeoff and Landing). Figure 1.3(c) shows a Hexacopter multicopter. Unlike a helicopter, the quick adjustment of the lift force is achieved by controlling the angular speeds of the propellers, and due to the multiple-rotor structure, their counter-torques can cancel each other out. Compared to other types of UAVs (Unmanned Aerial Vehicles), most multicopters suffer from autonomy issues (limited flight time) and low payload capacity.

(a) Fixed wing (b) helicopter (c) multicopter

Figure 1.3: The three models of unmanned aerial vehicles

However, it is necessary to highlight that the trend of using quadcopters is much more significant than that of Hexacopters[8], as illustrated in Figure 1.4, with the difference between the two types summarized as follows:
For the Hexacopter: illustrated in Figure 1.5(a), it has six rotors to generate thrust, pitch moment, roll moment, and yaw moment.
For the quadcopter: this type only has four rotors to generate thrust and the three moments see Figure 1.5(b).
This means that the fundamental difference between multicopters lies in the relationship between the number of rotors on one hand and the generation of thrust and the three moments on the other hand.
In addition to the three types of drones presented above, there are UAVs that result from certain combinations of these drones, as shown in Figure 1.6 One type of helicopter combines both a tricopter and

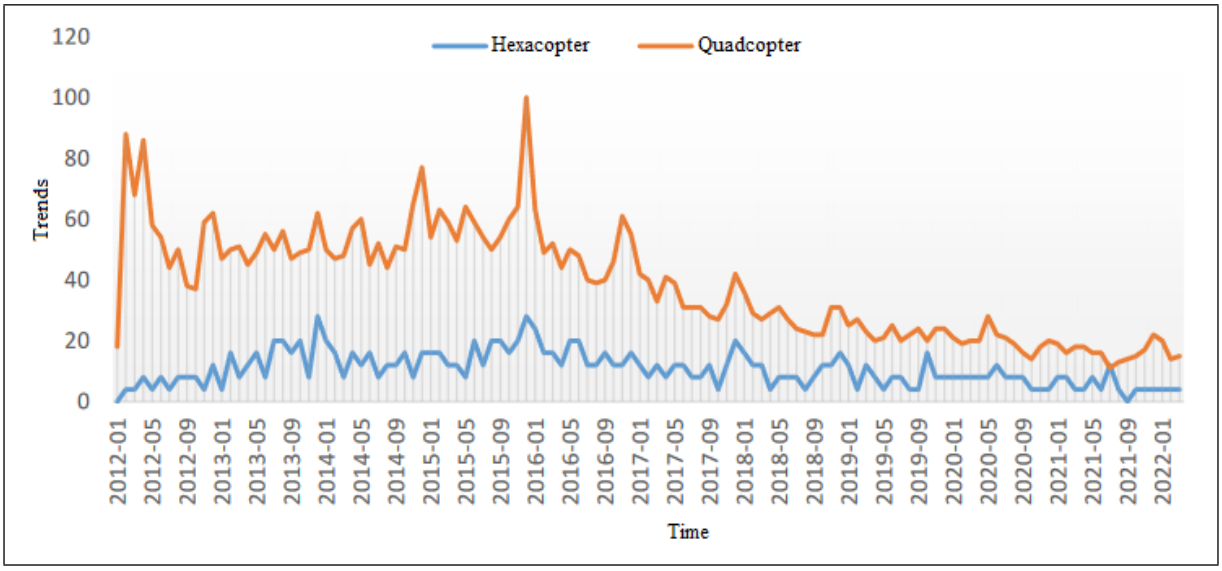

Figure 1.4: The trend of using quadcopters and hexacopters.

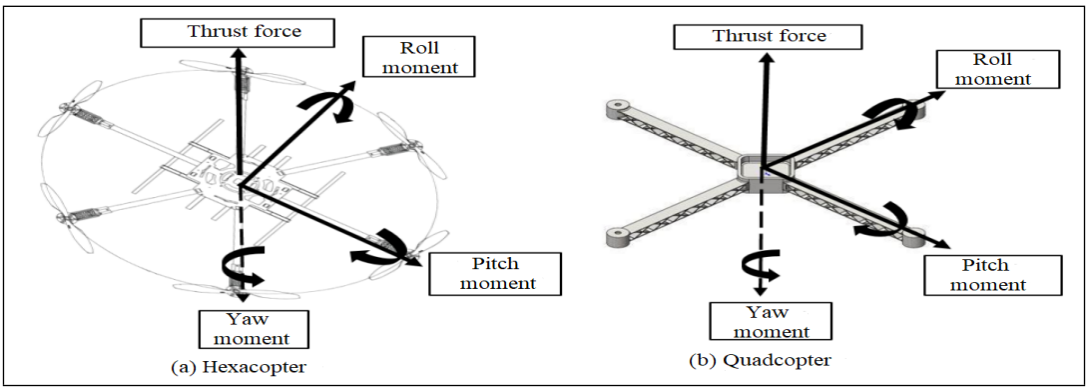

Figure 1.5: Two highly recognized multicopter models.

a fixed-wing aircraft [10] see Figure 1.6(a). With this configuration, the characteristics of a fixed-wing aircraft are combined with those of a helicopter. On the other hand, Figure 1.6(b) shows a combination of a quadcopter with a fixed-wing aircraft and a helicopter [7] [11].

(a) Combined helicopter

(b) Tiltrotor UAV

Figure 1.6: combination of The three models of unmanned aerial vehicles

1.3 Historical Overview of multicopters

In the previous section, the reason why people choose multicopters was discussed. However, another question is commonly asked: Why are multicopters more popular today?
The answer can be derived from the history of technological development in multicopters. In general, it can be divided into five periods as shown in Figure 1.7 below:

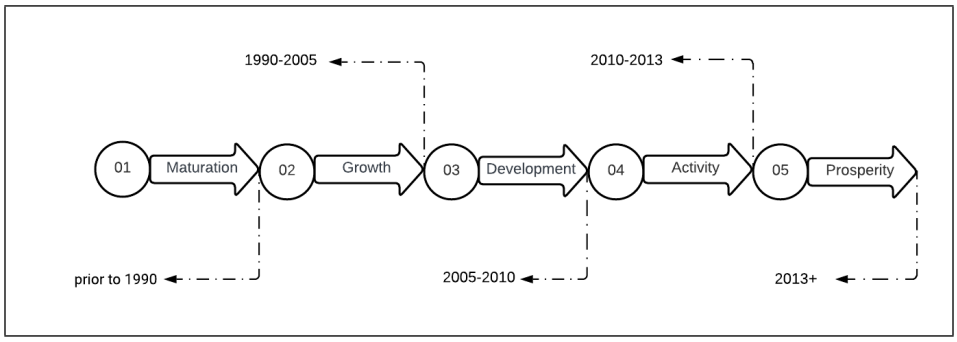

Figure 1.7: Diagram illustrating the technological evolution of multicopters.

1.3.1 The Maturation Period (pre-1990)

Since the beginning of 1907 in France, the Breguet brothers built their first multicopter, which was a quadcopter type Figure 1.8 called the Breguet-Richet Gyroplane. It was capable of carrying a payload equivalent to the weight of a human, as shown in Figure 1.9. During the initial test, the aircraft rose to approximately 60 cm. With modifications, it achieved 150 cm, and similar heights were reached in several subsequent trials. However, the Breguet-Richet aircraft was neither controllable nor maneuverable, so it was only capable of vertical takeoff and landing [12].

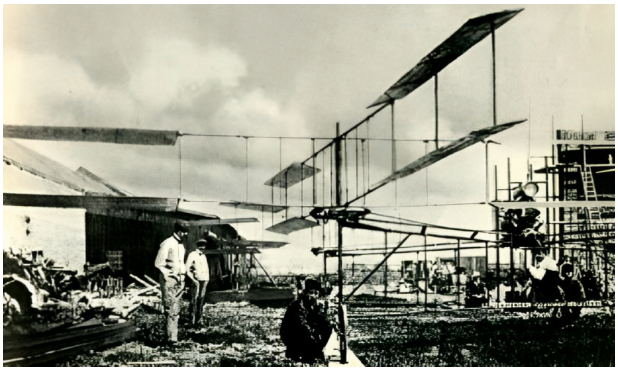

Figure 1.8: Gyroplane Breguet-Richet in flight.

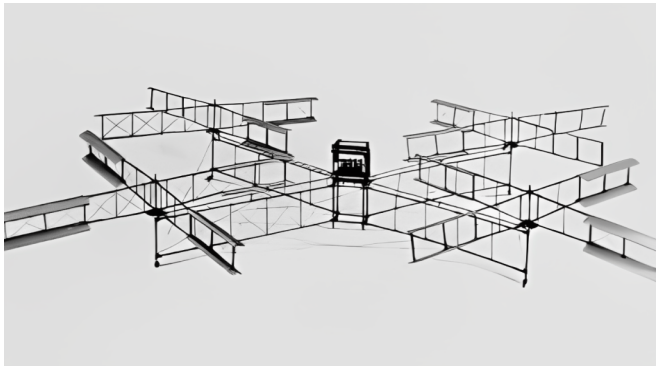

Figure 1.9: Gyroplane Breguet-Richet No. 1.

In 1920, Etienne Oehmichen, an employee of the French automobile company Peugeot, built a four-rotor machine [7]. His first model failed to take off from the ground. However, after some modifications, his second aircraft, Oehmichen No. 2, depicted in Figure 1.10, set a world record by staying in the air for up to 14 minutes, albeit at an altitude of only five meters.
These early models suffered from poor engine performance and could only reach a few meters in height. Little improvement was made to quadcopter design in the following three decades.

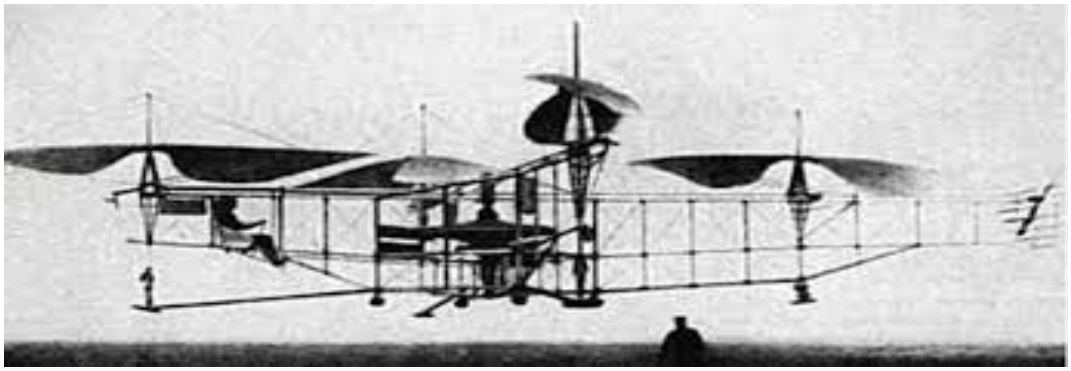

Figure 1.10: Oehmichen Model No. 2.

It was not until the mid-1950s that the first true quadcopter took flight, designed by Marc Adman Kaplan [12]. His quadcopter model, Convertawings Model "A" depicted in Figure 1.11, made its first flight in 1956 and proved to be a great success.

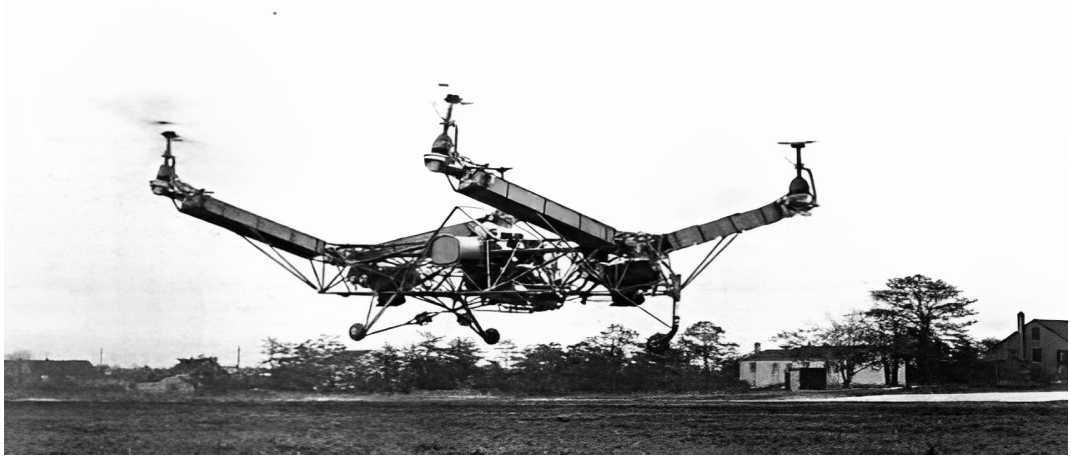

Figure 1.11: The Convertawings Model "A".

In 1957, the U.S. Army entered into a contract with Curtiss-Wright Corporation to develop a prototype of a vertical takeoff and landing aircraft (VZ-7) for transporting soldiers and supplies curtiss-Wright manufactured two VZ-7 prototypes in 1958 that were capable of easily performing hover flights and maneuvers, as shown in Figure 1.12. However, they were unable to meet the altitude and speed requirements specified in the contract [13], [14].
Before 1990, the electrical components of multicopters such as motors and sensors were bulky and expensive. Moreover, their performance was significantly lower compared to helicopters. As a result, multicopters were almost abandoned during this period. Over the next 30 years, there were not many improvements, and this type of aircraft received little attention.

1.3.2 The Growth Period (1990 - 2005)

Starting in the 1990s, researchers began developing micro-electromechanical systems (MEMS) and inertial measurement units (IMUs) weighing just a few grams. However, their use was initially limited due to issues related to additive and multiplicative noise. As a result, the measurements taken by these systems could only be effectively utilized after the introduction of algorithms designed to eliminate such noise [15].

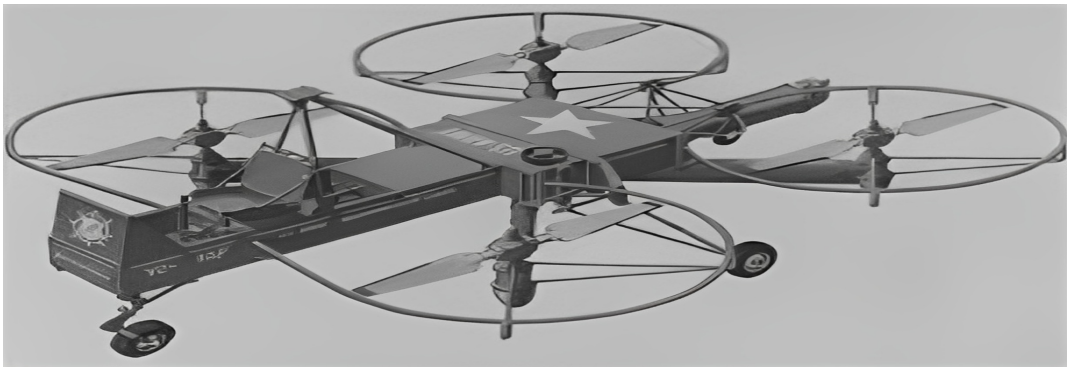

Figure 1.12: The Curtiss-Wright VZ-7 prototype.

The design of a multicopter requires not only algorithms but also microcomputers on which these algorithms can run. At this stage, the processing speed of microcomputers, such as single-chip microcomputers (SCMs) and digital signal processors (DSPs), has significantly improved. This advancement has encouraged researchers to develop models and design control algorithms [15],[16].

In the early 1990s, multicopters began to move away from the military domain and entered the civilian market. For example, the mini quadcopter (Keyence Gyrosaucer, Figure 1.13(a)) was commercialized in Japan [17]. This could be considered as the first generation of mini multicopters.

On the other side, in the United States, engineer Mike Dammar developed his own quadcopter powered by two rechargeable batteries. In 1999, he launched his aircraft under the name Roswell Flyer (Figure 1.13b), which was later adopted by the company Draganfly [18]. From this company, a series of multicopters were commercialized in 2002, such as the fixed-wing Tongo2 (Figure 1.13c), capable of flying for 90 minutes with two batteries, and the quadcopter X4-P.

(a) Keyence Gyrosaucer

(b) Roswell Flyer

(c) Tongo2

Figure 1.13: Drones developed during the growth period.

1.3.3 The Development Period (2005-2010)

This period is characterized by a sharp increase in scientific articles and global publications in the field of avionics related to multicopters, as shown in Figure 1.14.

Although a researcher's work on algorithms primarily encompasses the theoretical aspects, it was not easy for them to practically construct a real multicopter during this period, as e-commerce was not as popular as it is today. To address this issue, Jonathan P. How's team at the Massachusetts Institute of

Technology (MIT) created a real-time indoor testbed environment for reliable commercial autonomous vehicles, catering to the needs of the markets at that time [19].
In October 2005, Udo Juerss, Jan Wendel, and Daniel Schübeler founded Microdrones, and in April 2006, they began production of the md4-200, as shown in Figure 1.15(a). More than 250 units were sold in a short period of time.

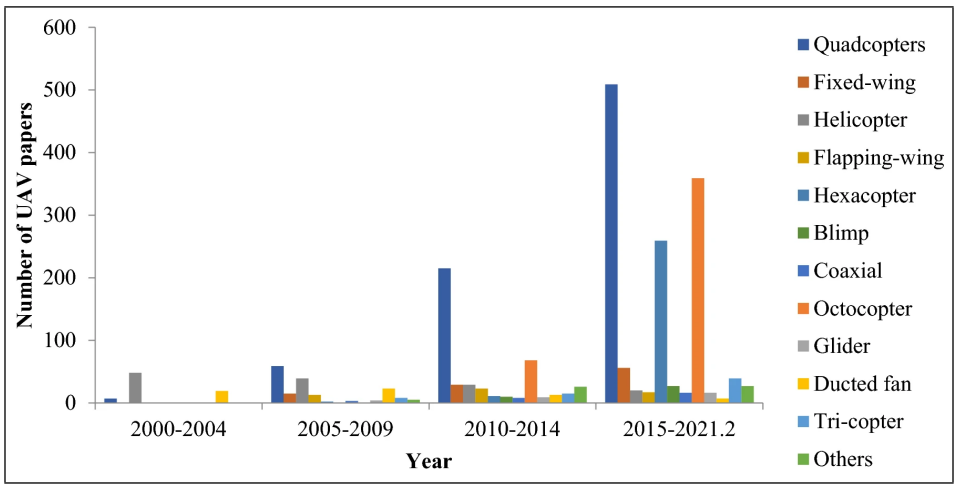

Figure 1.14: Number of publications related to multicopters.[1]

Four years later, the same company launched the md4-1000 Figure 1.15(b), which became the first drone to cross the Alps, covering a total distance of 12 kilometers [20]. Spectators were particularly impressed by the fact that the md4-1000 flew in GPS mode with well-defined waypoints to accomplish this mission, making the flight route fully automated.

(a) md4-200

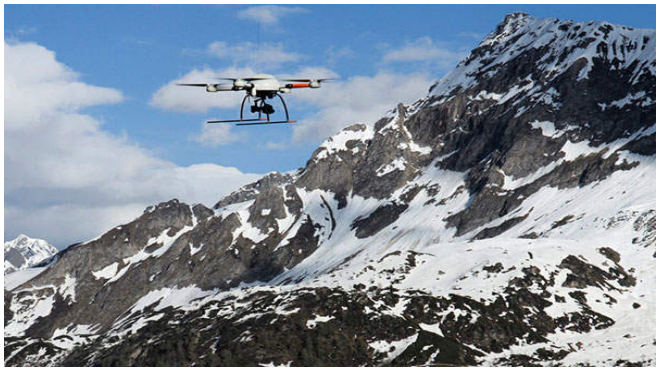

(b) md4-1000

Figure 1.15: Two drones from the company Microdrones.

1.3.4 The Activity Period (2010-2013)

In February 2012, Vijay Kumar from the University of Pennsylvania delivered a speech at the TED conference titled ”ideas worth spreading.” During his presentation, several videos showcased fleets of micro flying robots performing complex maneuvers and working together on tasks. This conference highlighted the immense potential of multicopters [21].

During this period, several open-source autopilot boards emerged for multicopters, which reduced their development costs. Table 1.2 presents major projects and their corresponding links.

Autopilot	**Website**
Ardupilot	http://ardupilot.com
Paparazzi	http://paparazziuav.org
Pixhawk	http://pixhawk.ethz.ch
Multiwii	http://multiwii.com
Parrot API (SDK)	http://projects.ardrone.org

Table 1.2: Open-Source Autopilot Systems

Some companies that previously focused solely on developing autopilots for multicopters also began designing ready-to-fly multicopter drones. For example, at the end of 2013, the Chinese company DJI specialized in the manufacturing of recreational drones. DJI introduced the "MATRICE 600 PRO" Hexacopter [9] to the market, which was ready to fly and had the specifications shown in Table 1.3 .

Specification	**Value**
Total Weight	9.5 kg (with six Li-Po batteries)
Maximum Speed	40 m/s
Autonomy	32 minutes
Obstacle Detection	Five directions
Battery	5700 mAh LiPo 6S
Stabilization	3-axis (Roll-Pitch-Yaw)

Table 1.3: Drone Specifications

On the other hand, the French company "AR. Drone" released the Parrot drone equipped with a front-facing camera, with the images being transmitted to a smartphone screen. The Parrot drone can be controlled using a smartphone or tablet. The pilot can see on their screen what the drone's camera sees, as if they were in the cockpit. The technical specifications of this drone are shown in Table 1.4 .

Specification	**Value**
Total Weight	420 g
Maximum Speed	12 m/s
Autonomy	12 minutes
Obstacle Detection	No obstacle avoidance module
Battery	1000 mAh LiPo 3S
Stabilization	3-axis (Roll-Pitch-Yaw)

Table 1.4: Drone Specifications

1.3.5 The period of prosperity (+2013)

In recent years, researchers working on multicopters have been striving to make them more autonomous and cooperative. By adding modules of artificial intelligence based on deep learning, multicopters have

become capable of playing with a ball, making decisions, handling faults, and delivering products (Amazon Project [22]).

In June 2015, a special edition of the journal "Nature" titled "Science, technology and the future of small autonomous drones" [23] was dedicated to the intelligence of machines. This publication summarizes the challenges in design and manufacturing, detection and control, as well as future research trends in the field of micro drones. Figure 1.16 shows an estimation based on two platforms, "Engineering Village" and "Web of Science," of the number of articles related to the development of multicopters worldwide from January 1990 to December 2015. It can be observed that the number of publications reached its peak in 2013. These preliminary research efforts laid a solid foundation for the development of the multicopter industry.

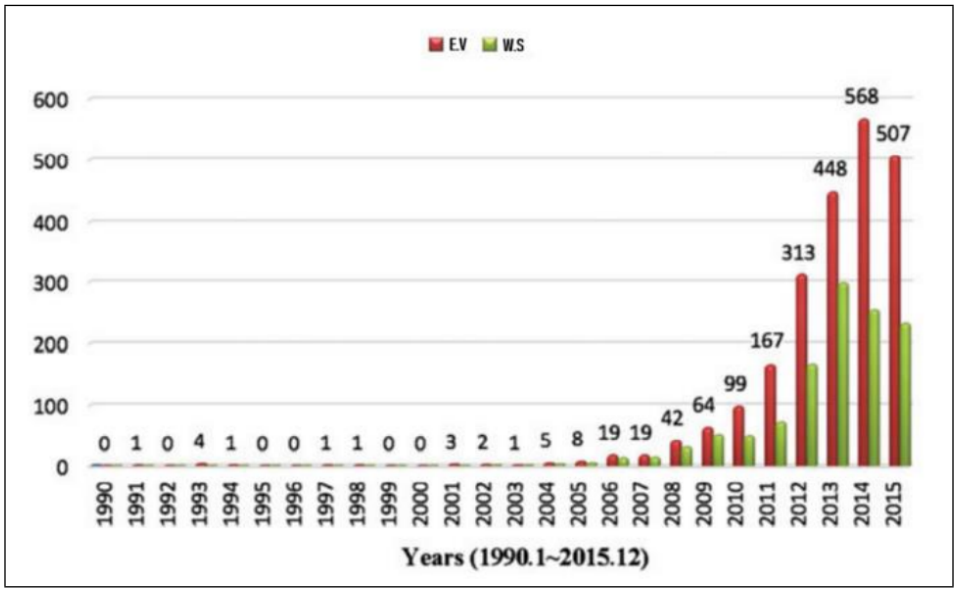

Figure 1.16: Estimation of the number of articles related to multicopters.

In late 2013, a video was released indicating that Amazon was aiming to deliver small packages to customers homes in just thirty minutes through "Prime Air," which is a delivery project involving only Hexacopter and Octorotor type multicopters [22] see Figure 1.(17).

In December 2016, Jeff Bezos, the CEO of Amazon, announced that the drone delivery service "Prime Air" had been successfully tested in Cambridge, UK, by delivering a TV streaming stick and a bag of popcorn directly to the backyard of a nearby customer.

Table 1.5 presents some of the multicopters that were developed between 2013 and September 2015.

In the war in Ukraine, multicopters, or drones, have been extensively used by both Ukrainian forces and separatist groups in the eastern regions of Donetsk and Luhansk. These drones have played various roles, including reconnaissance and intelligence gathering, targeting and artillery spotting, and even aerial attacks. They have provided valuable real-time information, enhanced artillery accuracy, and allowed for precision strikes. Counter-drone measures have been developed, but the use of smaller drones and tactics like swarm attacks have posed challenges. Foreign involvement and the supply of advanced drone technology have further escalated the drone warfare aspect of the conflict. Multicopters will likely continue to play a significant role as the conflict progresses, shaping the nature of warfare in the region.

1.3.6 Conclusion

From the historical development of multicopters, three conclusions can be drawn:

Figure 1.17: Prime Air delivery octocopter.

The multicopter is an old product that dates back 100 years, while small multicopters have been around for over 25 years. The development of multicopters has involved research in the areas of sensors, motors, and batteries and open-source autopilot boards that enable rapid improvement of guidance, navigation, and control algorithms.
For users, ready-to-fly multicopters are the future trend because they don't need to worry about assembly, parameter tuning, and improvement of algorithms embedded in multicopter autopilot boards.
The Hexacopter has not received as much research and development work compared to the quadcopter.

1.4 Evaluation of multicopter Performance

The evaluation of multicopter performance can be conducted based on the following five commonly used factors in the literature [7].

1.4.1 Ease of use

From a user's point of view, the ease of hovering or performing maneuvers with a drone is a highly interesting criterion.

1.4.2 Reliability

Reliability is often quantified as the mean time between failures. As drones integrate into our airspace, the need for improved reliability becomes even more evident.

1.4.3 Ease of maintenance

The two main characteristics of ease of maintenance are troubleshooting ease (the ease of performing scheduled maintenance) and maintenance ease (the ease of restoring service after a failure).

Name	Company	Date	Country	Characteristics
AR.Drone 2.0	Parrot	12/2013	France	Extremely precise control. Automatic stabilization without GPS.
AirDog	Helico Aerospace industries	6/2014	Latvia	Foldable drone. Follows and points the camera towards the user.
Inspire 1	DJI	12/2014	China	Carries 2 batteries during flight. Designed for professional photography.
Solo	3D Robotics	4/2015	USA	Aerial photography.
Phantom 3	DJI	4/2015	China	Stabilized 4K camera. Maximum range of 2,000 meters. Visual positioning system.
Micro Drone 3.0	Extreme Fliers	9/2015	UK	Small and intelligent. Real-time transmission of footage.
Feibot	Feibot	9/2015	China	Drone controller based on a smartphone.

Table 1.5: Commercialized drones from 2013 to 2015.

1.4.4 Autonomy

The autonomy of a drone is one of the most important performance criteria. In order to fly the drone with the longest possible payload, most consumer drones are equipped with lithium polymer (Li-Po) batteries. Despite technological advancements, there is still room for improvement in the field of electrical autonomy.

1.4.5 Maximum payload weight

The payload is the difference between the maximum allowable mass of a vehicle and its empty weight. It can be a package for civilian applications or even a missile for military applications.

In principle, the combination of the five performance factors actually determines user satisfaction. The three types of aircraft mentioned in section 1.2.2 are taken as examples and analyzed as follows.

Ease of use

The RC (Radio Control) of a multicopter is the simplest to use. As shown in Figure 1.18, the two sticks of an RC transmitter correspond to the movements of forward/backward, leftward/rightward, upward/downward, and yaw, respectively. In general, an adult can understand and master the operation within a few hours.

Flying a fixed-wing aircraft requires a larger airspace as it cannot hover in the air. Remote pilots of fixed-wing models need to perform control actions more frequently. Learning the operation and control of helicopters and airplanes takes a lot of time as the movements are coupled. Based on the above analysis, the multicopter excels in terms of ease of use.

Reliability The multicopter exhibits high reliability in terms of its mechanical structure. Fixed-wing aircraft and helicopters both have rotating joints in their structures (e.g., ailerons, elevator control surfaces), which can experience varying degrees of mechanical wear. In contrast, multicopters do not have such joints in their structure, eliminating this potential issue. Therefore, once again, multicopters excel in

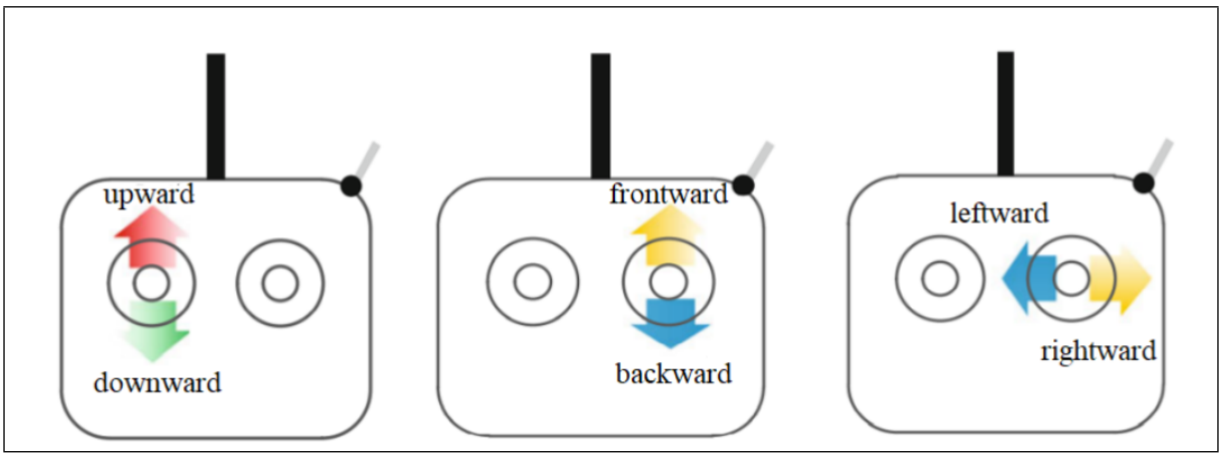

Figure 1.18: The movements performed by the arms of the Remote Controller.

terms of reliability.

Ease of maintenance multicopters are the easiest to maintain. They have a simple structure and can therefore be assembled with little effort. In contrast, airplanes and helicopters have more complex mechanical components and structures. Consequently, their assembly is not easy

Autonomy and payload These two criteria represent the weak point of multicopters, as their energy conversion efficiency is the lowest. Therefore, their flight time and payload capacity do not have any advantage compared to fixed-wing aircraft and helicopters.

A summary of their overall performance is presented in Table 1.6, where a "+" sign indicates a strong point.

According to Table 1.6, multicopters show remarkable advantages in terms of ease of use, reliability, and maintainability, while they have disadvantages in terms of endurance time and payload capacity.

Aspect	**Fixed-Wing**	**Helicopters**	**multicopters**
Ease of Use	++	+	+++
Reliability	++	+	+++
Maintenance	++	+	+++
Autonomy	+++	++	+
Payload Capacity	++	+++	+

Table 1.6: Comparison of Fixed-Wing, Helicopters, and multicopters

1.5 Bottleneck

The bottleneck in the development of multicopters lies in the inability to further push the existing compromise between the payload that can be carried and the size of the drone and its components. This challenge can be detailed as follows:

Firstly, as the radius of a propeller increases, the dynamic response becomes slower. On the other hand, helicopters increase or decrease lift by simultaneously changing the pitch angle of all blades equally, resulting in an ascent or descent behavior.

Secondly, the larger the radius of a propeller, the greater the fatigue in the center of the rotor due to propeller flapping effects. Propeller flapping refers to the continuous up-and-down motion of a rotor blade,

which occurs during the flight of multicopters as the motors rotate. The effects caused by propeller flapping are similar to repeatedly bending a flexible wire in one direction and then in the opposite direction. multicopters are typically equipped with lightweight plastic propellers with a fixed pitch, as excessively rigid propellers can transmit aerodynamic forces directly to the motor [24]. This can lead to mechanical failure of the motor or the frame itself.

Thirdly, the total load supported by the aircraft depends not only on the maximum torque of the motors but also on the aerodynamic characteristics of the propellers (such as the thrust and torque coefficients, radius, and pitch). Therefore, the bottleneck is primarily caused by the relationship between the payload and the propellers, which raises the issue of propeller flapping.

However, there is a hardware solution to increase the payload capacity supported by multicopters, which involves increasing the number of motors and using smaller propellers.

For example, the German company has designed a VC200 multicopter, shown in Figure 1.19, which can carry two passengers and achieve a flight endurance of over one hour. The trade-off is that the total weight of the aircraft has increased, and the endurance time is sacrificed. Additionally, since it has eighteen motors, the failure rate of a motor has increased [25]. However, there is a high level of redundancy in the control system. Through intelligent control algorithms, flight safety can be improved.

(a) VC-200 in flight

(b) VC-200 disassembled

Figure 1.19: The VC-200 transport UAV

1.6 Missions of multicopters

Most of the missions currently performed with manned aircraft can be carried out by drones. They allow for the execution of dangerous or repetitive missions at a lower cost and without risking the safety of a pilot. Furthermore, the miniaturization of these flying devices offers new possibilities that were not feasible with larger aircraft. Hexacopters, for example, have the ability to fly at low altitudes in urban areas or even inside buildings. Inspecting infrastructure, border surveillance, and photography are just a few examples of the applications of these flying devices. In this section, we will present some examples of their use in both civilian and military domains.

1.6.1 Civil Domain

Missions related to surveillance and security, which are typical in the military domain, can also be directly applicable to civil security. The Hexacopter can be used for traffic surveillance [26], maritime

surveillance, as well as fire detection [27]. In the field of audiovisual production, Hexacopters enable unique aerial shots for television programs and cinema.
Drones also find their place in the industry, especially Hexacopters, which with their motor redundancy, robustness, and stability, can perform missions that are difficult to achieve with manned aircraft. They are used, for example, for the inspection of infrastructure such as bridges, buildings, and wind turbines, as well as for the inspection of power lines or pipelines [28].
Hexacopters are also used for mapping missions. They can reconstruct high-resolution aerial images of the areas they fly over as well as a 3D model of the terrain [29]. This type of reconstruction is particularly useful, for example, for quarry operators or during archaeological excavations [30]. The use of multi-spectral cameras (visible, near-infrared, thermal) in agriculture is also common.
Drones are new diagnostic tools in emergency situations. For instance, during a flood or a fire, they can quickly map the affected area to assess the damages [30]. One example is the STaFF® system, a Tactical System for Forest Firefighting developed by the company Fly-n-Sense.

1.6.2 Military Domain

The search for intelligence on the adversary has always preceded and accompanied military actions. This imperative has taken new developments with the implementation of aerial capabilities. During the last conflicts of the 20th century, such as the American intervention in Vietnam, the Gulf War of 1991, or the fighting in Kosovo in 1999, air superiority was a decisive element in military operations. Similarly, the role of aviation was crucial in the recent Iraqi conflict and even in the 2022 Ukraine war. As an example, the combat Hexacopter drone ”I9” is capable of identifying targets using artificial intelligence and engaging them with a shotgun. Indeed, their missions are numerous, including: Observation and Surveillance; Communication relay; Bombing.

1.7 Challenges of Hexacopters

1.7.1 Endurance

The batteries used by UAVs are heavy and discharge quickly. Gasoline engines, on the other hand, are noisy and emit combustion gases. One of the proposed solutions to address this challenge is to use a fuel cell (hydrogen). Drones powered by a hydrogen fuel cell can fly farther and up to three times longer than Li-Po battery-powered aircraft of similar size [31]. They operate silently, emit only water vapor, and can be quickly recharged. For example, in 2018, the French company ”HEXADRONE” launched the ”HYCOPTER” UAV on the market, powered by 6 electric motors fueled by an ultralight hydrogen fuel cell from ”HES Energy Systems,” with a flight endurance of 3.5 hours [32] Figure 1.20.

1.7.2 Motion and Obstacle Detection

Flight of Hexacopters in urban environments poses a challenge when performing tasks such as aerial photography or package delivery. Without the aid of human eyes, the Hexacopter must navigate on its own. To do so, it needs to be equipped with visual sensing capabilities (e.g., camera, ultrasonic sensor, or LIDAR) that enable the detection of obstacles and external motion [33]. With the help of control algorithms, the Hexacopter becomes capable of avoiding obstacles and even performing online trajectory planning.

Figure 1.20: UAV HYCOPTER with a hydrogen fuel cell.

Among the technological solutions, there is the LIDAR (IntuVue RDR-84K Radar, as of September 2020) by Honeywell, which uses multiple beams to detect multiple objects simultaneously.
Figure 1.21(a) shows this device, and Figure 1.21(b) shows that it can be mounted on a Hexacopter. In addition to weather detection, the system can simultaneously scan and receive radar echoes from aircraft, ground vehicles, buildings, and even people.

(a) IntuVue RDR-84K device

(b) IntuVue RDR-84K mounted on a hexacopter

Figure 1.21: Radar detection system onboard a hexacopter drone.

1.7.3 Localization

Localization is a crucial task for aircraft navigation. It is performed by measurement instruments such as GPS, which provides the drone's position during flight. However, its use requires specific conditions (outdoor, good weather conditions). To overcome this problem, a technological solution is to use an inertial measurement unit (IMU). This unit contains a set of electronic components (Magnetometer, Gyroscope, and Accelerometer) all integrated into a single electronic chip to provide accurate information to the navigation system [34]. With an onboard IMU, the Hexacopter can determine its position, direction, and velocity.

1.7.4 Communication and Information Security

In December 2011, the American stealth drone RQ-170 Sentinel, shown on Iranian state television Figure 1.22(a), was captured by hacking its GPS coordinates, causing it to land in Iranian territory instead of its intended location. According to Iranian engineers, the technique used allowed the aircraft to land without hacking the remote control signals and communications between the American control center and the UAV. A document (PDF) presented in October 2012 at a conference in Chicago [35] [36] on flight security delved into GPS spoofing attacks, exposing the elements necessary for "seamless takeover" of drones and other aerial vehicles. Two years later, during a ceremony held in Tehran on May 11, 2013, Iran showcased an RQ-170 drone Figure 1.22(b) that was manufactured through reverse engineering based on the captured American Sentinel drone from December 2011.

(a) American stealth drone RQ-170 Sentinel.

(b) Iranian copy of RQ-170.

Figure 1.22: The RQ-170 drone.

1.7.5 Open-source/Closed-source Autopilot

The onboard autopilot board in the Hexacopter can be either open-source or closed-source, and this poses a challenge for developers who focus on implementing different navigation, guidance, and control techniques. Table 1.7 below presents some projects of autopilot boards. In general, an open-source system is one in which the source code is visible and modifiable, whereas a closed-source autopilot has restricted access. In the market, commercially available drones typically use closed-source autopilot boards, while open-source autopilot boards are sold for research and development purposes.

Open Source	**Closed Source**
Drone Paparazzi	NAZA M V2
ArduPilot	Freefly Alta 8
Dronecode	Parrot ANAFI
LibrePilot	WingtraOne Gen II

Table 1.7: Open Source vs Closed Source

1.7.6 Mechanical Structure and Propulsion System

The performance of Hexacopters is closely related to their propulsion system and mechanical structure. This challenge has become one of the most important areas of research and development in aviation [37],

[38]. It should be noted that multicopters have three types of propulsion systems, namely fuel-based, hybrid (fuel-electric), and pure electric. Additionally, there are several possible mechanical structures such as hexacopters, quadcopters, tricopters, and so on.

1.8 Conclusion

In this chapter, we began by providing definitions related to UAS (Unmanned Aircraft Systems). We then presented a brief history of multicopter development. Following that, we established criteria for evaluating the performance of multicopters. Finally, we explored the various applications of drones and the missions that can be assigned to them, including specific applications for Hexacopters.
In addition to the simplicity of design of multicopters, Hexacopters offer additional advantages compared to other multicopters, such as increased flight stability, motor redundancy, and payload capacity.
The next chapter presents the modeling of the Hexacopter drone, taking into consideration its flight mechanics and working assumptions.

Chapter 2

Modeling of the Hexacopter

2.1 Introduction

Mathematical modeling provides a representation of the system's evolution over time based on the inputs it receives. In the case of the Hexacopter, the mathematical model is used to predict the position and orientation of the drone over time based on the inputs, which are the voltages provided to the six motors. The Hexacopter model can then be utilized to develop control laws.
The modeling of the Hexacopter shown in Figure 2.1 can be broken down by modeling each subsystem separately, which will be developed in this chapter.

2.2 Principle of operation of the Hexacopter

The Hexacopter is a vertical take-off and landing (VTOL) UAV. It consists of six rotors with their propellers and can perform all six degrees of freedom in space, namely three rotations (roll, pitch, and yaw) and three translations (along the three axes). This description applies to the specific project object, which is an "X"-configured Hexacopter drone. Generally, the motion of the Hexacopter is controlled by the four channels (ch1...ch4) of the Radio Control.

2.2.1 Vertical Movement

Vertical movement corresponds to ascending or descending. It can be achieved by having equal speeds for all six motors to cancel out the gyroscopic torque generated. Ascending corresponds to a resultant thrust force greater than the weight of the Hexacopter, and vice versa for descending. Figure 2.2(a) shows the direction of rotation for each rotor.

2.2.2 Roll movement and lateral displacement along the axis

The roll movement is achieved by applying a torque around the longitudinal axis of the drone. This is accomplished by having a difference in thrust resulting from the rotation of the motors on the two sides of the axis. The roll movement is accompanied by lateral displacement along the axis. Figure 2.2(b) shows the selected motors to perform these two movements.

2.2.3 Pitch movement and longitudinal displacement

The pitch movement is achieved by applying a torque around the lateral axis of the vehicle. This is accomplished by creating a difference in thrust on either side of the axis. In the case of an X configuration Hexacopter, it should be noted that there are two rotors on the lateral axis that do not contribute to the pitch movement. The pitch movement is accompanied by a longitudinal displacement. Figure 2.2(c) shows the direction of rotation and the motors used to perform pitch movement and longitudinal displacement.

2.2.4 Yaw movement

The yaw movement involves rotating the drone around its vertical axis. This is achieved by the effect of the drag forces generated by the propellers. The sum of the speeds of the rotors rotating in the same direction must be different from the sum of the speeds of the rotors rotating in the opposite direction, as shown in Figure 2.2(d).

2.3 General Description of the Modeling

The modeling of the drone mainly consists of four parts [7]:

2.3.1 Kinematic model of a rigid body

Kinematics is independent of mass and force. It only studies variables such as position, velocity, attitude, and angular velocity. For the kinematic model of the Hexacopter, the inputs are velocity and angular velocity, and the outputs are position and attitude.

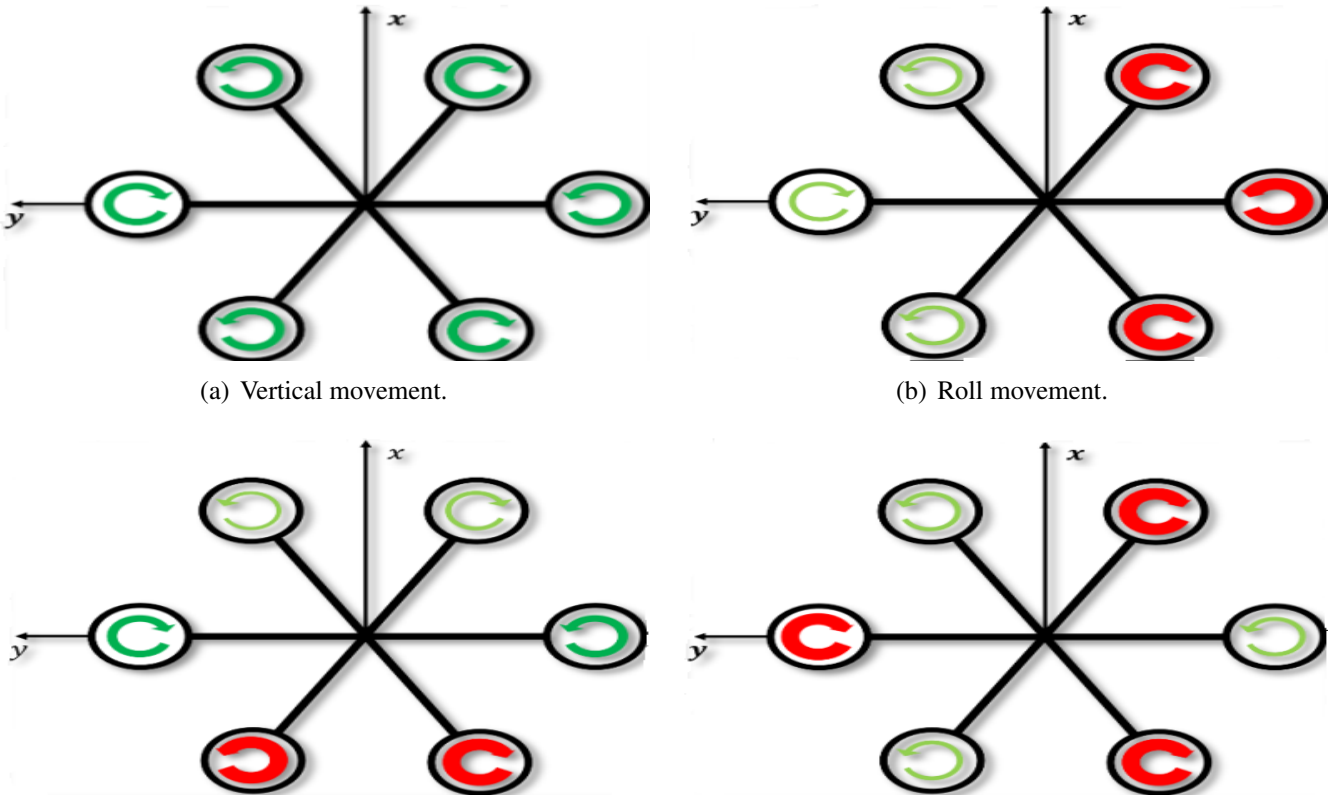

(a) Vertical movement. (b) Roll movement.

(c) Pitch movement. (d) Yaw movement.

Figure 2.1: Configurations used to achieve the six degrees of freedom.

2.3.2 The dynamic model of a rigid body

Dynamics involves both motion and force, and they are related to the mass and moments of inertia of the object. Equations such as Newton's second law, the kinetic energy equation, and the momentum equation are often used to study the mutual effect between different objects. For the dynamic model of the Hexacopter, the inputs are the thrust and moments (roll moment, pitch moment, and yaw moment), and the outputs are linear velocity and angular velocity. The kinematic model of the rigid body and the dynamic model together form the general rigid model for drone flight control.

2.3.3 Control efficiency model

The inputs are the angular velocities of the propellers, and the outputs are the thrust and moments. For multicopters, the thrust and moments are all generated by the propellers. Given the angular velocities of the propellers, the thrust and moments can be calculated using the control efficiency model. When the thrust and moments are obtained through controller design, the angular velocities of the propellers can be calculated using the control allocation model.

2.3.4 Propeller model

The propeller model is a complete power mechanism that includes a brushless direct current (BLDC) motor, an electronic speed controller (ESC), and a propeller. The input is a throttle command ranging from 0 to 1, and the outputs are the angular velocities of the propellers. In practice, a model with the throttle command as the input and the propeller thrust as the output can also be established.

2.4 Modeling assumptions

For convenience, the following assumptions are made when modeling the Hexacopter [39]:

- The Hexacopter is a rigid body.
- The mass and moments of inertia are constant.
- The geometric center and the center of gravity of the drone coincide.
- The thrust produced by the propellers is always perpendicular to the plane of the frame.
- The lift and drag force of a rotor are proportional to the square of its rotational speed.
- The rotors and propellers are identical.

2.5 Definition of reference frames

A preliminary step in developing the equations of motion for a system is the definition of reference frames. UAVs are typically defined in spatial orientation using two reference systems, as shown in Figure 2.3, and defined as follows [40]:
The Earth frame R_E is chosen as the inertial reference frame. The x_E axis points towards the North, the y_E axis points towards the West, the z_E axis points upwards relative to the Earth, and O_E is the origin of the frame. In this frame, the position $[x, y, z]^T$ and the attitude (roll, pitch, yaw) $[\Phi, \theta, \Psi]^T$ describe its linear and angular positioning [41].
The reference frame of the mobile R_B (body frame) is fixed to the body, its origin coincides with the center of gravity of the UAV. The x_B axis points forward of the Hexacopter, y_B points to its left. The rotor axes point in the positive direction of z_B. The vectors of the mobile frame describing the state of the drone are generally represented as follows: the translational velocities $[u, v, w]^T$ and the rotational velocities $[p, q, r]^T$ [40].

2.6 Modeling of the Hexacopter

The complete modeling of the Hexacopter will focus on the four parts already mentioned in this chapter, namely:
The kinematic model. The dynamic model. The control efficiency model. The rotor model.

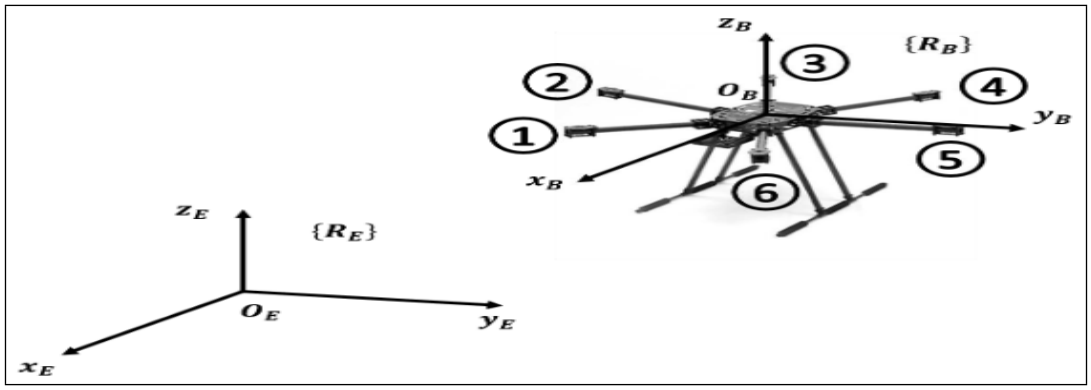

Figure 2.2: The two main frames.

The diagram in Figure 2.4 illustrates the complete model of the Hexacopter, which we will further analyze in the following sections.

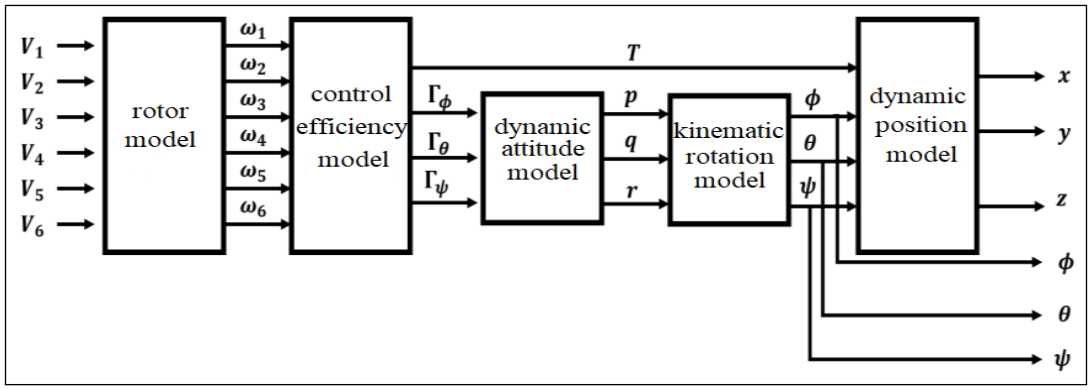

Figure 2.3: Block diagram presenting the complete model of the hexacopter.

2.6.1 Kinematic Modeling

Kinematics is a branch of mechanics that studies the motion of a body or a system of bodies without considering the forces and torques acting on it. To describe the motion of a rigid body with six degrees of freedom, we exploit the relationship between the two previously defined frames: the Earth frame and the body frame.
The relationship between the Earth frame and the frame attached to the drone can be illustrated by Figure 2.5.
The homogeneous transformation matrix R_{EB} is expressed as follows:

$$R_{EB} = Rotz(\psi) \times Roty(\theta) \times Rotx(\phi) \tag{2.1}$$

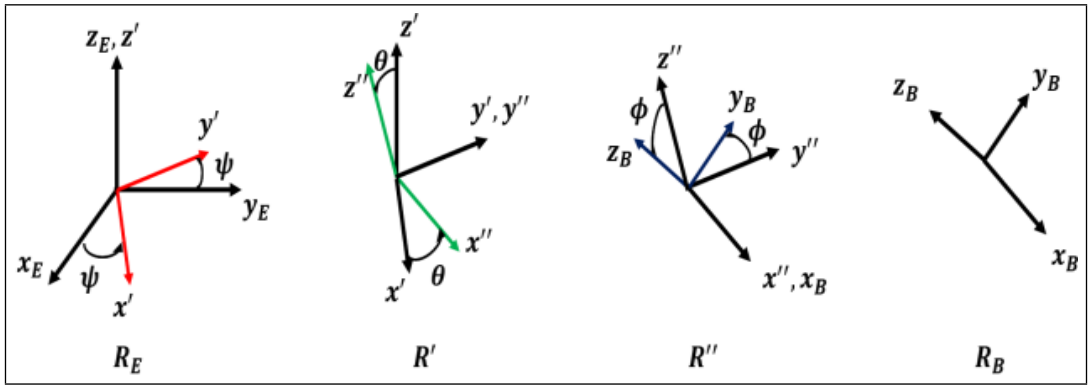

Figure 2.4: Transformation from the Earth frame to the body frame.

Where the matrices $Rot_x(\phi)$, $Rot_y(\theta)$, and $Rot_z(\psi)$ represent the transformation matrices for rotation around the x, y, and z axes, respectively.

$$Rotx(\phi) = \begin{pmatrix} 1 & 0 & 0 \\ 0 & \cos(\phi) & \sin(\phi) \\ 0 & -\sin(\phi) & \cos(\phi) \end{pmatrix} Roty(\theta) = \begin{pmatrix} \cos(\theta) & 0 & -\sin(\theta) \\ 0 & 1 & 0 \\ \sin(\theta) & 0 & \cos(\theta) \end{pmatrix}$$
$$Rotz(\psi) = \begin{pmatrix} \cos(\psi) & \sin(\psi) & 0 \\ -\sin(\psi) & \cos(\psi) & 0 \\ 0 & 0 & 1 \end{pmatrix} \tag{2.2}$$

The homogeneous transformation matrix is written as:

$$R_{EB} = \begin{pmatrix} C_\psi C_\theta & S_\phi S_\theta C_\psi - C_\phi S_\psi & S_\psi S_\phi + C_\phi S_\theta C_\psi \\ C_\psi S_\theta & C_\phi C_\psi + S_\phi S_\theta S_\psi & C_\phi S_\theta S_\psi - S_\phi C_\psi \\ -S_\theta & C_\theta S_\phi & C_\phi C_\theta \end{pmatrix} \tag{2.3}$$

Where S and C represent short notation of sin and cosine trigonometric functions.

Rotational Kinematics

The relationship between the angular velocity of the Euler angles and those expressed in the R_B frame is established as follows:
The angular velocity vector Ω can be expressed as:

$$\Omega = \begin{pmatrix} p \\ q \\ r \end{pmatrix} = \begin{pmatrix} \dot{\phi} \\ 0 \\ 0 \end{pmatrix} + Rotx(\phi)^T \cdot \begin{pmatrix} 0 \\ \dot{\theta} \\ 0 \end{pmatrix} + Rotx(\phi)^T \cdot Roty(\theta)^T \cdot \begin{pmatrix} 0 \\ 0 \\ \dot{\psi} \end{pmatrix} \tag{2.4}$$

Therefore, we obtain:

$$\begin{pmatrix} p \\ q \\ r \end{pmatrix} = \begin{pmatrix} 1 & 0 & 0 \\ 0 & \cos\phi & \sin\phi\cos\theta \\ 0 & -\sin\phi & \cos\phi\cos\theta \end{pmatrix} \begin{pmatrix} \dot{\phi} \\ \dot{\theta} \\ \dot{\psi} \end{pmatrix} \tag{2.5}$$

The inverse relationship is given by:

$$\begin{pmatrix} \dot{\phi} \\ \dot{\theta} \\ \dot{\psi} \end{pmatrix} = \begin{pmatrix} 1 & 0 & 0 \\ 0 & \cos\phi & -\sin\phi \\ 0 & \dfrac{\sin\phi}{\cos\theta} & \dfrac{\cos\phi}{\cos\theta} \end{pmatrix} \begin{pmatrix} p \\ q \\ r \end{pmatrix} \tag{2.6}$$

with $\theta \neq \pm\dfrac{\pi}{2}$

Translation Kinematics

The relationship between the linear velocities of the drone's center of gravity expressed in the R_{EB} and R_{EB} frames can be established by the equation:

$$\begin{pmatrix} \dot{x} \\ \dot{y} \\ \dot{z} \end{pmatrix} = R_{EB} \begin{pmatrix} u \\ v \\ w \end{pmatrix} \tag{2.7}$$

2.6.2 Dynamic Modeling

Dynamic modeling of a physical system takes into account not only the motions but also the causes of these motions, including the forces and moments acting on it, based on the assumptions already established in this chapter.

Dynamic Position Model

The dynamic modeling of the translation of the Hexacopter begins by enumerating the set of forces acting on it. Using the Newton-Euler formalism, the equation governing the dynamics of the drone's position can be written as follows:

$$m\ddot{\xi} = F_f + F_t + F_g \tag{2.8}$$

With:

- m: The total mass of the Hexacopter.
- ξ: The position vector of the center of gravity of the Hexacopter.
- F_f: The resultant of the thrust forces generated by the six rotors.

$$F_f = \begin{pmatrix} 0 \\ 0 \\ T \end{pmatrix}_{R_B} \tag{2.9}$$

where T is the resultant of the thrust forces generated by the six propellers.

- F_t: The resultant of the drag forces.

$$F_t = \begin{pmatrix} -K_{ftx} & 0 & 0 \\ 0 & -K_{fty} & 0 \\ 0 & 0 & -K_{ftz} \end{pmatrix} \dot{\xi} = - \begin{pmatrix} K_{ftx}\dot{x} \\ K_{fty}\dot{y} \\ K_{ftz}\dot{z} \end{pmatrix}_{R_E} \tag{2.10}$$

where K_{ftx}, K_{fty}, and K_{ftz} represent the coefficients of the drag forces in the $\mathbf{R}_E$ frame.
F_g: The force of gravity.

$$F_g = \begin{pmatrix} 0 \\ 0 \\ -mg \end{pmatrix}_{R_E} \tag{2.11}$$

Where g is the acceleration due to gravity.
By expanding the Newton-Euler formalism of equation (2.8), we obtain the following:

$$m \begin{pmatrix} \ddot{x} \\ \ddot{y} \\ \ddot{z} \end{pmatrix} = R_{EB} \begin{pmatrix} 0 \\ 0 \\ T \end{pmatrix} + \begin{pmatrix} -K_{ftx}\dot{x} \\ -K_{fty}\dot{y} \\ -K_{ftz}\dot{z} \end{pmatrix} + \begin{pmatrix} 0 \\ 0 \\ -mg \end{pmatrix} \tag{2.12}$$

$$\begin{cases} \ddot{x} = \dfrac{T}{m}\left(\cos\phi \sin\theta \cos\psi + \sin\psi \sin\phi\right) - \dfrac{K_{ft_x}\dot{x}}{m} \\ \ddot{y} = \dfrac{T}{m}\left(\cos\phi \sin\theta \sin\psi - \cos\psi \sin\phi\right) - \dfrac{K_{ft_y}\dot{y}}{m} \\ \ddot{z} = \dfrac{T}{m}\cos\phi \cos\theta - \dfrac{K_{ft_z}\dot{z}}{m} - mg \end{cases} \tag{2.13}$$

Dynamic attitude Model

The dynamic modeling of the Hexacopter's attitude takes into account all the moments exerted on it. By using the Newton-Euler formalism, the equation governing the dynamics of the drone's attitude can be written as follows:

$$J\dot{\Omega} = -\Omega \wedge J\Omega + M_f - M_a - M_g \tag{2.14}$$

with J the symmetric inertia matrix of the Hexacopter given by:

$$J = \begin{pmatrix} I_{xx} & 0 & 0 \\ 0 & I_{yy} & 0 \\ 0 & 0 & I_{zz} \end{pmatrix} \tag{2.15}$$

M_f : The resultant moment of thrust and drag forces of the rotors around the center of gravity of the drone:

$$M_f = \begin{pmatrix} \Gamma_\phi \\ \Gamma_\theta \\ \Gamma_\psi \end{pmatrix} \tag{2.16}$$

Where Γ_φ, Γ_θ, and Γ_ψ are the roll, pitch, and yaw moments performed by the drone respectively.

$$M_a = \begin{pmatrix} K_{fa_x} & 0 & 0 \\ 0 & K_{fa_y} & 0 \\ 0 & 0 & K_{fa_z} \end{pmatrix} \Omega^2 \tag{2.17}$$

$$\Omega^2 = \begin{pmatrix} p^2 \\ q^2 \\ r^2 \end{pmatrix} \tag{2.18}$$

Where K_{fa_x}, K_{fa_y}, and K_{fa_z} represent the coefficients of aerodynamic friction and Ω^2 represent the element wise square of Ω

M_g : The resultant of the couples due to gyroscopic effects.

$$M_g = \sum_{i=1}^{6} \Omega \wedge J_r \begin{pmatrix} 0 \\ 0 \\ (-1)^{i+1}\omega_i \end{pmatrix} = \Omega \wedge \begin{pmatrix} 0 \\ 0 \\ J_r\varpi \end{pmatrix} \tag{2.19}$$

J_r : inertia of the rotors and

$$\varpi = \omega_1 - \omega_2 + \omega_3 - \omega_4 + \omega_5 - \omega_6 \tag{2.20}$$

By explicitly stating the equation governing the attitude dynamics of the Hexacopter in equation (2.14), we obtain:

$$\begin{pmatrix} I_{xx}\dot{p} \\ I_{yy}\dot{q} \\ I_{zz}\dot{r} \end{pmatrix} = - \begin{pmatrix} p \\ q \\ r \end{pmatrix} \wedge \begin{pmatrix} I_{xx}p \\ I_{yy}q \\ I_{zz}r \end{pmatrix} + \begin{pmatrix} \Gamma_\phi \\ \Gamma_\theta \\ \Gamma_\psi \end{pmatrix} - \begin{pmatrix} K_{fax}p^2 \\ K_{fay}q^2 \\ K_{faz}r^2 \end{pmatrix} - \begin{pmatrix} p \\ q \\ r \end{pmatrix} \wedge \begin{pmatrix} 0 \\ 0 \\ J_r\varpi \end{pmatrix} \tag{2.21}$$

This yields:

$$\begin{cases} \dot{p} = \dfrac{1}{I_{xx}}(qr(I_{yy} - I_{zz}) - K_{fax}p^2 - J_r\varpi q + \Gamma_\phi) \\ \dot{q} = \dfrac{1}{I_{yy}}\left(pr(I_{zz} - I_{xx}) - K_{fay}q^2 + -J_r\varpi p + \Gamma_\theta\right) \\ \dot{r} = \dfrac{1}{I_{zz}}\left(pq(I_{xx} - I_{yy}) - K_{faz}r^2 + \Gamma_\psi\right) \end{cases} \tag{2.22}$$

Finally, we obtain the dynamics of the attitude (Euler angles: roll ϕ, pitch θ, and yaw ψ) through the transformation matrix already established in equation (2.6)

$$\begin{pmatrix} \dot{\phi} \\ \dot{\theta} \\ \dot{\psi} \end{pmatrix} = \begin{pmatrix} 1 & 0 & 0 \\ 0 & \cos\phi & -\sin\phi \\ 0 & \dfrac{\sin\phi}{\cos\theta} & \dfrac{\cos\phi}{\cos\theta} \end{pmatrix} \begin{pmatrix} p \\ q \\ r \end{pmatrix} \tag{2.23}$$

with $\theta \neq \pm\dfrac{\pi}{2}$

2.6.3 Control Efficiency Model

The control efficiency model highlights the relationship between the rotation speeds of the propellers and the resulting efforts (forces and moments).

The thrust force T_i generated by propeller i is given by:

$$T_i = C_{Li}\omega_i^2 \tag{2.24}$$

where C_{L_i} is the lift coefficient of propeller i and ω_i is the rotor speed of propeller i.
The drag torque T_i of rotor i is given by:

$$\Gamma_i = C_{Di}\omega_i^2 \tag{2.25}$$

The drag coefficient C_{Di} of rotor i is the coefficient of drag torque of rotor i.
The Hexacopter's flight is driven by the six propellers. The angular velocities of the propellers i, where i = 1, ..., 6, determine the total thrust T and the moments Γ.
The total thrust acting on the Hexacopter is given by:

$$T = \sum_{i=1}^{6} T_i = \sum_{i=1}^{6} C_{Li}\omega_i^2 \tag{2.26}$$

Taking into consideration that the six propellers are identical $(C_{L1} = ... = C_{L6} = C_L)$, we obtain:

$$T = C_L \sum_{i=1}^{6} \omega_i^2 = C_L \left(\omega_1^2 + \omega_2^2 + \omega_3^2 + \omega_4^2 + \omega_5^2 + \omega_6^2\right) \tag{2.27}$$

For an X-configuration of a Hexacopter, the resulting moments from the thrust forces generated by the rotation of the propellers are obtained geometrically, as shown in Figure 2.6.

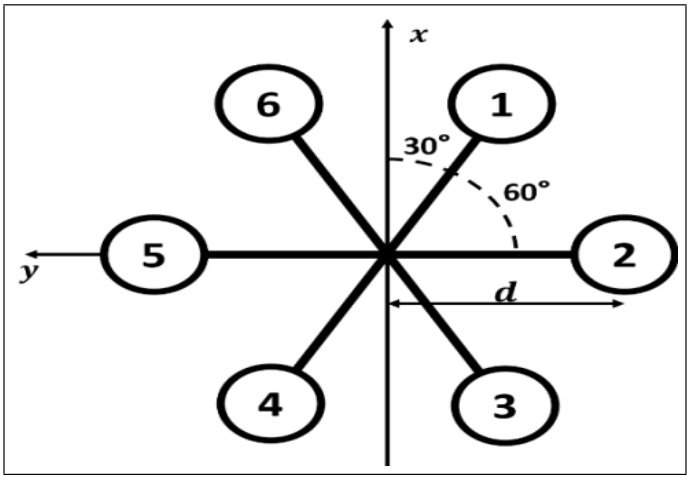

Figure 2.5: Geometric configuration of the rotors.

We therefore have:

$$\begin{aligned}
\Gamma_\phi &= d(-T_1 \sin\tfrac{\pi}{6} - T_2 - T_3 \sin\tfrac{\pi}{6} + T_4 \sin\tfrac{\pi}{6} + T_5 + T_6 \sin\tfrac{\pi}{6}) \\
&= dC_L(-\omega_1^2 \sin\tfrac{\pi}{6} - \omega_2^2 - \omega_3^2 \sin\tfrac{\pi}{6} + \omega_4^2 \sin\tfrac{\pi}{6} + \omega_5^2 + \omega_6^2 \sin\tfrac{\pi}{6}) \\
&= dC_L(-\tfrac{\omega_1^2}{2} - \omega_2^2 - \tfrac{\omega_3^2}{2} + \tfrac{\omega_4^2}{2} + \omega_5^2 + \tfrac{\omega_6^2}{2})
\end{aligned} \tag{2.28}$$

$$\begin{aligned}
\Gamma_\theta &= d(-T_1 \cos\tfrac{\pi}{6} + T_3 \cos\tfrac{\pi}{6} + T_4 \cos\tfrac{\pi}{6} - T_6 \cos\tfrac{\pi}{6}) \\
&= dC_L(-\omega_1^2 \cos\tfrac{\pi}{6} + \omega_3^2 \cos\tfrac{\pi}{6} + \omega_4^2 \cos\tfrac{\pi}{6} - \omega_6^2 \cos\tfrac{\pi}{6}) \\
&= \frac{dC_L\sqrt{3}}{2}(-\omega_1^2 + \omega_3^2 + \omega_4^2 - \omega_6^2)
\end{aligned} \tag{2.29}$$

$$\Gamma_\psi = C_D(-\omega_1^2 + \omega_2^2 - \omega_3^2 + \omega_4^2 - \omega_5^2 + \omega_6^2) \tag{2.30}$$

With d as the distance between the rotors and the center of gravity of the Hexacopter, all of the above can be rewritten in the form of a matrix called the "control efficiency matrix" as follows:

$$\begin{pmatrix} T \\ \Gamma_\phi \\ \Gamma_\theta \\ \Gamma_\psi \end{pmatrix} = \begin{pmatrix} C_L & C_L & C_L & C_L & C_L & C_L \\ -\frac{dC_L}{2} & -dC_L & -\frac{dC_L}{2} & \frac{dC_L}{2} & dC_L & \frac{dC_L}{2} \\ -\frac{dC_L\sqrt{3}}{2} & 0 & \frac{dC_L\sqrt{3}}{2} & \frac{dC_L\sqrt{3}}{2} & 0 & -\frac{dC_L\sqrt{3}}{2} \\ -C_D & C_D & -C_D & C_D & -C_D & C_D \end{pmatrix} \begin{pmatrix} \omega_1^2 \\ \omega_2^2 \\ \omega_3^2 \\ \omega_4^2 \\ \omega_5^2 \\ \omega_6^2 \end{pmatrix} \tag{2.31}$$

The inverse process of obtaining the propeller rotation speeds from the desired/produced forces is called "command allocation model." This relationship is utilized for the implementation of the flight controller. The flight performance of a multicopter vehicle heavily relies on the control allocation strategy used to map the control vector consisting of thrust and roll, pitch, and yaw moments to the propeller speeds [42] [43].

For a quadcopter drone, under normal circumstances, the command allocation matrix can be obtained by simply inverting the control efficiency matrix (a 4x4 matrix). However, for a Hexacopter UAV, the control efficiency matrix is not invertible (non-square), and the command allocation matrix cannot be directly obtained by inversion. Therefore, we resort to an approximation of the command allocation matrix, which can be obtained using various methods [44]. In our work, we used the method of pseudo-inverse for inversion.

Although the pseudo-inverse method is useful for obtaining the command allocation matrix, this strategy only exploits a limited range of the vehicle's capabilities to generate thrust and moments. To exploit a much wider range, another calculation method called "weighted pseudo-inverse" is proposed in the literature [45], [46]. There are also methods that use neural network-based learning to calculate the inverse with more precision. In our work, we used the "pseudo-inverse" inversion method.

2.6.4 Rotor Model

Generally, motors used in drones are either geared DC motors or brushless motors (BLDC) that drive the propellers. The rotor dynamics is approximated to that of a DC motor [41], and it is described by the following dynamic equations:

$$\begin{cases} V = ri + L\dfrac{di}{dt} + k_e\omega \\ k_m i = J_r\dfrac{d\omega}{dt} + Cs + k_r\omega^2 \end{cases} \tag{2.32}$$

With:

- V: The input voltage of the motor.
- ω: The angular velocity of the rotor.
- k_e, k_m: The electrical and mechanical torque constants, respectively.
- k_r: The load torque constant.
- r: The motor resistance.

- J_r: The rotor inertia.
- C_s: Represents the dry friction.

$$\dot{\omega} = \frac{k_m}{J_r}V - \frac{C_s}{J_r} - \frac{k_e k_m}{r J_r}\omega - \frac{k_r}{J_r}\omega^2 \tag{2.33}$$

2.7 Control Synthesis Model

Control of the Hexacopter can be achieved through different approaches, including model-based approaches. Model-based control approaches, as the name suggests, utilize the model for synthesizing the control law. However, using the full model to achieve the control objective may not be necessary and can be computationally expensive (in terms of computation time and memory usage). Therefore, we resort to simplified models, known as "synthesis models," for developing the control laws. The simplification is based on assumptions that are more or less valid during the system's evolution.
In the case of the Hexacopter, assuming that it performs small-amplitude angular movements, the angular velocity vector Ω expressed in the body frame R_B can be approximated as:

$$\Omega = \begin{pmatrix} p \\ q \\ r \end{pmatrix} \approx \begin{pmatrix} \dot{\phi} \\ \dot{\theta} \\ \dot{\psi} \end{pmatrix} \tag{2.34}$$

Considering the attitude control inputs as U_ϕ, U_θ, and U_ψ, representing the roll, pitch, and yaw torques, respectively, the synthesis model for attitude control is given by:

$$\begin{cases} \ddot{\phi} = \dfrac{1}{I_{xx}}[\dot{\theta}\dot{\psi}(I_{yy} - I_{zz}) - K_{fax}\dot{\phi}^2 - J_r\varpi\dot{\theta} + U_\phi] \\ \ddot{\theta} = \dfrac{1}{I_{yy}}[\dot{\phi}\dot{\psi}(I_{zz} - I_{xx}) - K_{fay}\dot{\theta}^2 + J_r\varpi\dot{\phi} + U_\theta] \\ \ddot{\psi} = \dfrac{1}{I_{zz}}[\dot{\phi}\dot{\theta}(I_{xx} - I_{yy}) - K_{faz}\dot{\psi}^2 + U_\psi] \end{cases} \tag{2.35}$$

Regarding the position control, the new model uses U_ϕ, U_θ, and U_ψ, as control inputs for position control in the x, y, and z directions, respectively. The synthesis model for position control is given by:

$$\begin{cases} \ddot{x} = \dfrac{T}{m}U_x - \dfrac{K_{ftx}}{m}\dot{x} \\ \ddot{y} = \dfrac{T}{m}U_y - \dfrac{K_{fty}}{m}\dot{y} \\ \ddot{z} = \dfrac{(\cos\phi\cos\theta)}{m}U_z - \dfrac{K_{ftz}}{m}\dot{z} - g \end{cases} \tag{2.36}$$

$$\begin{cases} U_x = \cos\phi\sin\theta\cos\psi + \sin\psi\sin\phi \\ U_y = \cos\phi\sin\theta\sin\psi - \cos\psi\sin\phi \end{cases} \tag{2.37}$$

The expressions for the desired roll angle (ϕ_d) and pitch angle (θ_d) based on equation (2.34) are:

$$\begin{cases} \phi_d = \sin^{-1}\left(U_x \sin\psi - U_y \cos\psi\right) \\ \theta_d = \sin^{-1}\left(\dfrac{U_x \cos\psi + U_y \sin\psi}{\cos\theta}\right) \end{cases} \tag{2.38}$$

2.8 Conclusion

This chapter presented a mathematical modeling approach for the Hexacopter drone. The system was modeled using subsystems kinematics of motion, dynamics of motion, control efficiency, and motor dynamics. We obtained the relationship between the motions position and orientation of the Hexacopter and the voltages provided to the six motors, which constitutes the complete model of the drone.

The Hexacopter model poses a major challenge for control due to a non-invertible control efficiency matrix and an inaccurate control allocation matrix.

In conclusion, we presented a reduced model of the Hexacopter that can be used in the synthesis of control laws using approaches or strategies based on the model.

Chapter 3

Control Techniques

3.1 Introduction

In this chapter, we present the control part of the hexacopter. Flying a hexacopter drone would be difficult without implementing a control law. This control law should allow for the calculation of the setpoint speed for each of the six motors to ensure the stability of the drone while following a position and/or attitude (orientation) reference. The objective of this chapter is to ensure that the hexacopter follows a predefined trajectory $(x_d(t), y_d(t), z_d(t), \psi_d(t))$ while remaining stable throughout its mission. To achieve this, three control approaches will be studied and synthesized: a PID controller as a classical technique, a non-linear Backstepping controller, and finally a sliding mode controller.
The simulation part concerns the implementation and validation of the three control. The objective of these controls is to perform two scenarios hovering and trajectory tracking, specifically the famous "circuit around the runway" test, which is well-known in the field of aviation. The simulation results using the three control techniques are obtained based on the parameters from [39] presented in Table 3.1.

Parameter	**Description**	**Value**
m	Total mass	0,65 kg
I_{xx}	Moment of inertia around x_B	7,5.10^{-3} kg.m^2
I_{yy}	Moment of inertia around y_B	7,5.10^{-3} kg.m^2
I_{zz}	Moment of inertia around z_B	1,3.10^{-2} kg.m^2
K_{ftx}	Drag coefficient along x_E	5,576.10^{-4} N/rad$^2/s^2$
K_{fty}	Drag coefficient along y_E	5,576.10^{-4} N/rad$^2/s^2$
K_{ftz}	Drag coefficient along z_E	6,354.10^{-4} N/rad$^2/s^2$
K_{fax}	Aerodynamic friction coefficient around x_B	5,576.10^{-4} N/rad$^2/s^2$
K_{fay}	Aerodynamic friction coefficient around y_B	5,576.10^{-4} N/rad$^2/s^2$
K_{faz}	Aerodynamic friction coefficient around z_B	6,354.10^{-4} N/rad$^2/s^2$
C_L	Lift coefficient	4,2.10^{-5} N/rad$^2/s^2$
C_D	Drag coefficient	$3,2320.10^{-7}$ N.m/ rad$^2/s^2$
d	Half wingspan	0,425 m
J_r	Motor inertia	6.10^{-5} kg.m^2
K_e	Electrical torque constant	0,0216 N.m/A
C_s	Dry friction	$5,3826.10^{-3}$ N
K_r	Load torque constant	$3,2320.10^{-7}$ N.m/ rad$^2/s^2$
K_m	Mechanical torque constant	0,65 kg
r	Motor resistance	0,6 Ω

Table 3.1: Simulation parameters

The aerodrome circuit navigation scenario is a maneuver performed by airplanes around the runway in a rectangular pattern, with left turns, and at a desired height above the aerodrome, which presents the challenge of the test we have set the mission duration to 100 seconds. The reference trajectory (Figure 3.1) is defined by the equations:

$$x_d(t) = \begin{cases} 0\,\text{m} & \text{for } t \in [0, 5) \\ 5\,\text{m} & \text{for } t \in [5, 25) \\ -7\,\text{m} & \text{for } t \in [25, 100] \end{cases}$$

$$y_d(t) = \begin{cases} 0\,\text{m} & \text{for } t \in [0, 15] \\ 5\,\text{m} & \text{for } t \in [15, 35] \\ -7\,\text{m} & \text{for } t \in [35, 100] \end{cases}$$

$$z_d(t) = \begin{cases} 5\,\text{m} & \text{for } t \in [0, 80] \\ 0\,\text{m} & \text{for } t \in [80, 100] \end{cases}$$

$$\psi_d(t) = \begin{cases} 0\,\text{rad} & \text{for } t \in [0, 60] \\ 1\,\text{rad} & \text{for } t \in [60, 70] \\ 0\,\text{rad} & \text{for } t \in [70, 100] \end{cases}$$

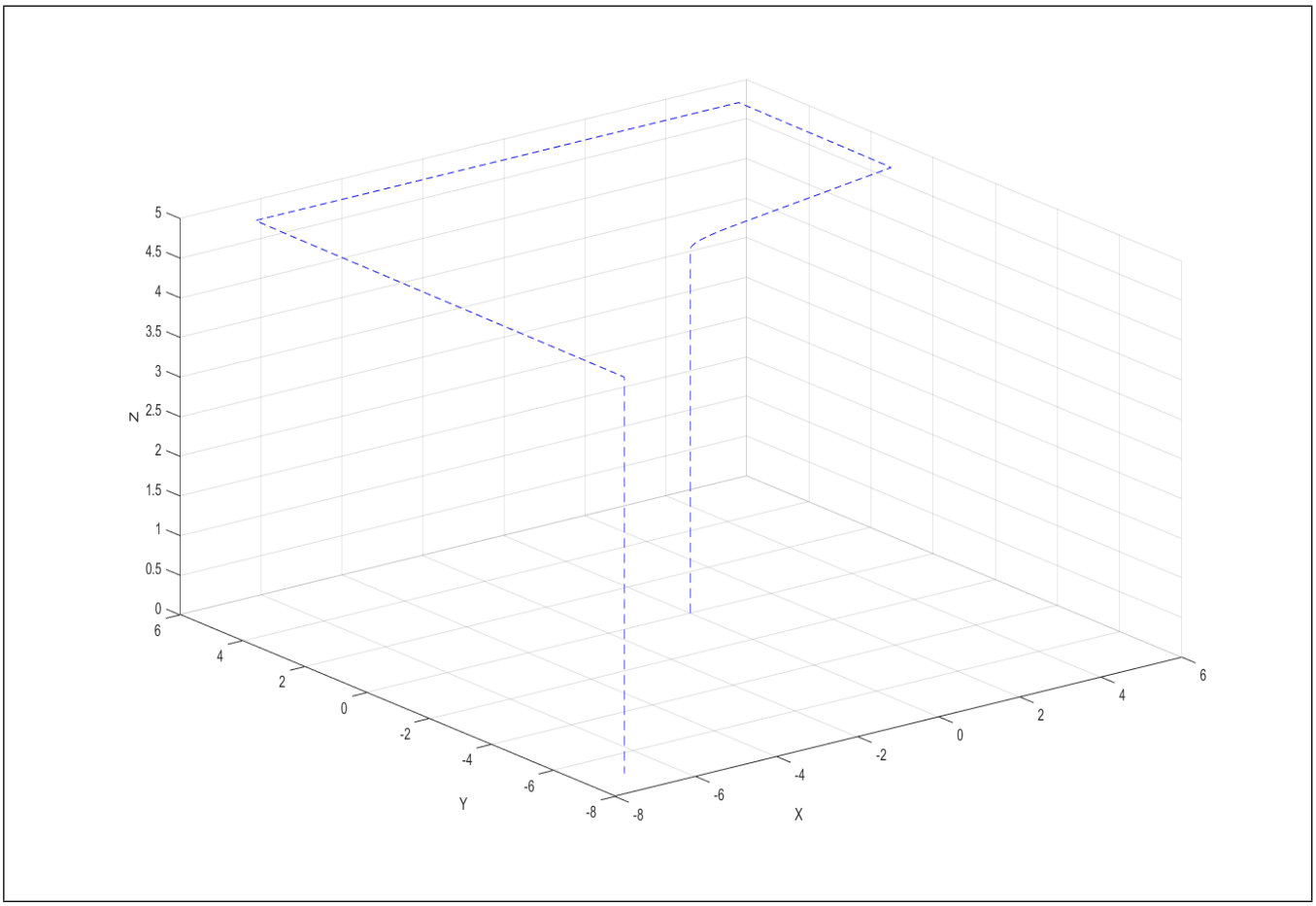

Figure 3.1: The aerodrome circuit navigation scenario

3.2 State of the art on the control of multicopters

Drones have several specific characteristics that make the design of control algorithms challenging. Rotary-wing drones, in general, are underactuated systems, sensitive to aerodynamic disturbances, and exhibit highly nonlinear dynamics. Moreover, they exhibit significant coupling between different state variables of the system and their control inputs. With the objective of reducing or eliminating these

undesirable effects, the development of control strategies for autonomous aerial vehicles has been the subject of hundreds of publications in recent decades. This section is dedicated to presenting the control architectures found in the literature.
In general, different control strategies are classified as linear or nonlinear based on the mathematical representation of the vehicle used for synthesizing the control laws. Linear control approaches are very popular because their design and implementation are relatively straightforward, which has led to their integration into the majority of autonomous aerial vehicles. Conversely, the implementation of nonlinear control approaches on drones is somewhat limited, but they are highly regarded for their theoretical contributions.

3.3 Linear Approaches

In the context of linear systems theory, control synthesis is based on a linear approximation of the vehicle's dynamic model. This approach allows for decoupling the dynamics into four Single Input - Single Output (SISO) loops associated with a single control input [47]. Typically, these four loops describe the longitudinal position or velocity of the drone, the lateral position or velocity, the vertical position or velocity, and the orientation around the vertical axis. Several linear control architectures are now presented.

- Linear PID Control: The PID control strategy is undoubtedly the most intuitive and straightforward approach to implement on a processor. It allows for easy understanding of the physical role of each control term, enabling the gains to be adjusted accordingly. This approach has been successfully tested on various experimental platforms, such as quadrotors [48] and hexacopters [49] [50] [51].

- Pole Placement Control: Pole placement control is a method that involves determining a gain matrix to place the eigenvalues of the closed-loop system at predefined positions. To ensure stability of the closed-loop system, the eigenvalues should be chosen with strictly negative real parts. This control architecture has been used by the authors of [52] [53] [54] for the control of a helicopter, hexacopter, and fixed-wing drone, respectively.

The aforementioned linear approaches are very interesting as they allow for precise determination of closed-loop stability, performance, and robustness. However, these techniques rely on the assumption that the system is linear, which is only true in a region of the state space around a particular operating point. Consequently, stability proof is not guaranteed if the vehicle deviates from this operating point. Special control algorithms must be developed to expand the operational range of the aerial vehicle.

3.4 Nonlinear Approaches

In most applications, the implemented control is based on a linearized model of the considered vehicle's dynamics. However, in recent years, there has been an increasing focus on control approaches based on a nonlinear representation of aerial vehicle dynamics. These nonlinear approaches offer significant theoretical contributions, although their application remains somewhat limited. The most commonly used nonlinear control architectures for drone piloting and guidance are:

- Backstepping Control: One of the most well-known methods in nonlinear control is the Backstepping theory. This method provides a recursive control design tool based on Lyapunov theory

[55] [56]. In the field of UAVs, it has been applied to helicopters [57][58][59]and hexacopters [60][61][62].

- Sliding mode control: (SMC) is a type of nonlinear control system methods that change the dynamics of the system by designing a multiple control structure to make sure that trajectories slide towards a switching surface. The control law works by switching from one continuous structure to another depending on position in state space. It is a robust control technique, which has the ability to compensate modeling errors, system's parameter differences and work for nonlinear and time varying systems. However, it has a draw back in forming a chattering effect that gives a high frequency oscillation [63] [64].

3.5 General Control Structure

The control of the hexacopter is achieved through a cascade structure consisting of two loops. The inner loop controller, related to attitude dynamics, is responsible for tracking the drone's orientation reference, i.e., following $(\phi_d, \theta_d, \psi_d)$ The outer loop controller, related to position dynamics, generates the desired roll and pitch angles as well as the total lift force required for positioning the drone at a given altitude.
The derivatives of the hexacopter's position and orientation form its complete dynamics. The overall system can be subdivided into two subsystems describing the rotation dynamics and the translation dynamics. Figure 3.1 presents a simplified block diagram illustrating the controller structure of a hexacopter drone.
The controller for translation motion (x , y) outputs the desired orientation (roll, pitch) of the hexacopter due to the coupling existing between these variables. The synthesis of a second controller then stabilizes the attitude towards the desired heading. For example, to perform a hover, the roll and pitch angles should be maintained at zero. The tilting of the aircraft causes its movement in the (x, y) plane, highlighting the importance of the attitude controller's accuracy.
In the first case, controlling orientation and altitude is relatively straightforward, as it is completely independent of controlling other degrees of freedom. In the second case, control is performed for all three position coordinates plus the yaw orientation. However, this mode of control utilizes both roll and pitch orientation controllers. In summary, the control signals from the three position controllers define a lift force vector in the inertial frame. The orientation of this force defines the setpoint sent to the roll and pitch controllers.

3.6 Synthesis of PID Control Laws

PID control (Proportional-Integral-Derivative) is certainly the most commonly used control structure in the industry. It has been adopted in over 90% of control architectures, many of which consist only of proportional and integral actions. The dominance of this approach stems not only from its simplicity but also from the performance it offers to closed-loop systems, regardless of their application domain.

3.6.1 Principle of Control

The central idea of this type of controller is to generate a control signal based on the difference between a setpoint y_{ref} and a measurement y. Let e be the error defined as $e = y_{ref} - y$. The expression for the

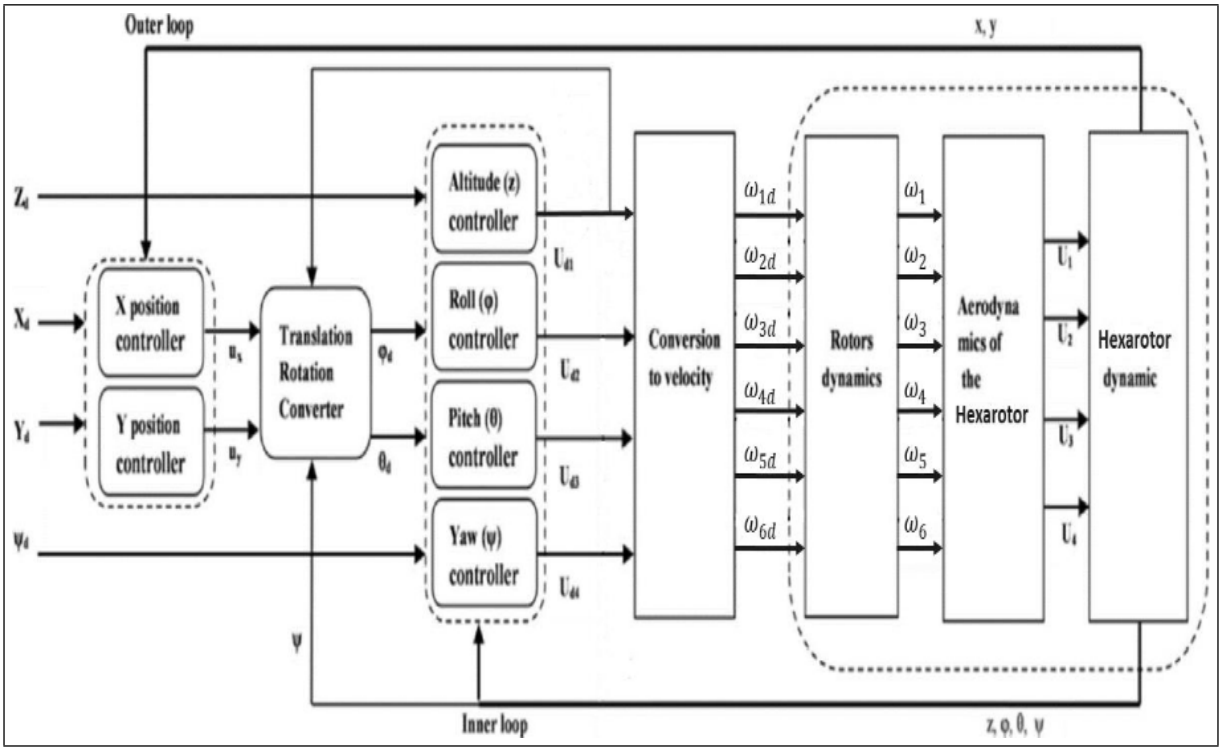

Figure 3.2: Diagram of the General Control Structure.

control signal u generated by a PID controller in the time domain is given by:

$$u(t) = K_P e(t) + K_I \int_0^t e(\tau)d\tau + K_D \frac{de(t)}{dt} \tag{3.1}$$

The control signal is therefore the sum of three terms: a term proportional to the error, a term proportional to the integral of the error, and a term proportional to the derivative of the error. The integral, proportional, and derivative components can be considered as control actions based on the past, present, and future, respectively. Adapting the control signal u to the requirements of the closed-loop system is achieved by appropriately selecting the proportional gain K_P, the integral gain K_I, and the derivative gain K_D.

3.6.2 Control objectives

In our case, the objective is to design a classical controller (PID) for trajectory tracking. The controller parameters will be adjusted empirically. However, the hexacopter is a six-degree-of-freedom robot, while the structure of the PID is single-variable. Therefore, we are developing a set of PIDs for all the measured variables of the hexacopter.

Figure 3.2 shows the control structure when a trajectory (x, y, z, ψ) is planned. In general, the stabilization of an hexacopter can be achieved by a PD controller for each degree of freedom. However, a residual error remains uncancelled at the altitude z when the hexacopter is in hover due to the effect of its weight. For this reason, a PD controller is designed for each degree of freedom except for altitude, for which a PID controller has been chosen.

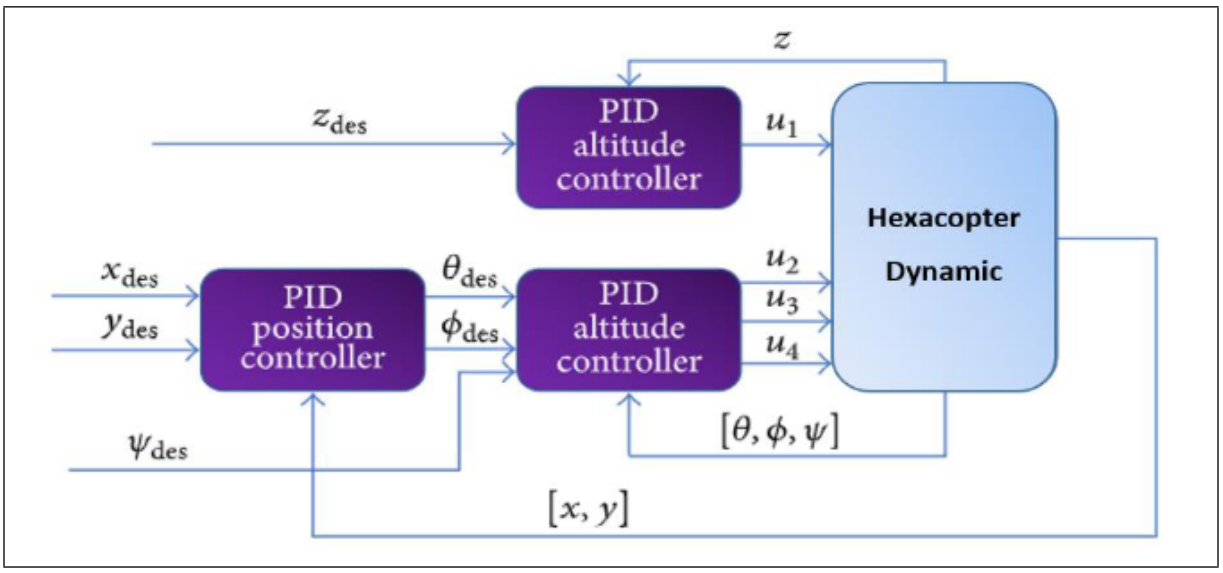

Figure 3.3: Structure of PID Control.

3.6.3 Control Laws

In the hexacopter, we need to control six variables (6 DOF). For this purpose, the control laws for these variables using PID are as follows:

- For the control loop:

$$\begin{cases} U_\phi(t) = K_{P\phi}e_\phi(t) + K_{I\phi}\int_0^t e_\phi(\tau)d\tau + K_{D\phi}e_\phi(t) & ; e_\phi(t) = \phi_d(t) - \phi(t) \\ U_\theta(t) = K_{P\theta}e_\theta(t) + K_{I\theta}\int_0^t e_\theta(\tau)d\tau + K_{D\theta}e_\theta(t) & ; e_\theta(t) = \theta_d(t) - \theta(t) \\ U_\psi(t) = K_{P\psi}e_\psi(t) + K_{I\psi}\int_0^t e_\psi(\tau)d\tau + K_{D\psi}e_\psi(t) & ; e_\psi(t) = \psi_d(t) - \psi(t) \end{cases} \tag{3.2}$$

- For the guidance loop:

$$\begin{cases} U_x(t) = K_{Px}e_x(t) + K_{Ix}\int_0^t e_x(\tau)d\tau + K_{Dx}e_x(t) & ; e_x(t) = x_d(t) - x(t) \\ U_y(t) = K_{Py}e_y(t) + K_{Iy}\int_0^t e_y(\tau)d\tau + K_{Dy}e_y(t) & ; e_y(t) = y_d(t) - y(t) \\ U_z(t) = K_{Pz}e_z(t) + K_{Iz}\int_0^t e_z(\tau)d\tau + K_{Dz}e_z(t) & ; e_z(t) = z_d(t) - z(t) \end{cases} \tag{3.3}$$

the following is the simulation result for the two seniors hovering and trajectory tracking using PID control

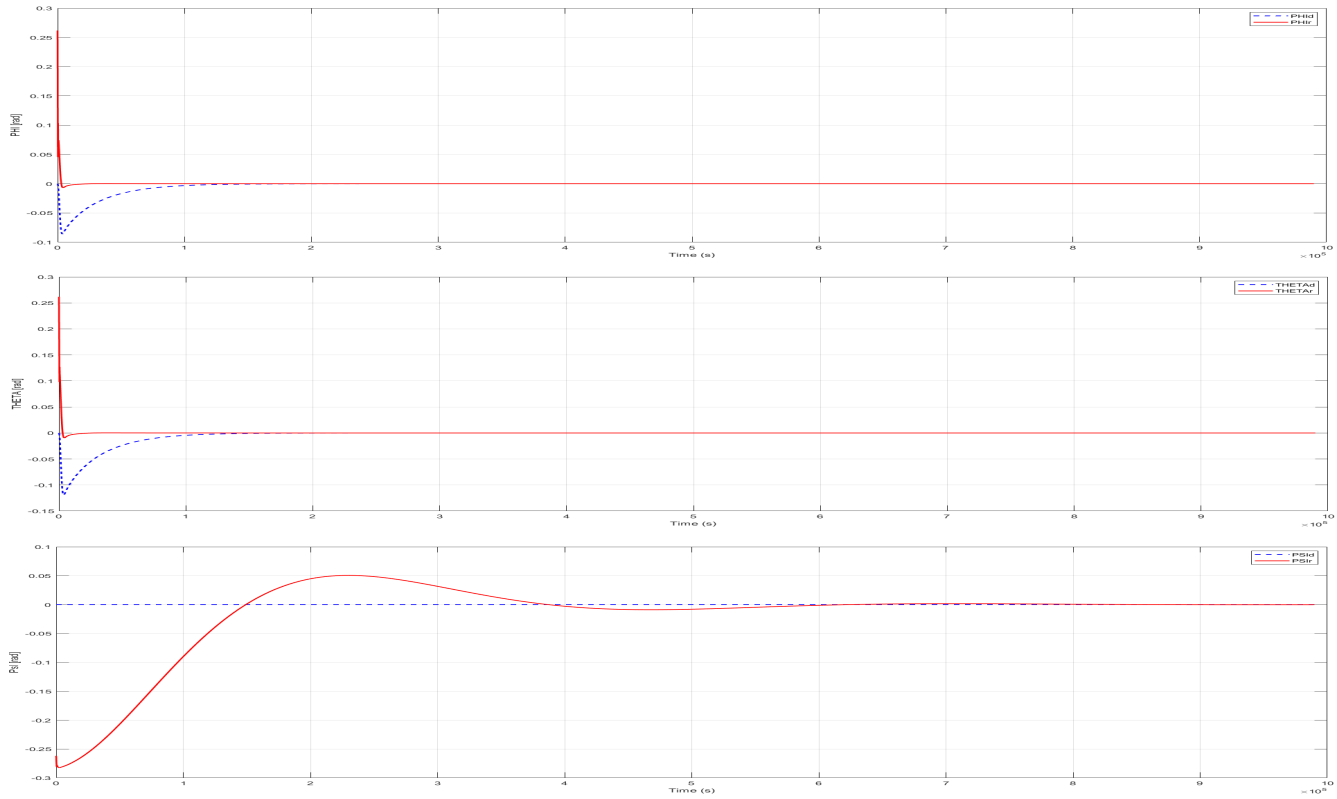

Figure 3.4: PID attitude hovering

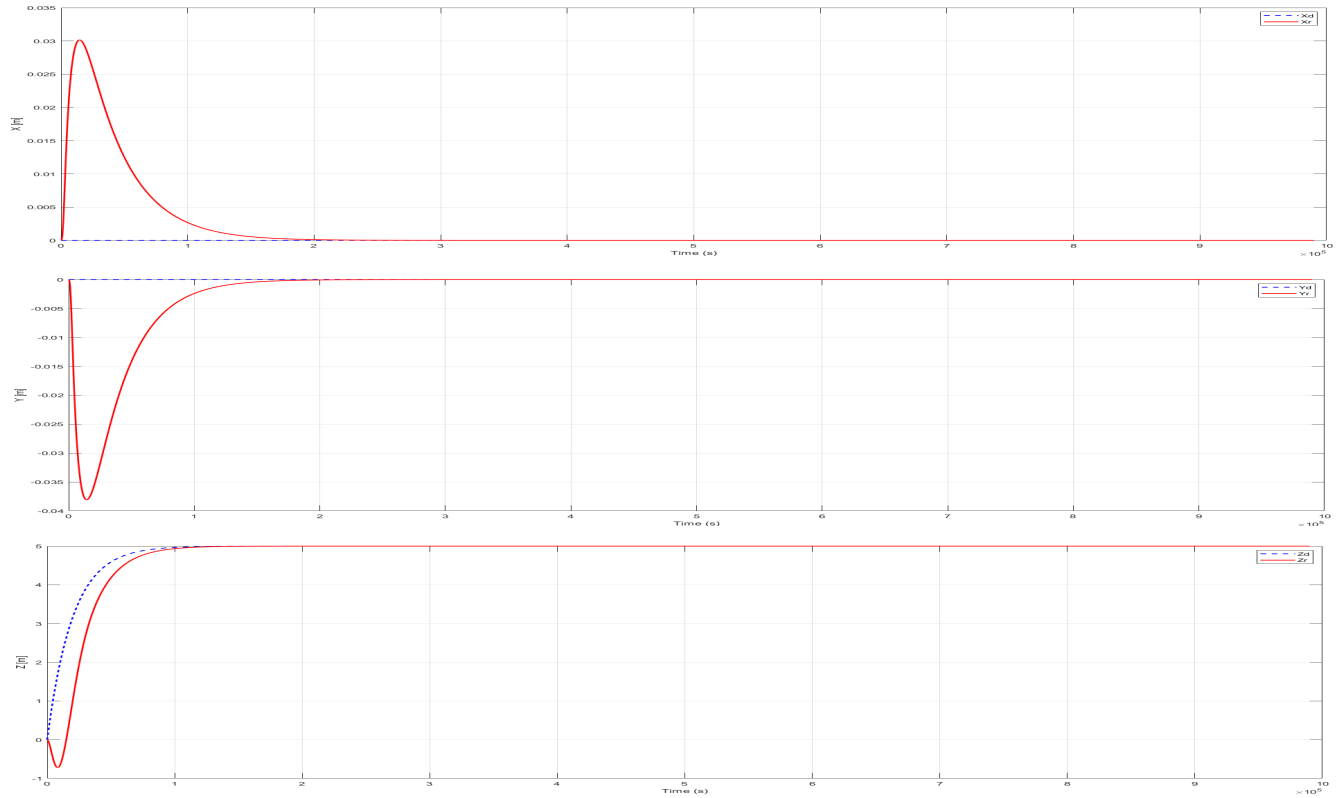

Figure 3.5: PID position hovering

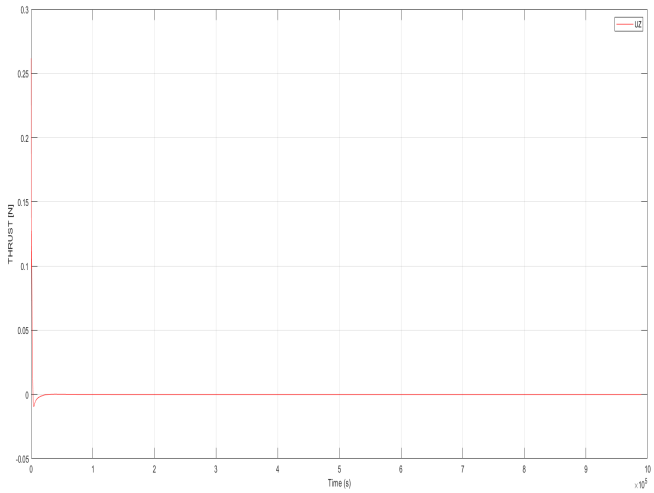

(a) Uz

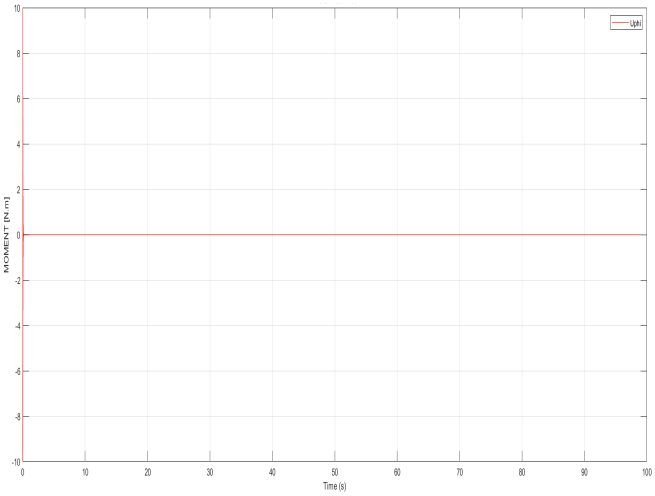

(b) Uphi

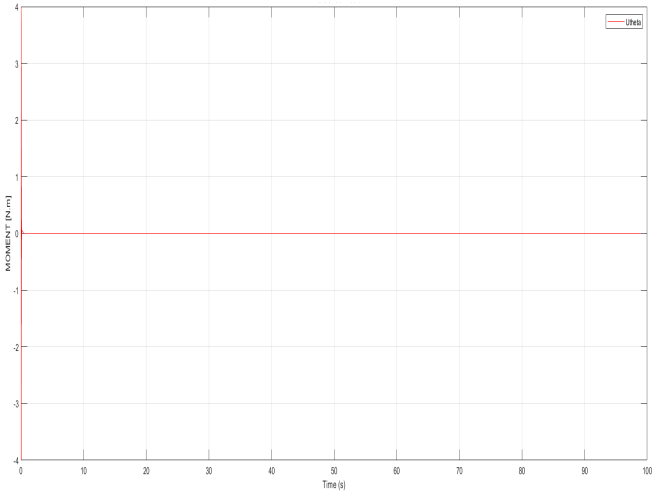

(c) Utheta

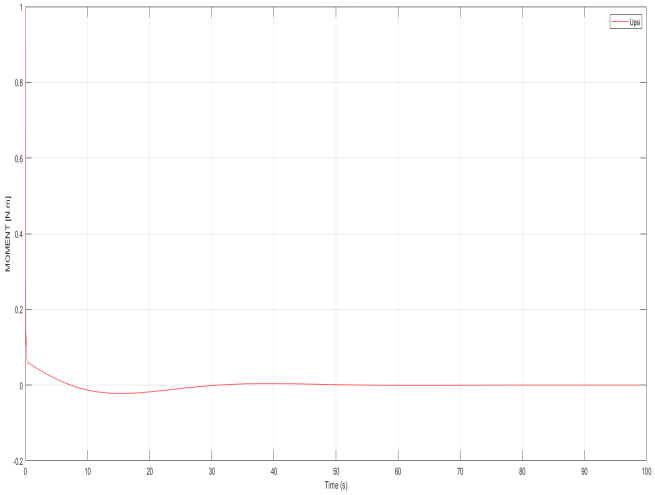

(d) Upsi

Figure 3.6: PID thrust and moments hovering.

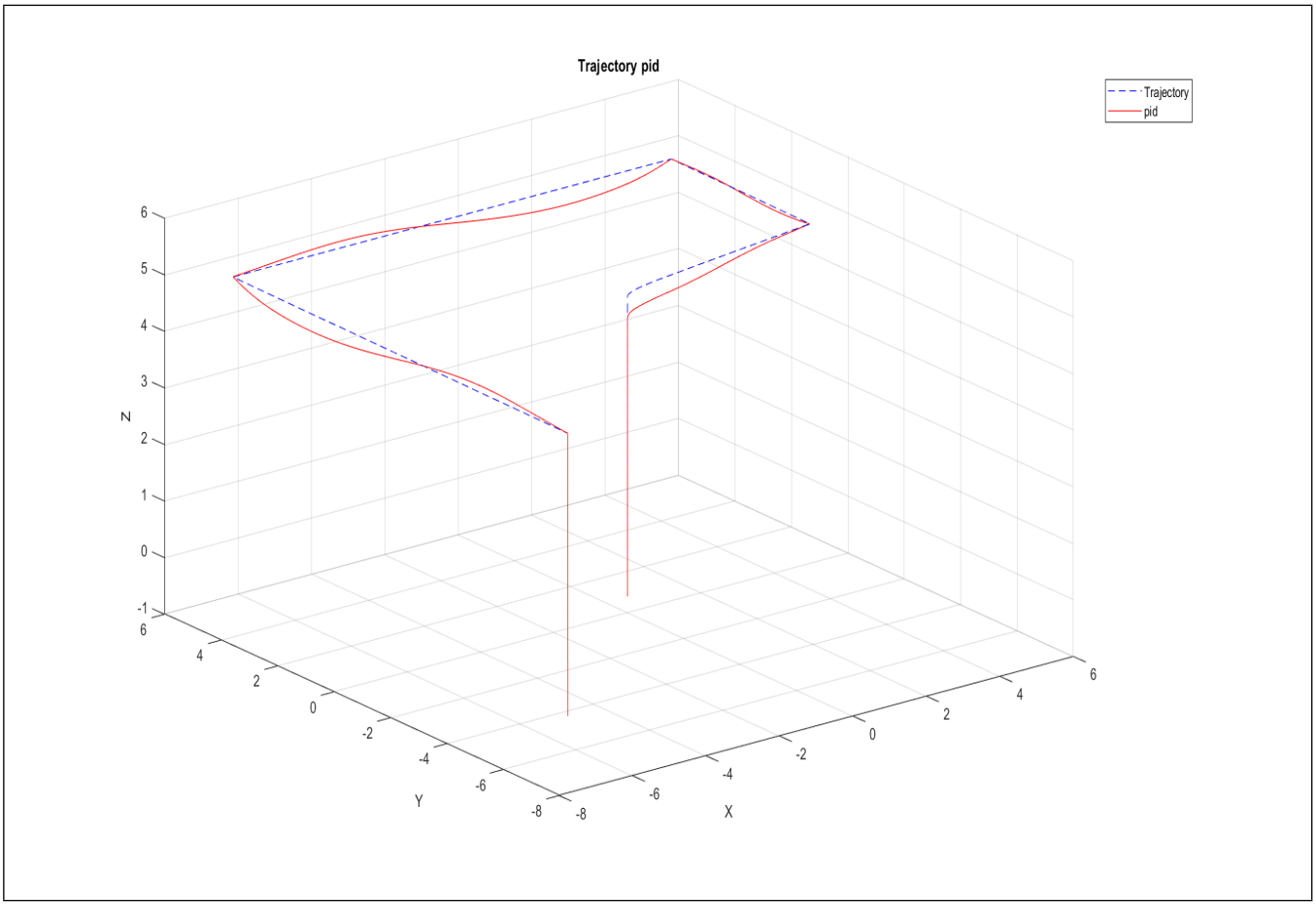

Figure 3.7: trajectory tracking using PID

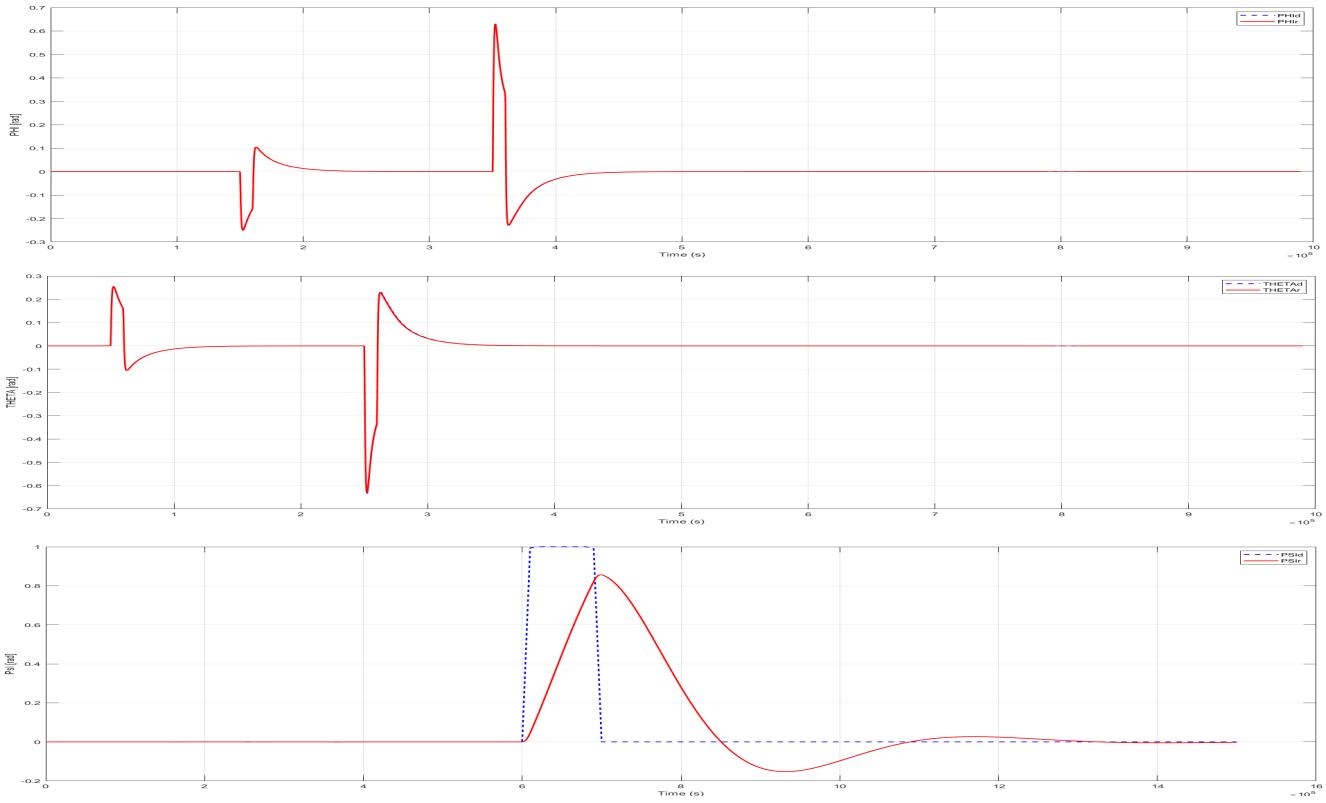

Figure 3.8: PID attitude trajectory

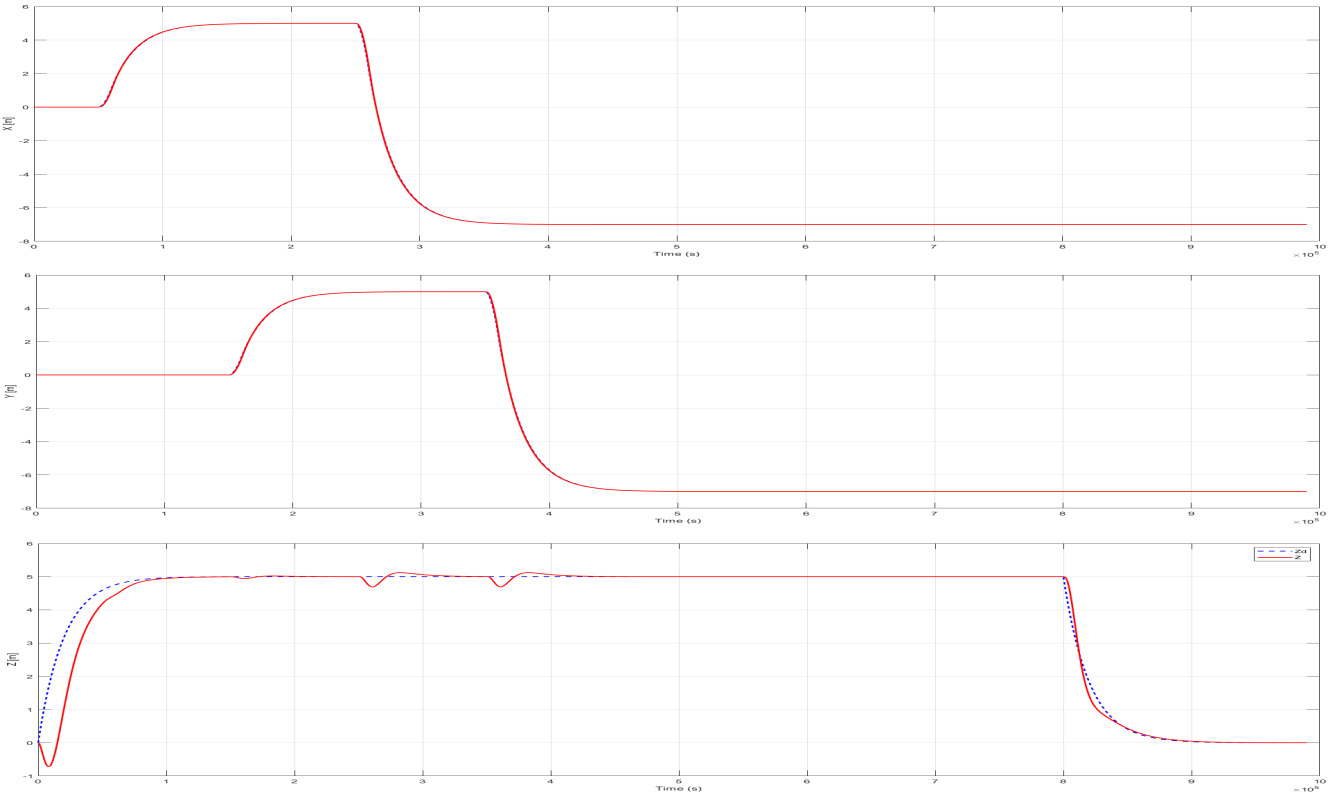

Figure 3.9: PID position trajectory

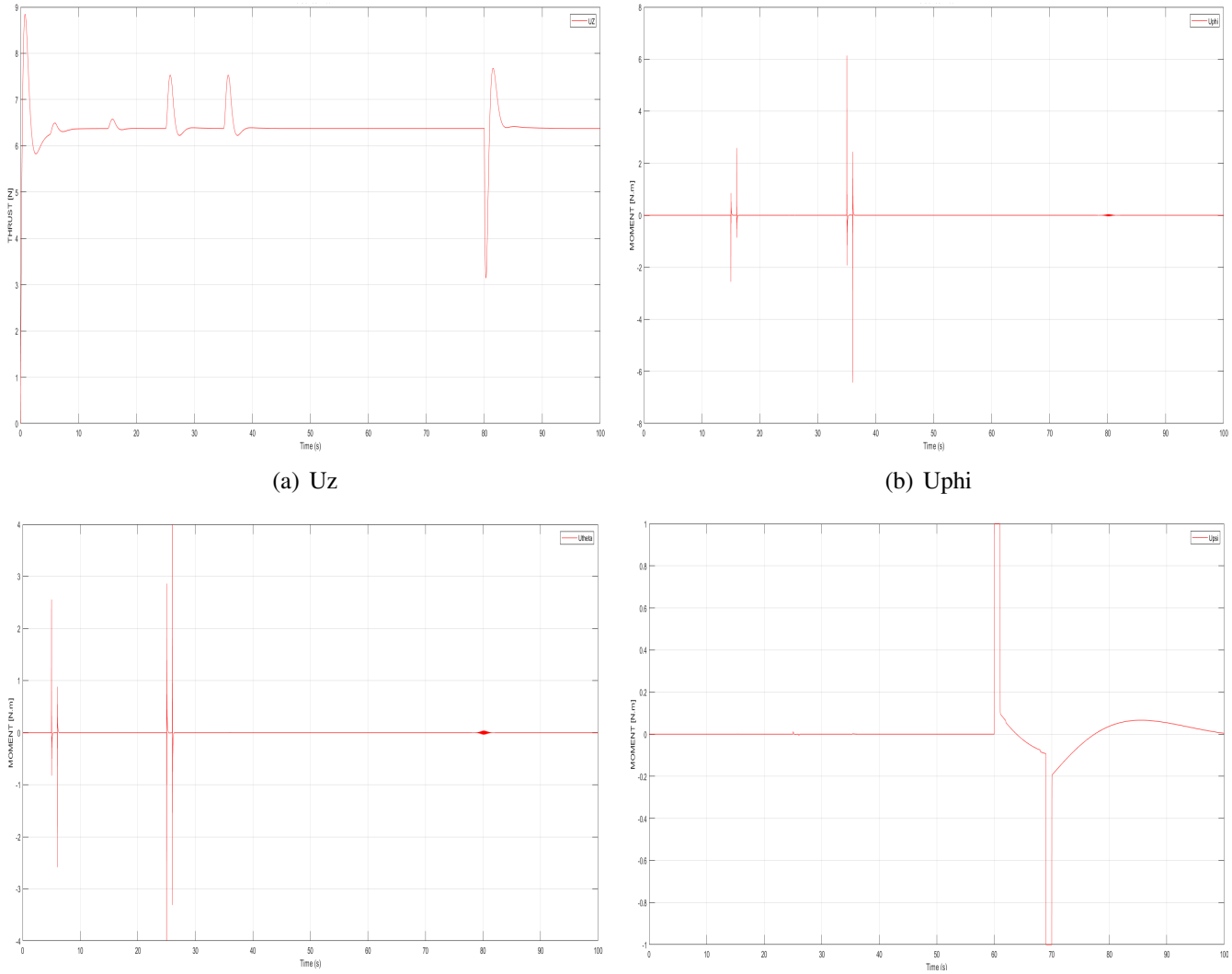

(a) Uz (b) Uphi

(c) Utheta (d) Upsi

Figure 3.10: PID thrust and moments trajectory.

3.7 Synthesis of Backstepping Control Laws

During recent years, a significant portion of the scientific community has focused on researching procedures for developing control laws for nonlinear systems, such as Backstepping. Numerous works addressing this new theoretical approach have emerged, with notable mentions of [58] [60] [62] . Applications of this approach to real systems have also been presented in the literature.

3.7.1 Backstepping theory

The backstepping technique was developed in the early 1990s. The introduction of backstepping control breathed new life into the control of nonlinear systems, which, despite significant progress, lacked general approaches. This technique is a systematic and recursive method for synthesizing nonlinear control laws that utilize the Lyapunov stability principle and can be applied to a wide range of nonlinear systems.
The basic idea of backstepping control is to make the closed-loop systems equivalent to stable cascade subsystems of order one in the sense of Lyapunov, which leads to global asymptotic stability. In other words, it is a multi-step method. At each step of the process, a virtual control signal is generated to ensure the convergence of the system to its equilibrium state. This can be achieved using Lyapunov functions that step-by-step stabilize each synthesis stage. It should be noted that backstepping is characterized by:

- It is applicable to strictly feedback systems, meaning that the derivative of each state vector component must be a function of previous components and depend additively on the next component.
- We start with the first differential equation of the system $\dot{x}_1$ which is further away from the control input u, and we complete the control law in the final step.
- In our case, we can synthesize the control laws for the control loop $(U_\phi, U_\theta, U_\psi)$ and the guidance loop (U_x, U_y, U_z), thus compelling the system to follow the desired trajectory.

3.7.2 Control objective

In the context of trajectory tracking, the control objective is a pursuit problem, meaning we want the state $x_i(t)$ to follow a time-varying reference $x_d(t)$ as t approaches t_f.

3.7.3 Description of the design steps

The design method of the Backstepping controller is primarily based on the Lyapunov stability theory of dynamical systems. The core of the theory is presented in (Khalil, 1992). In our work, we consider the nonlinear state model for the roll synthesis of the hexacopter to illustrate the design method:

$$\ddot{\phi} = \frac{1}{I_x}[\dot{\theta}\dot{\psi}(I_y - I_z) - K_{fax}\dot{\phi}^2 - J_r\varpi\dot{\theta} + U_2] \tag{3.4}$$

Let the state vector be:

$$X = [\ \phi\ \ \dot{\phi}\ \ \theta\ \ \dot{\theta}\ \ \psi\ \ \dot{\psi}\ \ x\ \ \dot{x}\ \ y\ \ \dot{y}\ \ z\ \ \dot{z}\ ]^T$$

Hence, equation (3.4) becomes the following state-space form:

$$\begin{cases} \dot{x_1} = x_2 \\ \dot{x_2} = a_1 x_4 x_6 + a_2 x_2^2 + a_3 x_4 \varpi + b_1 U\phi \end{cases} \tag{3.5}$$

$$a_1 = \frac{I_y - I_z}{I_x}, a_2 = -\frac{K_{fax}}{I_x}, a_3 = -\frac{J_r}{I_z}, b_1 = \frac{d}{I_x}$$

- First step:
  Let's define the first variable of the procedure as e, which represents the error between the state and the desired state, such that $e_1 = x_1 - x_{1d}$. The derivative with respect to time is given by:

$$\dot{e_1} = x_2 - \dot{x}_{1d} = x_2 - x_{2d} \tag{3.6}$$

  And a second variable of the Backstepping, denoted as $z_1 = x_2 - x_2^*$, where x_2^* is a virtual control law that will be determined later. To find this control law, we construct a partial quadratic Lyapunov function:

$$V_1(e) = \frac{1}{2}e_1^2 \tag{3.7}$$

  Its derivative with respect to time:

$$\dot{V}_1(e) = e_{11} = e_1(x_2 - \dot{x}_{1d}) \tag{3.8}$$

  x_2^* is chosen such that $\dot{V}(e_1)_1$ is negative definite:

$$x_2^* = \dot{x}_{1d} - k_1 e \tag{3.9}$$

  Where $k_1 > 0$ is a positive control constant. Noting that x_2^* has been chosen such that $\dot{V}_1(e_1) < 0$. Substituting x_2^* into $\dot{V}_1(e_1)$, we find:

$$\dot{V}_1(e_1) = e_1(-k_1 e_1 + z_1) = -k_1 e_1^2 + e_1 z_1 \tag{3.10}$$

$$z_1 = x_2 - \dot{x}_{1d} + k_1 e_1 \tag{3.11}$$

  For global stability, the last term $e_1 z_1$ will be eliminated in the next step.

- Second step:

  We now need to define a new system based on this new state. It is typically referred to as the "augmented system". We also note that in the second design step, the state x_1 will no longer appear explicitly. It is implicitly taken into account through the error state. The augmented system can be written as follows:

$$\begin{cases} \dot{e}_1 &= -k_1 e_1 + z_1 \\ \dot{z}_1 &= a_1 x_4 x_6 + a_2 x_2^2 + a_3 x_4 \varpi + b_1 U_\phi - \ddot{x}_{1d} + k_{11} \end{cases} \tag{3.12}$$

  Let the candidate Lyapunov function$V(e_1, z_1)$ of the augmented system be given by:

$$V_2(e_1, z_1) = V_1(e_1) + \frac{1}{2}z_1^2 \tag{3.13}$$

  The derivative with respect to time is:

$$\dot{V}_2(e_1, z_1) = e_1\dot{e}_1 + z_1\dot{z}_1 = e_1(-k_1e_1 + z_1) + z_1(a_1x_4x_6 + a_2x_2^2 + a_3x_4\varpi + b_1U_\phi - \ddot{x}_{1d} + k_1\dot{e}_1) \quad (3.14)$$

By choosing the following controller for roll:

$$U_\phi = \frac{1}{b_1}\left(-a_1x_4x_6 - a_2x_2^2 - a_3x_4\varpi + \ddot{x}_{1d} - k_1\dot{e}_1 - k_2z_1\right) \quad (3.15)$$

We obtain:

$$\dot{V}_2(e, z_1) = -k_1e^2 - k_2z_1^2 \quad (3.16)$$

With: k_1, k_2 are positive tuning gains. This ensures that the system is globally asymptotically stable (GAS). Therefore, our control objective is achieved.

Following exactly the same steps for the roll controller, the control input U_θ responsible for generating the pitch rotation and U_ψ responsible for generating the yaw rotation are given by

$$\begin{cases} U_\phi = \dfrac{1}{b_1}(-a_1x_4x_6 - a_2x_2^2 - a_3x_4\varpi + \ddot{x}_{1d} - k_1(-k_1e_1 + z_1) - k_2z_1) \\ U_\theta = \dfrac{1}{b_2}(-a_4x_2x_6 - a_5x_4^2 - a_6x_2\varpi + \ddot{x}_{4d} - k_3(-k_3e_2 + z_2) - k_4z_2) \\ U_\psi = \dfrac{1}{b_3}(-a_7x_2x_4 - a_8x_6^2 + \ddot{x}_{6d} - k_5(-k_5e_3 + z_3) - k_6z_3) \end{cases} \quad (3.17)$$

The altitude control U_z, longitudinal control U_x, and lateral control U_y are obtained using the same approach described previously, yielding:

$$\begin{cases} U_x = \dfrac{m}{U_z}(-a_9x_8 + \ddot{x}_d + k_7(-k_7e_7 + e_8) + k_8e_8 + e_7) \\ U_y = \dfrac{m}{U_z}(-a_{10}x_{10} + \ddot{y}_d + k_9(-k_9e_9 + e_{10}) + k_{10}e_{10} + e_9) \\ U_z = \dfrac{m}{\cos(x_1)\cos(x_3)}(-a_{11}x_{12} + g + \ddot{z}_d + k_{11}(-k_{11}e_{11} + e_{12}) + k_{12}e_{12} + e_{11}) \end{cases} \quad (3.18)$$

The z_i represents the tracking errors for the state variables, and the different k_i are tuning gains for each degree of freedom.
the following is the simulation result for the two seniors hovering and trajectory tracking using backstepping control

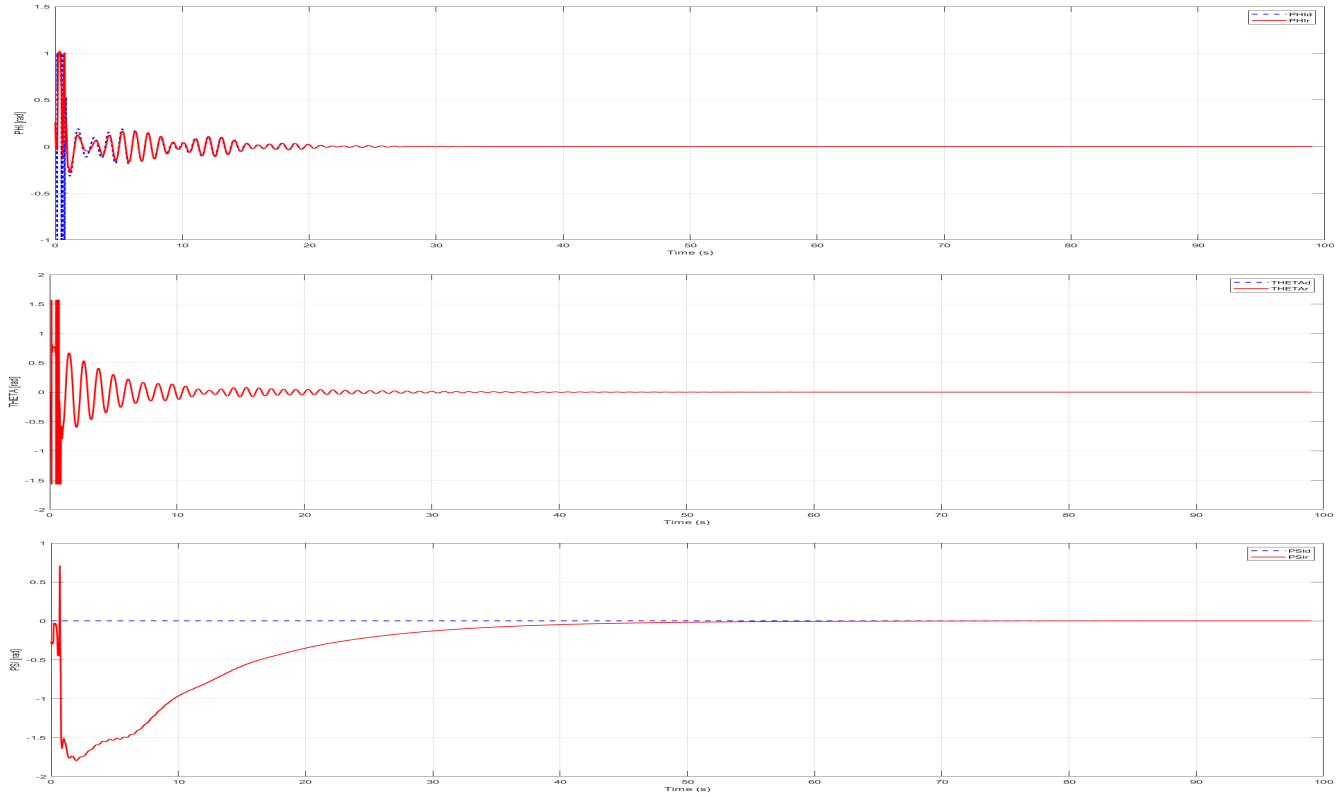

Figure 3.11: backstepping attitude hovering

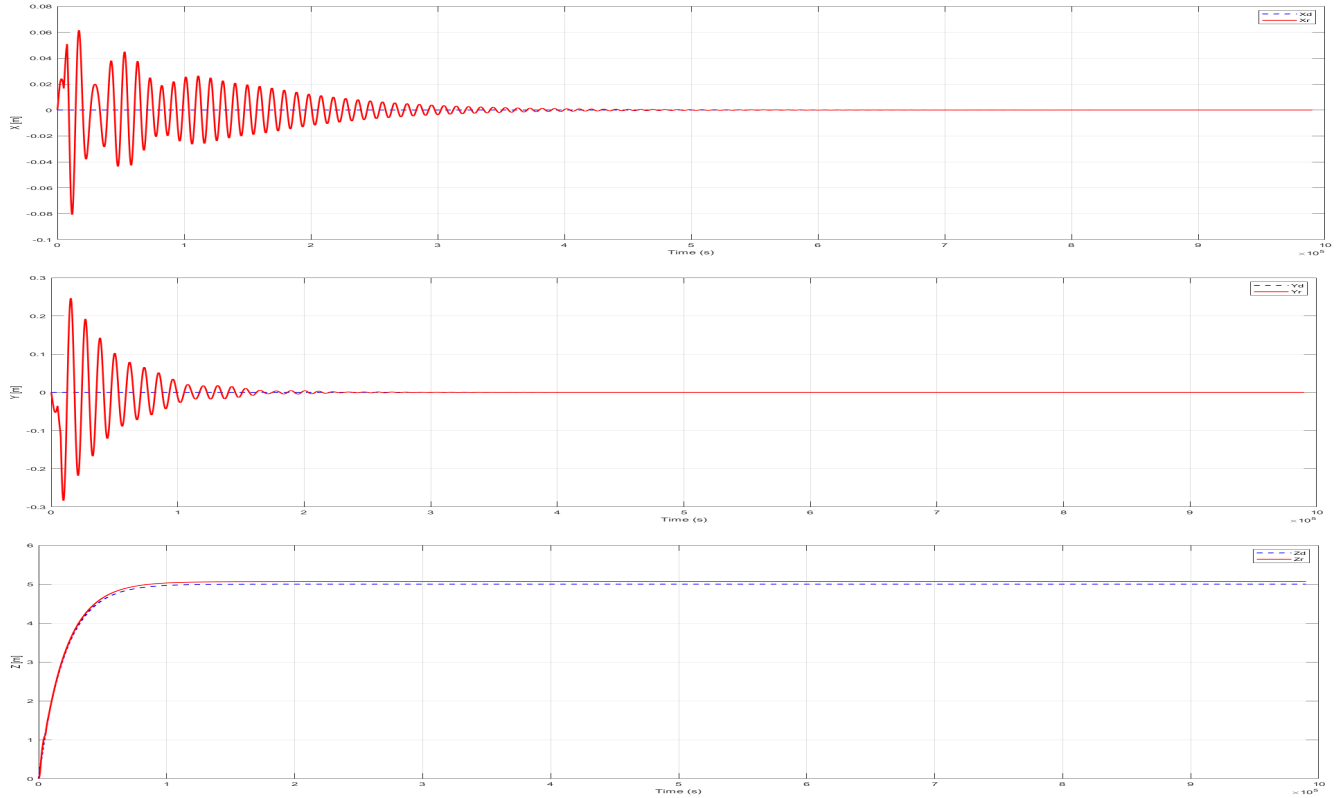

Figure 3.12: backstepping position hovering

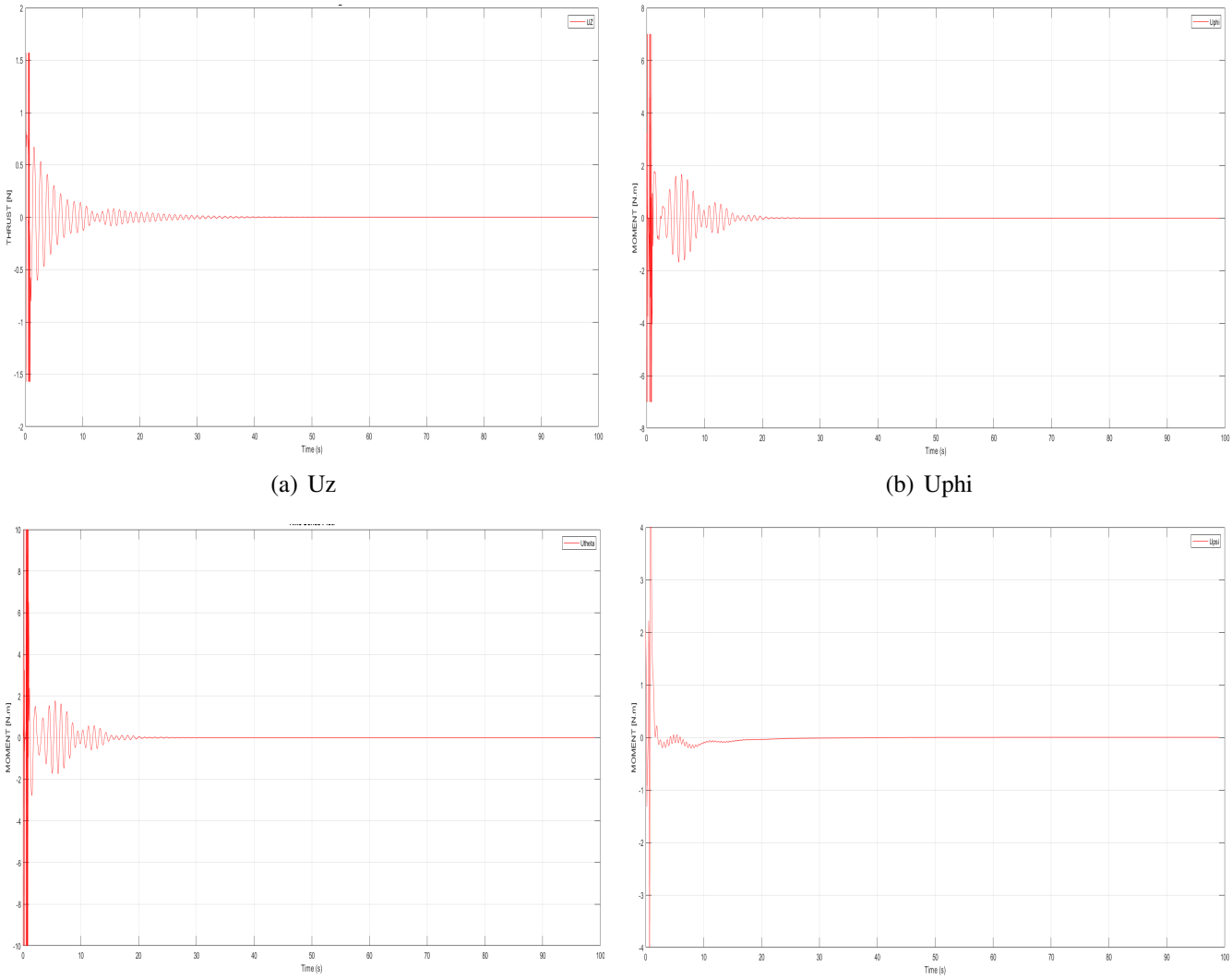

(a) Uz (b) Uphi

(c) Utheta (d) Upsi

Figure 3.13: backstepping thrust and moments hovering.

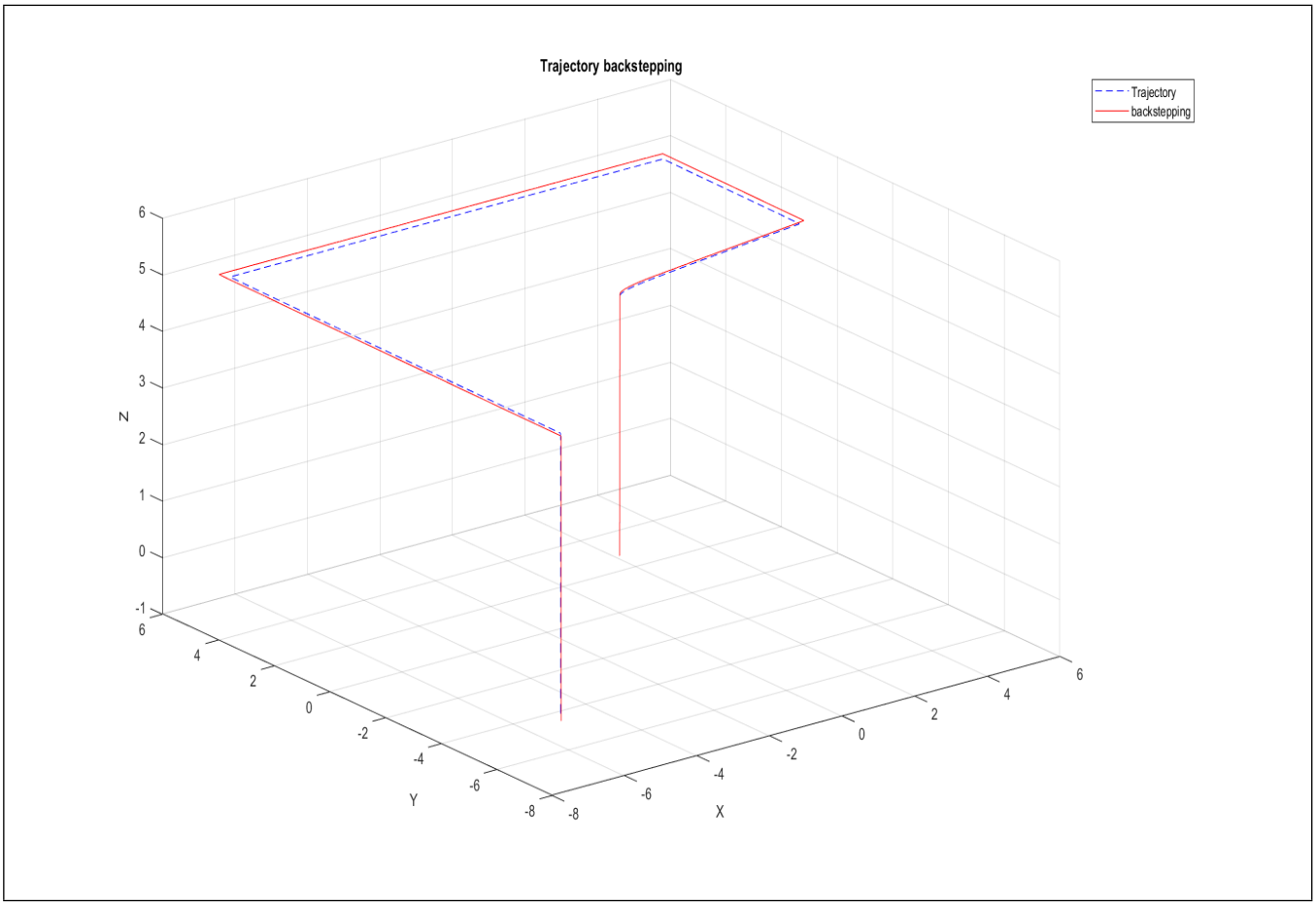

Figure 3.14: trajectory tracking using backstepping

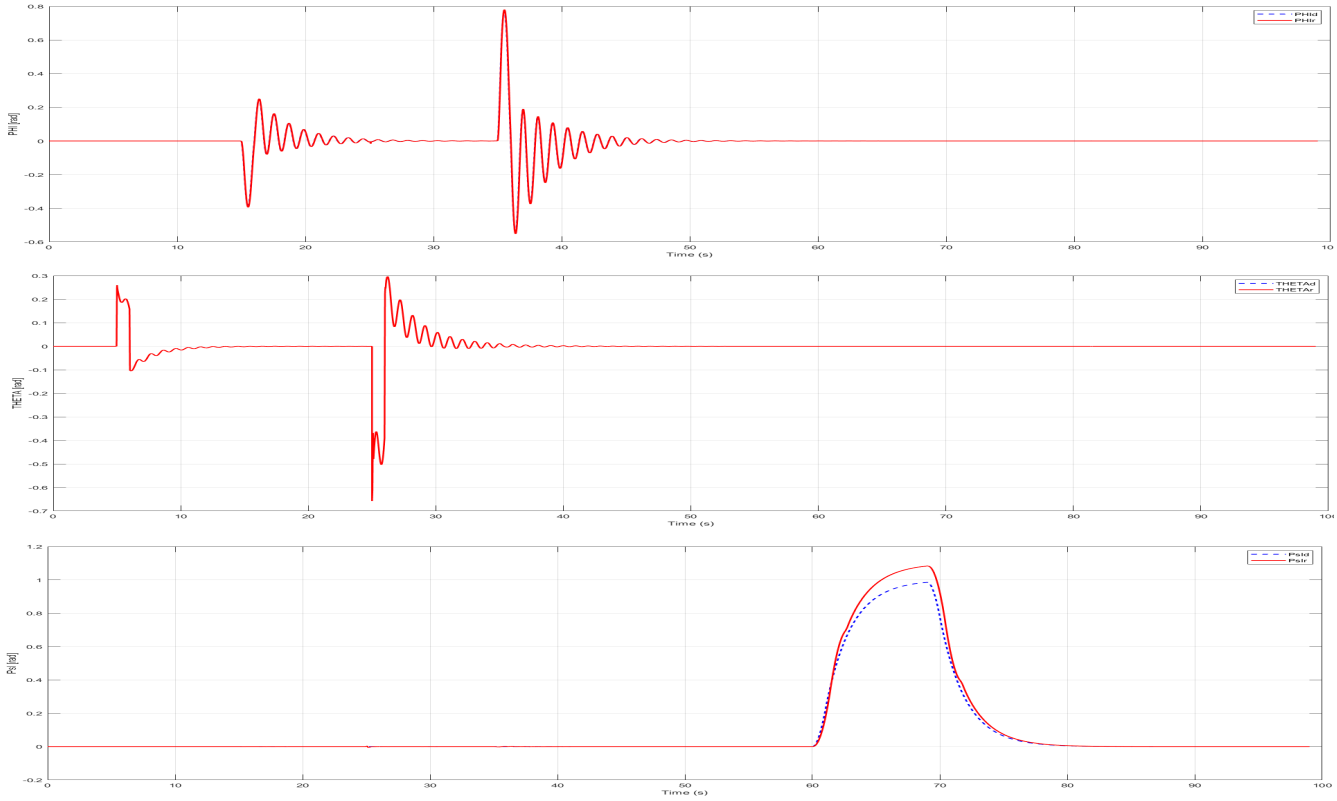

Figure 3.15: backstepping attitude trajectory

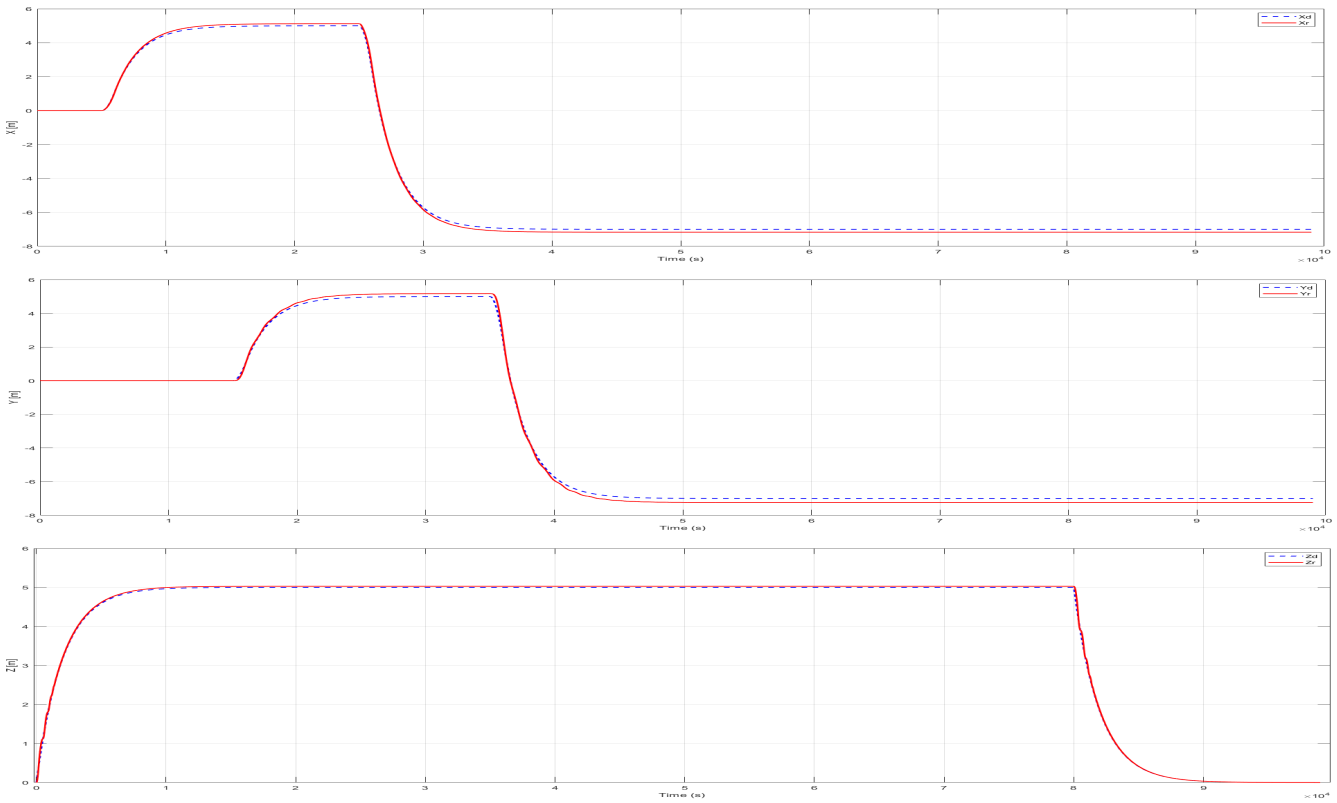

Figure 3.16: backstepping position trajectory

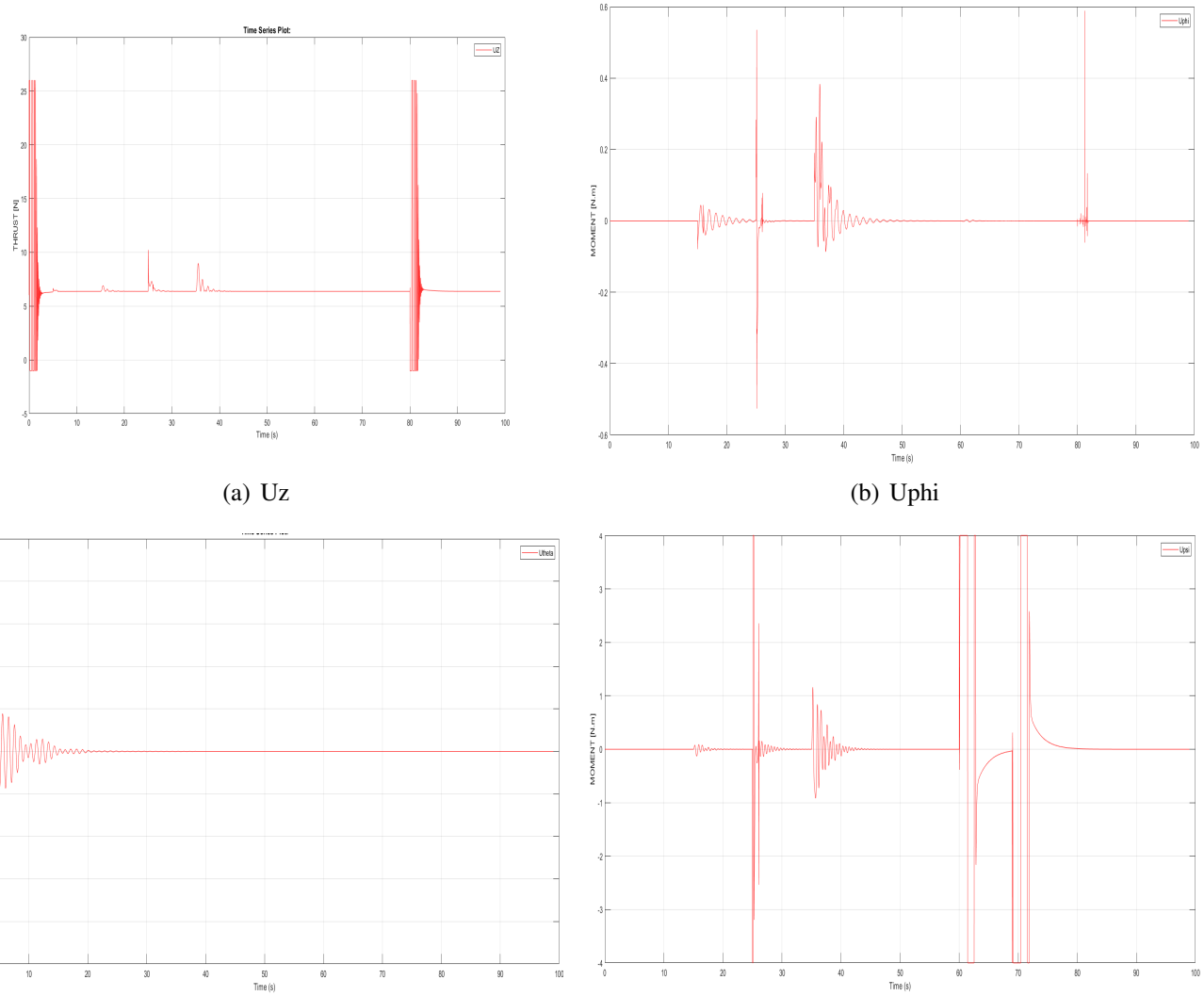

(a) Uz (b) Uphi

(c) Utheta (d) Upsi

Figure 3.17: backstepping thrust and moments hovering.

3.8 Synthesis of Sliding Mode Control Laws

In control systems, Sliding Mode Control (SMC) is a nonlinear control method that modifies the dynamics of a nonlinear system by applying a discontinuous control signal (or, more rigorously, a fixed-value control signal) that forces the system to "slide" along a cross-section of the normal behavior of the system. The feedback control law is not a continuous-time function. Instead, it can transition from one continuous structure to another depending on the current position in the state space. Therefore, Sliding Mode Control is a variable-structure control method. Multiple control structures are designed such that trajectories always move towards an adjacent region with a different control structure, and thus the final trajectory does not exist entirely within one control structure. Instead, it slides along the boundaries of the control structures. The motion of the system, when it slides along these boundaries, is referred to as sliding mode, and the geometric locus formed by the boundaries is called the sliding (hyper)surface. In the context of modern control theory, any variable-structure system, such as a system under SMC, can be considered as a special case of a hybrid dynamical system since the system moves both in a continuous state space and transitions between different discrete control modes.

3.8.1 Control objective

In the context of trajectory tracking, the control objective is a pursuit problem, meaning we want the state $x_i(t)$ to follow a time-varying reference $x_d(t)$ as t approaches t_f.

3.8.2 Description of the design steps

We consider the sliding surface:

$$S_0 = \dot{e} + \lambda e \tag{3.19}$$

Considering the dynamics of the sliding surface, we can deduce the equivalent control U_{eq}, knowing that $U = U_{eq} + U_n$ where U_n is the discontinuous control.

$$\dot{S}_0 = \ddot{e} + \lambda\dot{e} = \dot{x}_2 - \ddot{x}_{1d} + \lambda\dot{e} = f(X) + g(X)U - \ddot{x}_{1d} + \lambda\dot{e} \tag{3.20}$$

$$\dot{S}_0 = 0 \Rightarrow U_{eq} = \frac{1}{g(X)}(-f^*(X) + \ddot{x}_{1d} - \lambda\dot{e}) \tag{3.21}$$

We propose the Lyapunov function V_c in such a way that

$$V_c(S_0) = \frac{1}{2}S_0^2 \tag{3.22}$$

calculation of its temporal derivative gives:

$$\dot{V}_c = S_0\dot{S}_0 = S_0\left(f(X) + g(X)U - \ddot{x}_{1d} + \lambda\dot{e}\right) \tag{3.23}$$

Hence, we can obtain a discontinuous control of the form:

$$u_n = -\gamma g(X)\text{sign}(S_0) \tag{3.24}$$

With γ being a positive tuning gain.

$$U = U_{eq} + U_n$$

$$U = \frac{1}{g(X)}(-f^*(X) + \ddot{x}_1 d - \lambda \dot{e} - \gamma \text{sign}(S_0)) \tag{3.26}$$

Following exactly the same steps for the roll controller, the control input U_θ responsible for generating the pitch rotation and U_ψ responsible for generating the yaw rotation are given by:

$$\begin{cases} U_\phi = I_{xx}\left(\frac{-1}{I_{xx}}(\dot{\theta}\dot{\psi}(I_{yy} - I_{zz}) - K_{fax}\dot{\phi}^2 - J_r\omega_r\dot{\phi}) + \ddot{\phi}_d - \lambda_\phi \dot{e}_\phi - \gamma_\phi \text{sign}(S_{0_\phi})\right) \\ U_\theta = I_{yy}\left(\frac{-1}{I_{yy}}(\dot{\phi}\dot{\psi}(I_{zz} - I_{xx}) - K_{fay}\dot{\theta}^2 + J_r\omega_r\dot{\phi}) + \ddot{\theta}_d - \lambda_\theta \dot{e}_{\theta - \gamma_\theta \text{sign}(S_{0_\theta})}\right) \\ U_\psi = I_{zz}\left(\frac{-1}{I_{zz}}(\dot{\phi}\dot{\theta}(I_{xx} - I_{yy}) - K_{faz}r^2) + \ddot{\psi}_d - \lambda_\psi \dot{e}_\psi - \gamma_\psi \text{sign}(S_{0_\psi})\right) \end{cases} \tag{3.27}$$

The altitude control U_z, longitudinal control U_x, and lateral control U_y are obtained using the same approach described previously, yielding:

$$\begin{cases} U_x = \frac{m}{T}\left(\frac{K_{ftx}}{m}\dot{x} + \ddot{x}_d - \lambda_x \dot{e}_x - \gamma_x \text{sign}(S_{0_x})\right) \\ U_y = \frac{m}{T}\left(\frac{K_{fty}}{m}\dot{y} + \ddot{y}_d - \lambda_y \dot{e}_y - \gamma_y \text{sign}(S_{0_y})\right) \\ U_z = \frac{m}{\cos(\phi)\cos(\theta)}\left(\frac{K_{ftz}}{m}\dot{z} + g + \ddot{z}_d - \lambda_z \dot{e}_z - \gamma_z \text{sign}(S_{0_z})\right) \end{cases} \tag{3.28}$$

the following is the simulation result for the two seniors hovering and trajectory tracking using sliding mode control

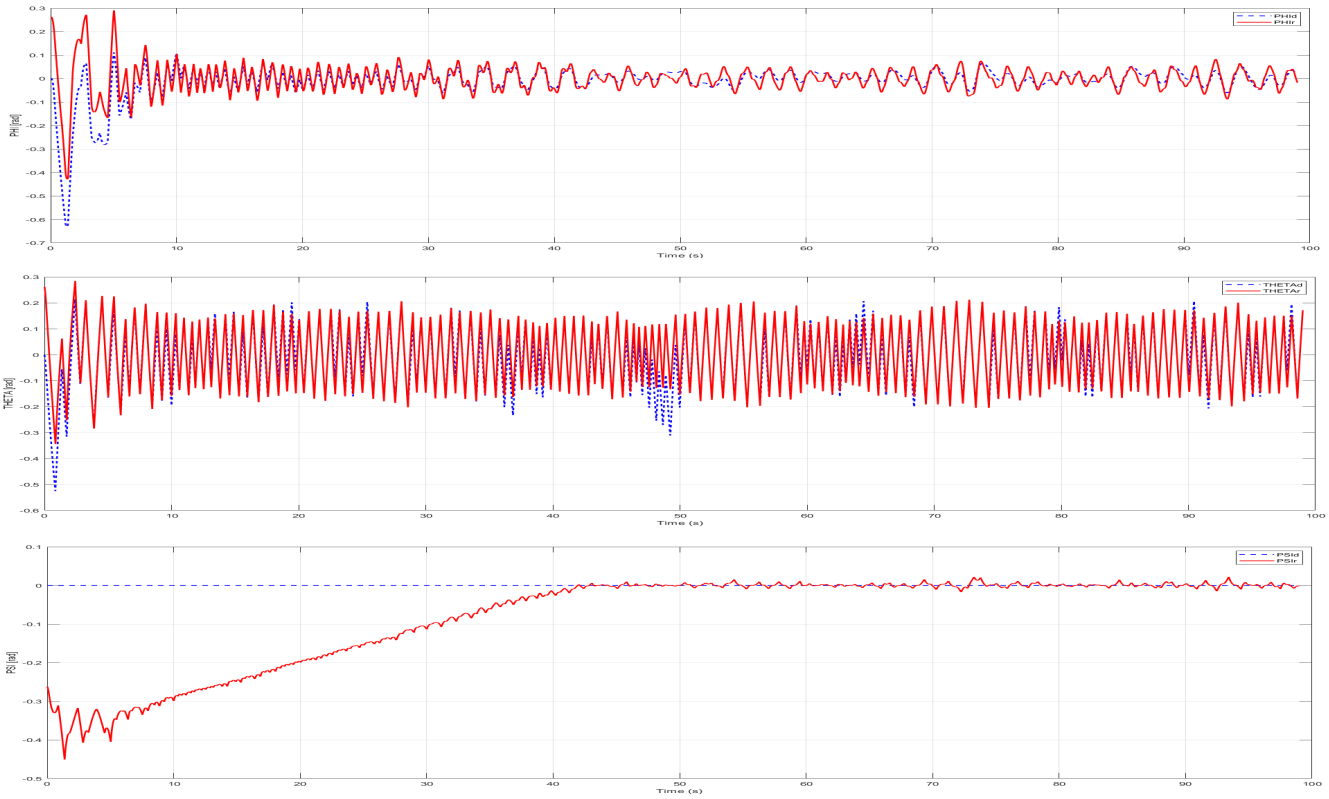

Figure 3.18: sliding mode attitude hovering

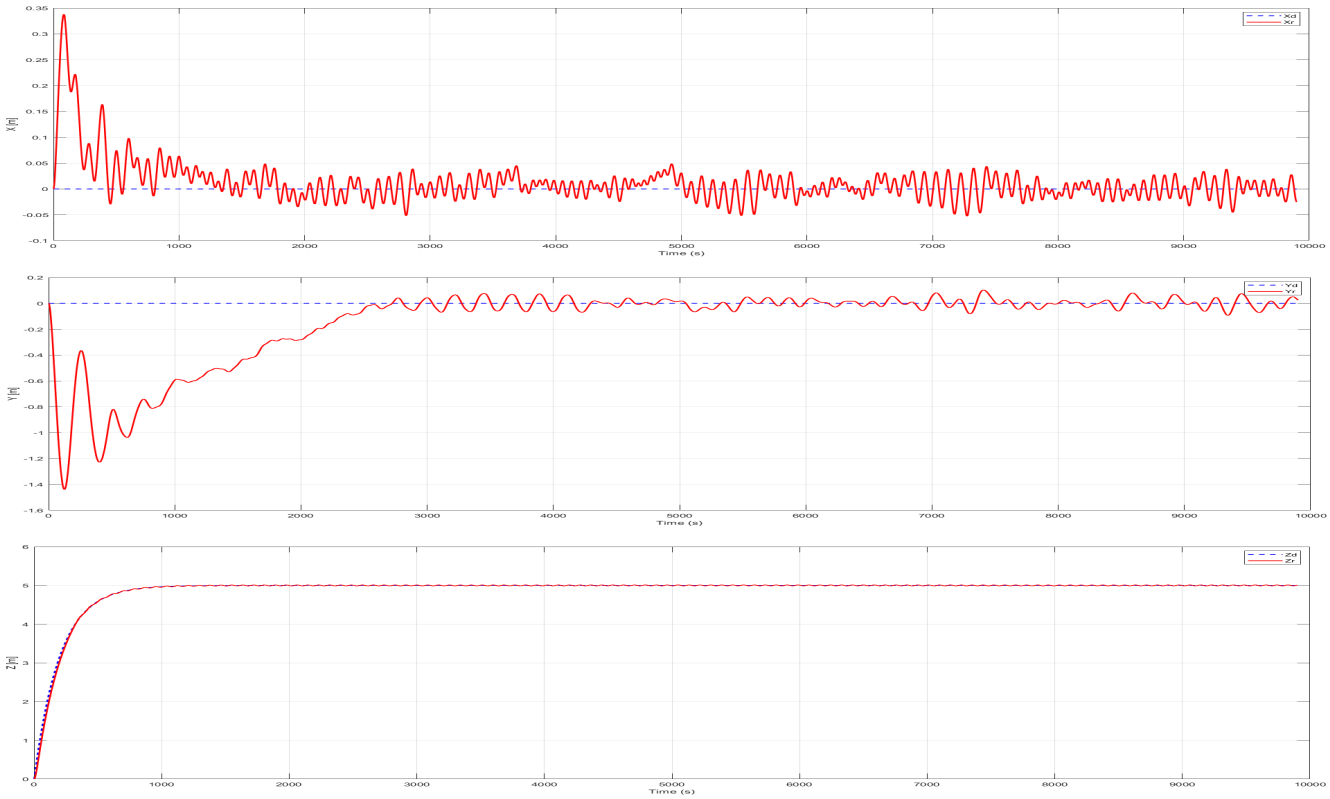

Figure 3.19: sliding mode position hovering

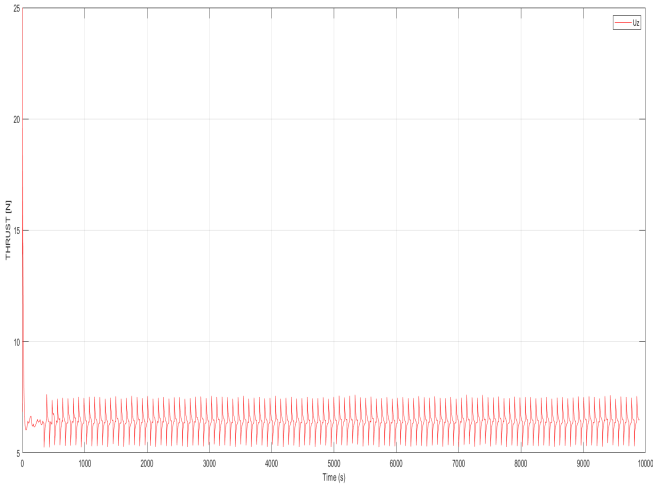

(a) Uz

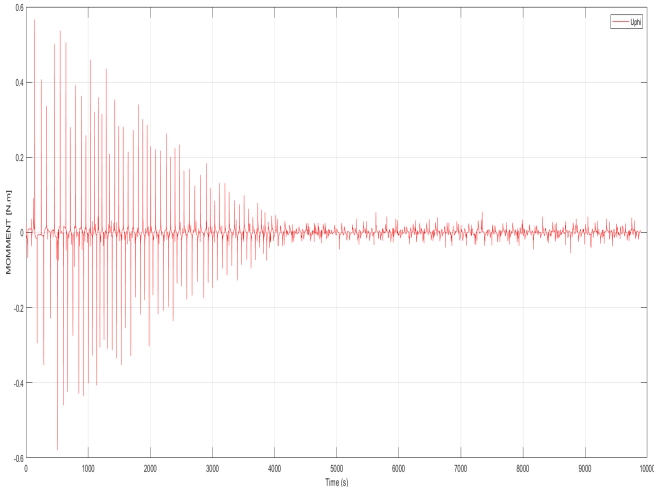

(b) Uphi

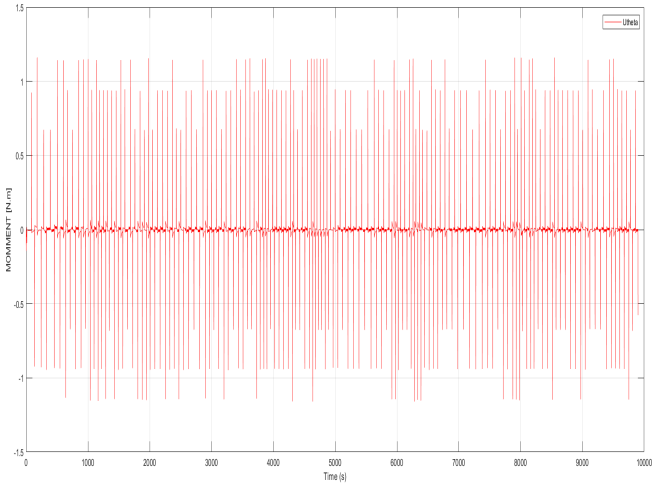

(c) Utheta

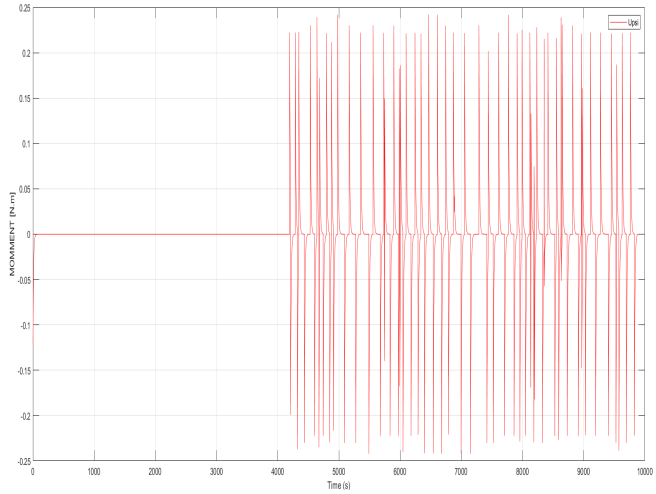

(d) Upsi

Figure 3.20: backstepping thrust and moments hovering.

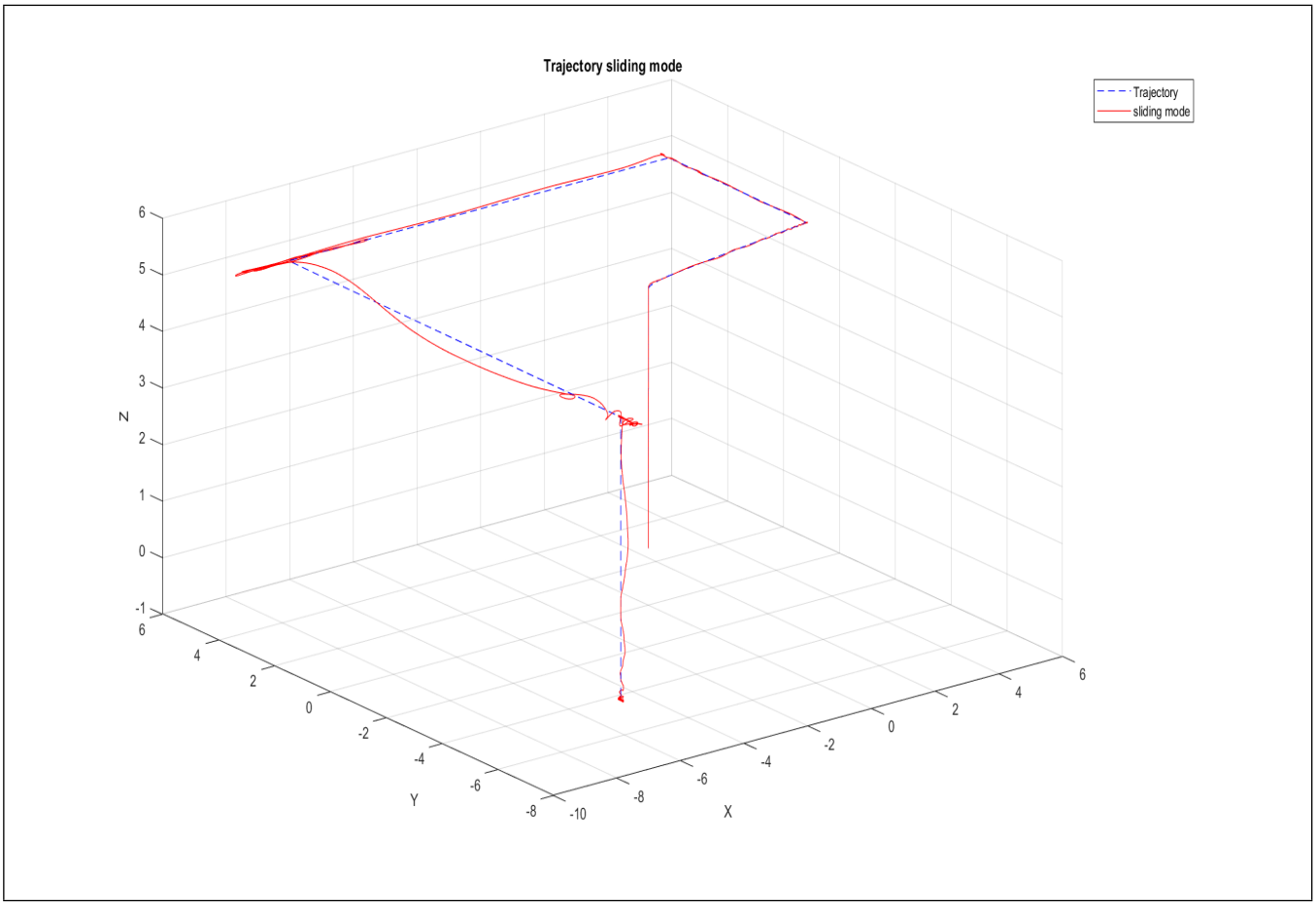

Figure 3.21: trajectory tracking using sliding mode

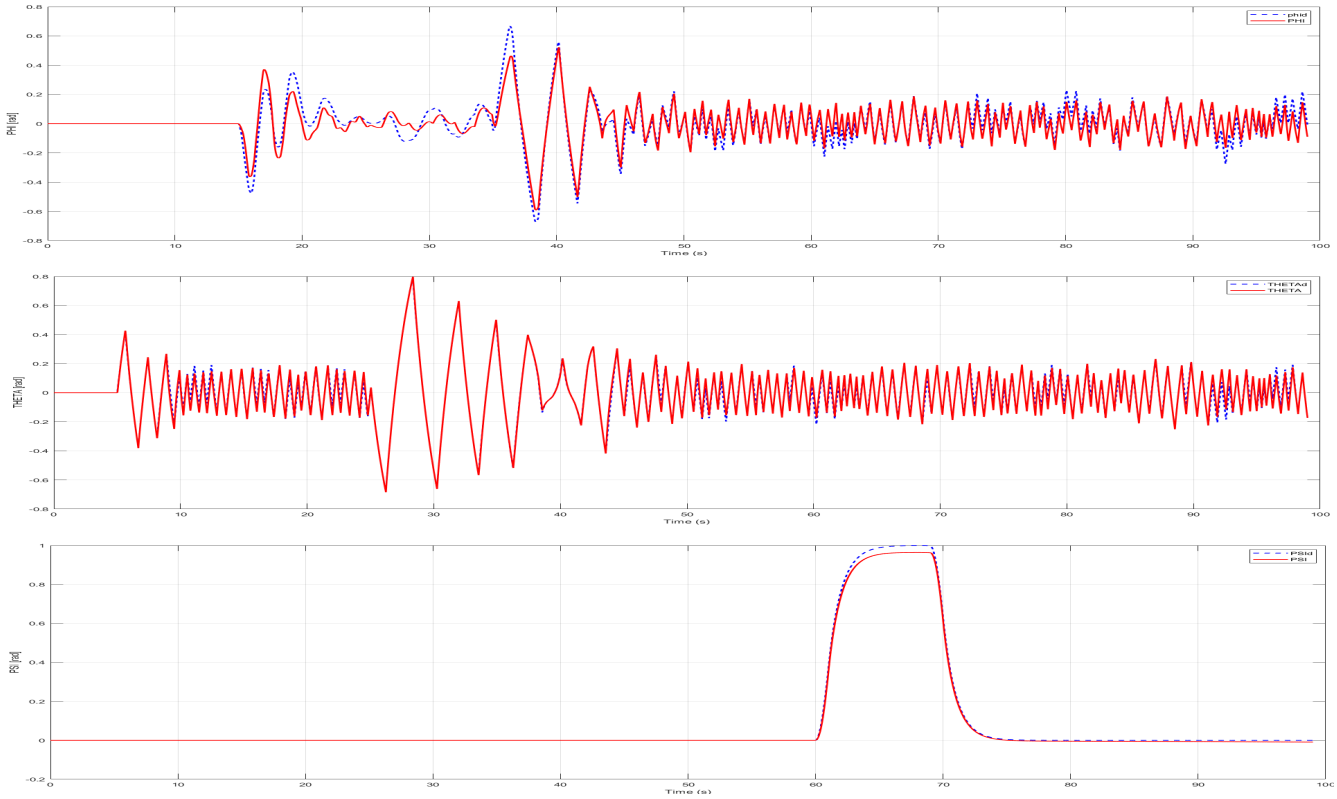

Figure 3.22: sliding mode attitude trajectory

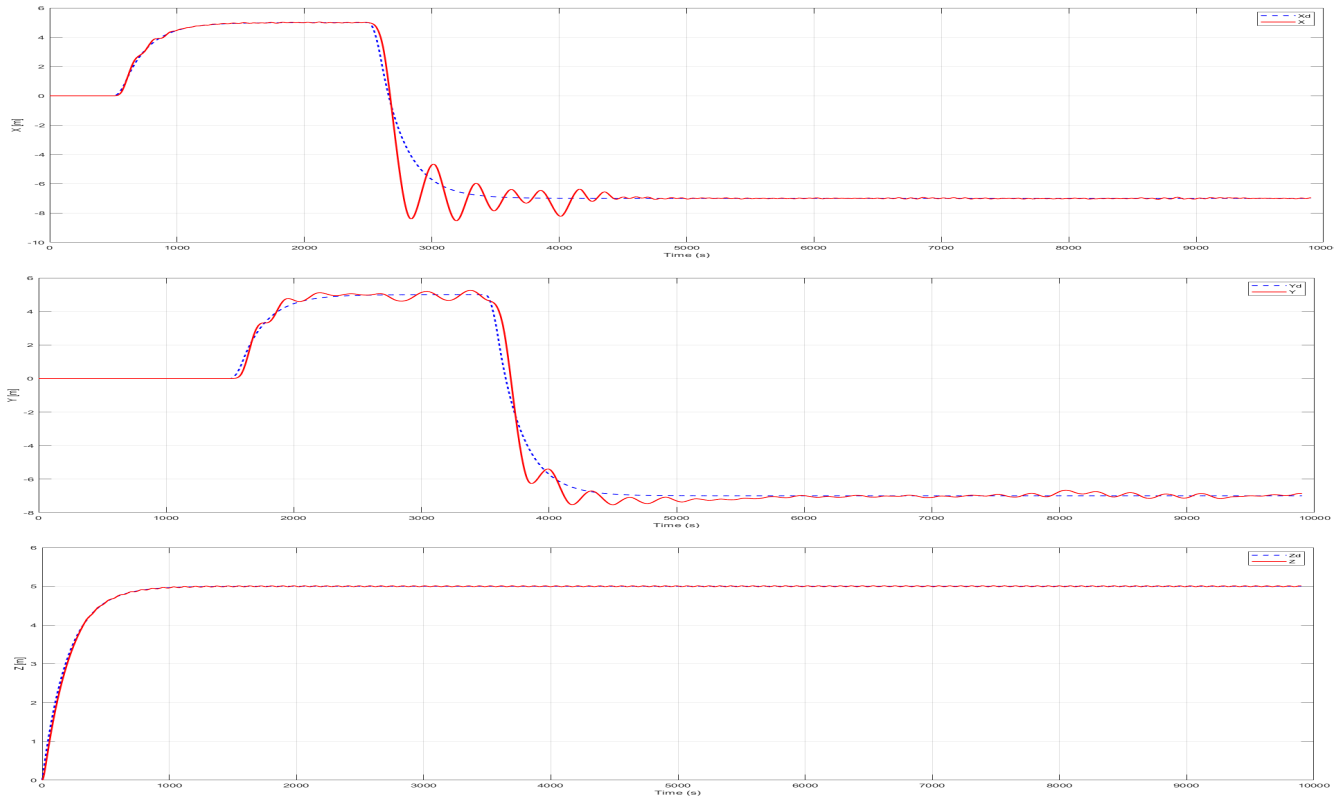

Figure 3.23: sliding mode position trajectory

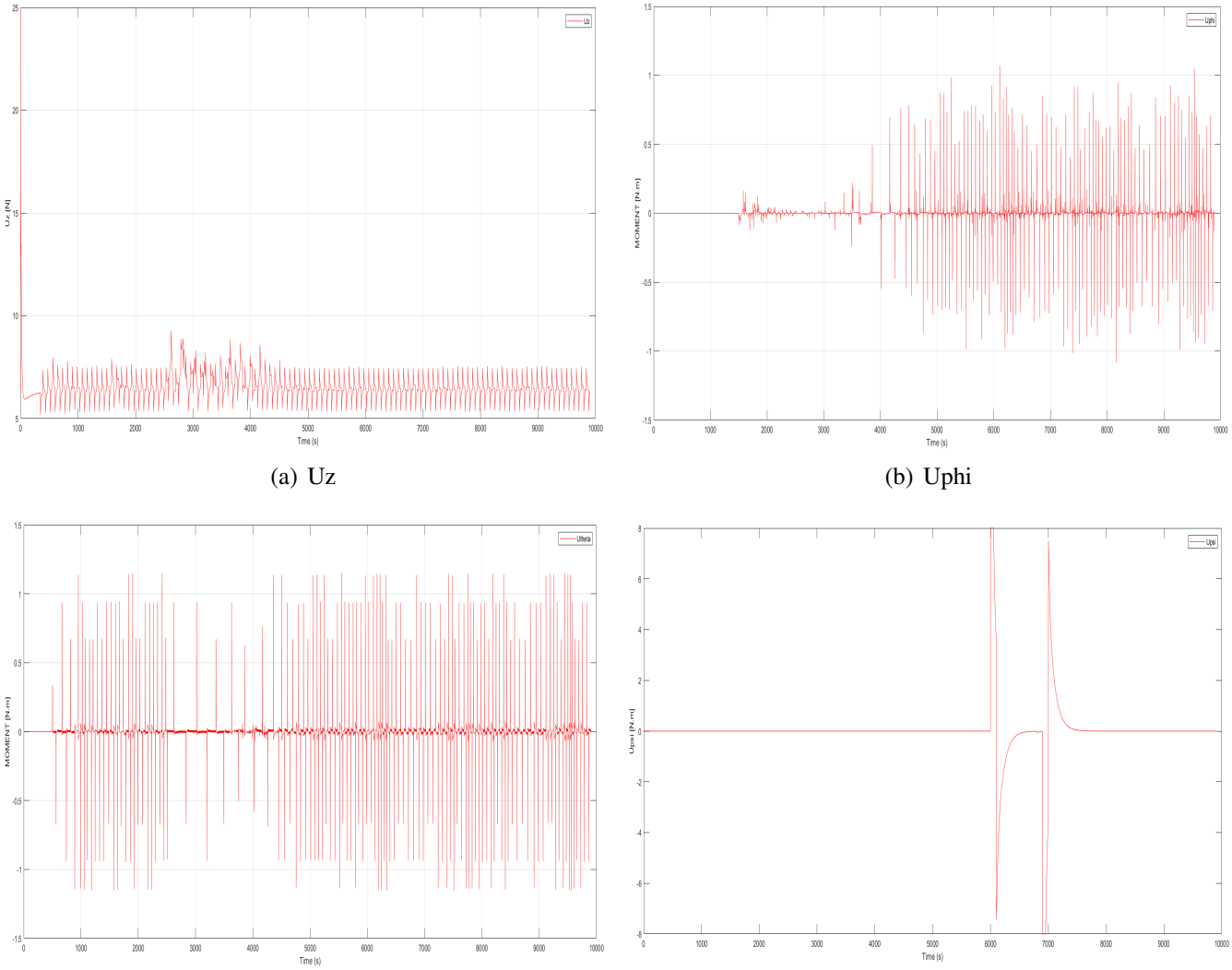

(a) Uz (b) Uphi

(c) Utheta (d) Upsi

Figure 3.24: sliding mode thrust and moments trajectory.

3.9 conclusion

Comparing PID, backstepping, and sliding mode control for a hexacopter, the following conclusions can be drawn:

PID control is a widely used control technique due to its simplicity and effectiveness. It provides good stability and steady-state performance for hexacopter control. However, PID control may struggle with handling nonlinearities and disturbances, which can limit its performance in complex flight scenarios.

Backstepping control is a nonlinear control approach that can handle system uncertainties and nonlinearities effectively. It provides better tracking performance and disturbance rejection compared to PID control. Backstepping control requires a good understanding of the system dynamics and can be more complex to design and implement.

Sliding mode control is a robust control technique that can handle uncertainties and disturbances by driving the system state onto a predefined sliding surface. It offers excellent robustness and disturbance rejection capabilities, making it suitable for challenging flight conditions. However, sliding mode control can introduce high-frequency control inputs, leading to increased wear and tear on the actuators. In conclusion, the choice of control strategy for a hexacopter depends on the specific requirements and flight conditions. PID control is simple and effective for basic stabilization tasks. Backstepping control is suitable for handling nonlinearities and uncertainties, providing improved tracking performance. Sliding mode control offers robustness and disturbance rejection capabilities at the cost of potentially higher actuator wear. The selection should be based on the specific control objectives, system dynamics, and the trade-offs between simplicity, performance, and robustness.

conclusion

Hexacopter drones have advantages over more commonly used quadrotors in terms of the stability they can provide during flight, which is crucial for missions such as surveillance and aerial photography. They are also more tolerant to motor failures that may occur at any moment during the flight. However, controlling this type of multirotor poses a challenge in terms of command allocation, which is performed using an approximately calculated matrix.

The complete model simulation of the hexacopter, under realistic assumptions, involved the utilization of three distinct control techniques: linear controllers specifically linear PID control, nonlinear controllers Backstepping control, and sliding mode control. These three categories represent different approaches to controlling the hexacopter system.

During the simulation, all three control methods exhibited their ability to effectively guide and govern the hexacopter system toward the desired objectives. This was achieved through the careful selection of appropriate gains for each control technique. Despite the system's inherent complexity and pronounced nonlinearity, as well as the challenge posed by the inaccurate allocation matrix, the control methods showcased their proficiency in maintaining control over the hexacopter.

The linear PID control approach relied on proportional, integral, and derivative components to regulate the system's altitude. This classical yet effective method allowed for swift error correction and the maintenance of a stable altitude.

On the other hand, the Backstepping control technique, which falls under the category of nonlinear control, employed a cascading approach to achieve precise altitude control. By accounting for the intricate interactions between various degrees of freedom within the hexacopter system, Backstepping control demonstrated enhanced performance and accuracy.

Additionally, the sliding mode control technique was also utilized. Sliding mode control leverages discontinuous control actions and seeks to keep the system's state trajectory within a designated sliding surface. This approach can handle uncertainties and disturbances, making it suitable for controlling the hexacopter system under challenging conditions.

In conclusion, all three control techniques—linear PID control, Backstepping control, and sliding mode control—proved their effectiveness in steering the hexacopter system towards desired objectives. The comparison of these techniques, however, necessitates the optimal selection of tuning gains for each controller. This ensures a fair and meaningful evaluation, leading to the attainment of optimal performance for the hexacopter system.

Bibliography

[1] Faiyaz Ahmed, JC Mohanta, Anupam Keshari, and Pankaj Singh Yadav. Recent advances in unmanned aerial vehicles: a review. *Arabian Journal for Science and Engineering*, 47(7):7963–7984, 2022.

[2] Christopher Van Tilburg. First report of using portable unmanned aircraft systems (drones) for search and rescue. *Wilderness & environmental medicine*, 28(2):116–118, 2017.

[3] H. Marcovitz. *Military Drones*. World of Drones. ReferencePoint Press, Inc., San Diego, CA, 2021.

[4] Philip Boucher. Domesticating the drone: the demilitarisation of unmanned aircraft for civil markets. *Science and engineering ethics*, 21(6):1393–1412, 2015.

[5] Gyula Mester. Modeling of autonomous hexa-rotor microcopter. In *Proceedings of the IIIrd International Conference and Workshop Mechatronics in Practice and Education (MechEdu 2015)*, pages 88–91, 2015.

[6] Reg Austin. *Unmanned aircraft systems: UAVS design, development and deployment*. John Wiley & Sons, 2011.

[7] Quan Quan. *Introduction to multicopter design and control*. Springer, 2017.

[8] Google trends. Online, 2023.

[9] DJI Automative. MATRICE 600 PRO. Online, 2010.

[10] PH Fan. *Design and control of multi-rotor aircraft*. PhD thesis, B.U.I.C., 2010.

[11] RF Zhang. *A study on quadrotor compound helicopter oriented to reliable flight control*. PhD thesis, B. and University, 2011. (In Chinese).

[12] Jacques Noetinger. *L'histoire de l'aviation, de 1905 à nos jours en 1000 photographies: 1er série de Clément Ader à 1910*. Paris, 1948.

[13] Theodore P Wright. Factors affecting the cost of airplanes. *Journal of the aeronautical sciences*, 3(4):122–128, 1936.

[14] Curtiss-Wright VZ-7 helicopter - development history, p., technical data. Online, n.d.

[15] Nikolaus Koeniger, Gudrun Koeniger, Michael Gries, and Salim Tingek. Drone competition at drone congregation areas in four apis species. *Apidologie*, 36(2):211–221, 2005.

[16] Erdinc Altug. *Vision based control of unmanned aerial vehicles with applications to an autonomous four-rotor helicopter, quadrotor*. University of Pennsylvania, 2003.

[17] Gyrosaucer- the ultimate Indoor RC. Online, n.d. [Retrieved April 19].

[18] The story behind Draganfly Innovations. Online, n.d.

[19] Jonathan P How, Brett Behihke, Adrian Frank, Daniel Dale, and John Vian. Real-time indoor autonomous vehicle test environment. *IEEE Control Systems Magazine*, 28(2):51–64, 2008.

[20] Microdrones profile. Online, n.d.

[21] Nathan Michael, Jonathan Fink, and Vijay Kumar. Cooperative manipulation and transportation with aerial robots. *Autonomous Robots*, 30:73–86, 2011.

[22] Prime Air. Online, n.d.

[23] Dario Floreano and Robert J Wood. Science, technology and the future of small autonomous drones. *nature*, 521(7553):460–466, 2015.

[24] Larry Lipera, Jason D Colbourne, Mark B Tischler, M Hossein Mansur, Michael C Rotkowitz, and Paul Patangui. The micro craft istar micro air vehicle: Control system design and testing. In *Annual Forum Proceedings-American Helicopter Society*, volume 57, pages 1998–2008. AMERICAN HELICOPTER SOCIETY, INC, 2001.

[25] Volocopter. Online, n.d.

[26] Anuj Puri. A survey of unmanned aerial vehicles (uav) for traffic surveillance. *Department of computer science and engineering, University of South Florida*, pages 1–29, 2005.

[27] Michael Kontitsis, Kimon P Valavanis, and Nikos Tsourveloudis. A uav vision system for airborne surveillance. In *IEEE International Conference on Robotics and Automation, 2004. Proceedings. ICRA'04. 2004*, volume 1, pages 77–83. IEEE, 2004.

[28] Dieter Hausamann, Werner Zirnig, and Gunter Schreier. Monitoring of gas transmission pipelines-a customer driven civil uav application. In *ODAS Conference*, page 15, 2003.

[29] Sebastian Siebert and Jochen Teizer. Mobile 3d mapping for surveying earthwork projects using an unmanned aerial vehicle (uav) system. *Automation in construction*, 41:1–14, 2014.

[30] Horea Bendea, Filiberto Chiabrando, F Giulio Tonolo, and Davide Marenchino. Mapping of archaeological areas using a low-cost uav. the augusta bagiennorum test site. In *XXI International CIPA Symposium*, volume 1. Citeseer, 2007.

[31] Christophe De Wagter, Bart Remes, Ewoud Smeur, Freek van Tienen, Rick Ruijsink, Kevin van Hecke, and Erik van der Horst. The nederdrone: A hybrid lift, hybrid energy hydrogen uav. *international journal of hydrogen energy*, 46(29):16003–16018, 2021.

[32] H2 drones. Online, n.d. [Retrieved April 20].

[33] Margarida Faria, António Sérgio Ferreira, Héctor Pérez-Leon, Ivan Maza, and Antidio Viguria. Autonomous 3d exploration of large structures using an uav equipped with a 2d lidar. *Sensors*, 19(22):4849, 2019.

[34] Fernando Vanegas and Felipe Gonzalez. Enabling uav navigation with sensor and environmental uncertainty in cluttered and gps-denied environments. *Sensors*, 16(5):666, 2016.

[35] Renato Ferreira, João Gaspar, Pedro Sebastião, and Nuno Souto. A software defined radio based anti-uav mobile system with jamming and spoofing capabilities. *Sensors*, 22(4):1487, 2022.

[36] Yongho Ko, Jiyoon Kim, Daniel Gerbi Duguma, Philip Virgil Astillo, Ilsun You, and Giovanni Pau. Drone secure communication protocol for future sensitive applications in military zone. *Sensors*, 21(6):2057, 2021.

[37] Salwa Elouarouar and Hicham Medromi. Hexacopter drones overview. In *2022 2nd International Conference on Innovative Research in Applied Science, Engineering and Technology (IRASET)*, pages 1–7. IEEE, 2022.

[38] Isad Saric, Adnan Masic, and Muamer Delic. Hexacopter design and analysis. In *New Technologies, Development and Application IV*, pages 74–81. Springer, 2021.

[39] Hakim Bouadi, M Bouchoucha, and M Tadjine. Modelling and stabilizing control laws design based on backstepping for an uav type-quadrotor. *IFAC Proceedings Volumes*, 40(15):245–250, 2007.

[40] Sumaila Musa. Techniques for quadcopter modeling and design: A review. *Journal of unmanned system Technology*, 5(3):66–75, 2018.

[41] Hakim Bouadi and Félix Mora-Camino. Modeling and adaptive flight control for quadrotor trajectory tracking. *Journal of Aircraft*, 55(2):666–681, 2018.

[42] Denis Kotarski and Josip Kasać. Generalized control allocation scheme for multirotor type of uavs. *Drones—Applications; Dekoulis, G., Ed.; IntechOpen: London, UK*, pages 43–58, 2018.

[43] Duc-Tien Nguyen, David Saussie, and Lahcen Saydy. Fault-tolerant control of a hexacopter uav based on self-scheduled control allocation. In *2018 international conference on unmanned aircraft systems (ICUAS)*, pages 385–393. IEEE, 2018.

[44] Johannes Tjønnås and Tor A Johansen. Adaptive control allocation. *Automatica*, 44(11):2754–2765, 2008.

[45] Zhihui Wang, Jing Zhang, and Lingyu Yang. Weighted pseudo-inverse based control allocation of heterogeneous redundant operating mechanisms for distributed propulsion configuration. *Energy Procedia*, 158:1718–1723, 2019.

[46] Xingyue Shao, Zixuan Liang, Bai Chen, and Cunjia Liu. A modified weighted pseudo-inverse control allocation using genetic algorithm. In *2015 34th Chinese Control Conference (CCC)*, pages 5554–5559. IEEE, 2015.

[47] I.K. Peddle, T. Jones, and J. Treurnicht. Practical near hover flight control of a ducted fan (slade). *Control Engineering Practice*, 17(1):48–58, 2009.

[48] A. Tayebi and S. McGilvray. Attitude stabilization of a four-rotor aerial robot. In *2004 43rd IEEE Conference on Decision and Control (CDC) (IEEE Cat. No.04CH37601)*, 2004.

[49] N.D. Salim et al. Pid plus lqr attitude control for hexarotor mav in indoor environments. In *2014 IEEE International Conference on Industrial Technology (ICIT)*. IEEE, 2014.

[50] K.V. Rao and A.T. Mathew. Dynamic modeling and control of a hexacopter using pid and back stepping controllers. In *2018 International Conference on Power, Signals, Control and Computation (EPSCICON)*. IEEE, 2018.

[51] J.T. Zou, G.W. Huang, and C.Y. Hsu. The design and implementation of hexa-rotor aerial robot. In *Applied Mechanics and Materials*. Trans Tech Publ, 2013.

[52] A.A. Wahab, R. Mamat, and S.S. Shamsudin. The effectiveness of pole placement method in control system design for an autonomous helicopter model in hovering flight. *International Journal of Integrated Engineering*, 1(3), 2009.

[53] E. Pfeifer and F. Kassab Jr. Dynamic feedback controller of an unmanned aerial vehicle. In *2012 Brazilian Robotics Symposium and Latin American Robotics Symposium*. IEEE, 2012.

[54] S. Pouya and F. Saghafi. Autonomous runway alignment of fixed-wing unmanned aerial vehicles in landing phase. In *2009 Fifth International Conference on Autonomic and Autonomous Systems*. IEEE, 2009.

[55] M. Krstic, P.V. Kokotovic, and I. Kanellakopoulos. *Nonlinear and adaptive control design*. John Wiley & Sons, Inc., 1995.

[56] D. Arzelier. *Théorie de Lyapunov, commande robuste et optimisation*. PhD thesis, Université Paul Sabatier-Toulouse III, 2004.

[57] R. Mahony, T. Hamel, and A. Dzul. Hover control via lyapunov control for an autonomous model helicopter. In *Proceedings of the 38th IEEE Conference on Decision and Control (Cat. No. 99CH36304)*. IEEE, 1999.

[58] E. Frazzoli, M.A. Dahleh, and E. Feron. Trajectory tracking control design for autonomous helicopters using a backstepping algorithm. In *Proceedings of the 2000 American Control Conference. ACC (IEEE Cat. No. 00CH36334)*. IEEE, 2000.

[59] R. Mahony and T. Hamel. Robust trajectory tracking for a scale model autonomous helicopter. *International Journal of Robust and Nonlinear Control: IFAC-Affiliated Journal*, 14(12):1035–1059, 2004.

[60] G.P. Falconí and F. Holzapfel. Position tracking of a hexacopter using a geometric backstepping control law-experimental results. In *2014 IEEE International Conference on Aerospace Electronics and Remote Sensing Technology*. IEEE, 2014.

[61] S. Di Lucia, G.D. Tipaldi, and W. Burgard. Attitude stabilization control of an aerial manipulator using a quaternion-based backstepping approach. In *2015 European conference on mobile robots (ECMR)*. IEEE, 2015.

[62] G. Mester. Backstepping control for hexa-rotor microcopter. *Acta Technica Corviniensis-Bulletin of Engineering*, 8(3):121, 2015.

[63] Andrzej Bartoszewicz. *Sliding mode control*. Intech Publisher, India, 1st edition, March 2011.

[64] Pablo Proano, Linda Capito, Andres Rosales, and Oscar Camacho. Sliding mode control: Implementation like pid for trajectory-tracking for mobile robots. In *IEEE Asia-Pacific Conference on Control and Automation (APCCA)*, pages 220–225, Asia, 2015.

Abstract

arabtex utf8
This thesis focuses on achieving effective control of a hexacopter drone, highlighting its advantages over other multicopters, including stable hovering and fault tolerance for successful and safe mission accomplishment. The initial phase involves modeling the drone under specific assumptions, followed by synthesizing three distinct control laws for the development of controllers. The study then proceeds to simulate the drone's control using three different techniques: PID, Backstepping, and sliding mode. A comprehensive comparison of these control techniques is conducted, providing valuable insights into their performance and applicability. The findings contribute to advancing the understanding and implementation of efficient control strategies for hexacopter drones.

Keywords : control, hexarotor, modeling, simulation, PID, backstepping, sliding mode

Résumé

Ce mémoire se concentre sur la réalisation d'un contrôle efficace d'un drone hexarotor. Ce type de drone présente plusieurs avantages par rapport aux autres multicoptères, tels que la stabilité en vol stationnaire et la tolérance aux défaillances, ce qui lui permet d'accomplir ses missions avec succès et en toute sécurité. La première étape du travail consiste à modéliser le drone en fonction d'un ensemble d'hypothèses, puis à synthétiser trois lois de contrôle différentes pour la conception des contrôleurs. L'étude se poursuit ensuite par une simulation du contrôle du drone en utilisant trois techniques différentes : PID, Backstepping et le mode glissant. Une comparaison approfondie de ces techniques de contrôle est réalisée, fournissant des informations précieuses sur leurs performances et leur applicabilité. Les résultats contribuent à faire progresser la compréhension et la mise en œuvre de stratégies de contrôle efficaces pour les drones hexarotor.

Mots clés : commande, hexarotor, modélisation, simulation, PID, backstepping, mode glissant.

ملخص:

يهدف العمل المقدم في هذه الأطروحة إلى التحكم في طائرة بدون طيار سداسية المحركات. يتمتع هذا النوع من الطائرات بدون طيار بالعديد من المزايا مقارنة بالطائرات المتعددة المحركات الأخرى مثل استقرار في الحركة وتجاوز العيوب، مما يسمح لها بإنجاز مهامها بنجاح وأمان. يتضمن العمل مرحلة النمذجة الأولية للطائرة بدون طيار وتطوير وحدات التحكم باستخدام ثلاثة قوانين تحكم متميزة. تمت دراسة تحكم الطائرة بدون طيار باستخدام ثلاث تقنيات مختلفة: التحكم التناسبي التكاملي التفاضلي والتراجع ووضع الانزلاق. تمت مقارنة شاملة لهذه التقنيات لتحليل أدائها وقابليتها للتطبيق. تساهم النتائج في تعزيز الفهم وتوجيه استراتيجيات التحكم الفعالة للطائرات بدون طيار سداسية المحركات.

الكلمات الرئيسية: التحكم، السداسية، الطائرة بدون طيار، المحاكاة، التحكم التناسبي التكاملي التفاضلي، التراجع، وضع الانزلاق